The Role of Interfaces in Enzyme Activity and Cell Adaptation

Dissertation zur Erlangung des Doktorgrades
der mathematisch-naturwissenschaftlichen Fakultät
der Universität Augsburg

vorgelegt von

Stefan Nuschele

Lehrstuhl für Experimentalphysik I
Institut für Physik
Universität Augsburg
Juli 2010

Erstgutachter:	Prof. Dr. M. F. Schneider
Zweitgutachter:	Prof. Dr. A. Reller
Tag der mündlichen Prüfung:	27. Juli 2010

Abstract

The second derivatives of thermodynamic potentials are directly related to thermodynamic susceptibilites like heat capacity and compressibility. Such susceptibilites are strongly enhanced in the phase transition of lipid membranes corresponding to high fluctuations in the variables, e.g. in enthalpy and area. Not only are phase transitions found in simple component lipid membranes but they also occur in biological membranes of simple organisms. When growth parameters of bacterias are changed then also the measured transition temperatures changes. In the context of enzyme-membrane interaction, phase transitions mark the temperature at which the activation energies of various lipid vesicle bound enzymes decreases when the membranes melted from the gel to the fluid phase. In addition, the activity of lipid vesicle bound Phospholipase A2 has been found to exhibit a maximum when the membrane is in its phase transition.

In the present study the attention was directed at the investigation of membrane-enzyme-hydration-layers based biological interfaces. One of the fastest enzymes in biology, Acetylcholinesterase, was incorporated into lipid monolayers and the activity as well as monolayer phase states were simultaneously recorded on a Langmuir-trough - photometer hybrid. We were able to detect a dramatic increase in the activity of Acetylcholinesterase by a factor of 2-3 when the monolayers were driven through the phase transitions. The finding proved to be invariant upon changes in thermodynamic properties induced through variations in lipids, pH and temperature and therefore was regarded as being of general character. The results were demonstrated to suggest a correlation of area fluctuations and activity. This is also conform with the theory of Konrad Kaufmann which states that biological interfaces obtain their own entropy and, further, that critical states within these systems resemble high fluctuations that can lead to enhanced enzyme activities.

In addition, the membranes of both bacterial and human cells were investigated in terms of their phase behaviour and their adaptation to changes in temperature. The thermodynamic properties of the cell membranes were analyzed by applying a variety of methods including calorimetry, Langmuir monolayers, black lipid membranes, fatty acid analyses, enzyme activity assays and population studies. We found that human cell membranes exhibit phase transitions and probably a critical point as well as they adapt to changes in growth temperature. Due to the similarity of these results

to the properties found in bacterias, the underlying principles of these phenomena were supposed to originate from an universal mechanism. Based on the experimental findings we therefore developed a thermodynamic model of adaptation. For this purpose we applied the entropy potential to biological membranes and therefrom derived adaptation as the evolution of the entropy potential.

The findings strongly suggest a crucial role of biological interfaces in cell function.

Contents

Abstract iii

I Introduction 1

II Theory and Methods 4

1 Thermodynamics in Biology 5
1.1 Entropy . . . 5
1.2 Susceptibilities . . . 8

2 Lipids and Lipid Membranes 10
2.1 Lipid Structure and Membranes . . . 10
2.2 Biological Membranes . . . 12
2.3 Critical States of Membranes . . . 14

3 Enzymes 19
3.1 Kinetics and Single Enzyme Fluctuations . . . 19
3.2 On Konrad Kaufmann's Theory of Catalysis . . . 22
3.3 Membrane-Enzyme-Interaction . . . 25

4 Methods 27
4.1 Differential Scanning Calorimetry . . . 27
4.2 Langmuir Trough - Photometer Hybrid . . . 28
4.3 Black Lipid Membranes . . . 31
4.4 Cell Growth . . . 32
4.5 Extraction of Membranes and Desaturase . . . 34

III Results 35

5 Phase State Dependent Activity of Acetylcholinesterase 36
5.1 The Enzyme Acetylcholinesterase (AChE) . . . 36
5.2 Prestudies on Membrane-Bound AChE . . . 39

5.3 The Role of Protons in Monolayer-Enzyme Systems 46
5.4 Maximum Activity of AChE in Monolayer Phase Transition 50
5.5 Invarianz of the Maximum Activity 56
5.6 Theory and Discussion 58

6 The Physics of Adaptation in Biological Membranes 64
6.1 Crucial Role of Membranes in Cell Function 64
6.2 Adaptation of Bacterial Membranes 66
6.3 Experimental Proof of Phase Transitions in Human Cell Membranes 70
6.4 Adaptation of Human Cells 80
6.5 The Activity of Membrane Bound Desaturases 88
6.6 A General Model of Cell Adaptation 94

IV Summary and Outlook 102

V Appendix 107

A Procedures 108
A.1 Desaturase Activity Assay 108
A.2 Fatty Acid Analysis with Gas Chromatography 109

B Lipids 110
B.1 Nomenclature 110
B.2 Cardiolipin 110

Bibliography 111

Danksagung 124

Curriculum Vitae 126

Part I

Introduction

Our biological means of gaining knowledge of nature are based on using the senses of our body as well as on cognition. Over the past milenias these abilities have been utilized to develop an ensemble of methods and theories to study nature in more detail.

In biological research, numerous advanced techniques and methods have been developed within the last centuries. They allow researchers of various subjects to gain a very detailed insight into structure and functions of our biological environment. Here, in particular the decoding of our gensequences within the human genome project and the improved steric resolution of biological structures have lead to enormeous progresses in the understanding of the functioning of cells and of whole organisms. In this sense the "gen" and the "detail" way of studying biological objects over the last decades can be considered as very successful. However, they have produced a somewhat one-sided character of approaching the goal of understanding life. A rather dominating genetics and the focus on steric detailed resolutions of frozen molecule structures may have overgrown the idea of fundamental general approaches to biological research. Do we, to some extent, neglect such systemic and general approaches to biological questions?

Enzymes, and in particular membrane-bound enzymes, are embedded in an aqueous and lipid environment rather than being isolated within the cells. Concerning their function they are very sensitive to the particular state of the surrounding region. This becomes obvious considering the pH depedence of enzymatic reactions. Enzymes are also sensitive to the state of the lipid membranes. Some of them show a distinct change in their activitation energy when the surronding membrane is in its phase transition. Evenmore, for the ubiquitous enzyme Phospholipase A2 the activity has been found to be maximal in the phase transition regimes of membranes. It is of crucial interest wether the behaviour of Phospholipase A2 displays an exception or wether it features the tip of an iceberg hiding a much more general mechanism that applies for other enzymes, too.

It is reasonable to assume that membranes influence biological functions in a strong manner. In particular, this has become obvious when it was shown that cell membranes of simple organisms exhibit distinct phase behaviour. Further, it has been found that simple organisms like bacterias or yeasts adapt their lipid compositions and therefore also adapt their phase states to environmental changes. Such findings indicate that the occurance of distinct phase states in biological membranes seems to be crucial for cell functioning. This might hold especially for the enzymes refered to above.

In the present thesis the aforementioned phenomena of membrane phase state dependent enzyme activity and of adaptation are adressed. If membranes are directly involved into enzyme kinetics then as a consequence the surrounding aqueous

environment must be involved. Motivated by the results of membrane sensitive enzymes and by the adaptation of simple organisms, the aim of the present work was to clarify to what extend membrane interfaces play a role in these processes. It will be demonstrated that, indeed, the physical properties of membranes are directly related to enzymatic turn. In addition, it will be proven that human cell membranes exhibit distinct phase states leading to adaptation and critical states. By means of a thermodynamic approach both experimental findings are studied in a general unifying way.

The leading thought in this thesis is an interfacial thermodynamic approach to both mentioned topics in whose center the lipid membrane features a dominant role. The main topics of the thesis are evolved as follows:

In the first part theoretical aspects will be introduced from a thermodynamic perspective laying the foundation for the interpretations of the experimental reults below. The main focus in this theoretical part will be the role of entropy in biological interfaces. Furthermore, lipid membranes, enzymes and the applied materials and methods are described.

In the second part the obtained results are presented. It is separated into two chapters, where the first one is devoted to the interaction of enzymes and membranes. It will be shown, that if the enzyme Acetylcholinesterase is incorporated into lipid monolayers, its activity is strongly dependent on the physical state of the monolayer. In the phase transition regime of the membrane the activity exhibits a distinct maximum.

In the second results chapter the adaptive behaviour of cells is investigated. Cells and cell membranes are studied in terms of their adaptation to changes in environmental conditions. Not only were thermotropic phase transitions recored for bacterias, but also in membranes human cells they will be presented to occur. These transitions shifted to a new phase transition temperature after an environmental change has taken place. Including the results from part two a general thermodynamic model of cell adaptation is presented.

Part II

Theory and Methods

1 Thermodynamics in Biology

Thermodynamics is one of the most fundamental concepts in Physics. Its laws have never been observed to be falsified since their description was completed one century ago. The first law of Thermodynamics states the conservation of energy:

$$dE = \delta Q + \delta W \tag{1.1}$$

where E is the inner energy, Q is the heat and W denotes the work. In the second law of thermodymics Q is associated with the entropy S and the temperature T. For irreversibel processes the entropy is never decreasing, for reversibel processes the entropy is:

$$dS = \frac{\delta Q}{T} \tag{1.2}$$

In the following Einstein's definition of the second law and the entropy will be introduced as well as the proper entropy of interfaces which was first thoroughly described by Kaufmann [70]. Subsequently basic properties of lipids and membranes are illustrated. Phase transitions and susceptibilites of biological matter are then treated from the viewpoint of entropy. The last section is devoted to enzymes and to the state of the art of catalysis.

1.1 Entropy

Following Einstein [35] an entropy potential is proposed. Consequences of Einstein's definition of entropy are thermodynamic forces and fluctuations directly derived from the entropy potential. Based on Einstein's work, Kaufmann has developed a theory of soft interfaces like they appear in biological membranes and on enzymes. A summary of the main ideas is given in the following.

1.1.1 Einstein's Formulation of the Second Law of Thermodynamics

Before Einstein, Clausius was the first to state that for the fully reversible steps in the heat engine entropy is a function of state. This assumption means that the

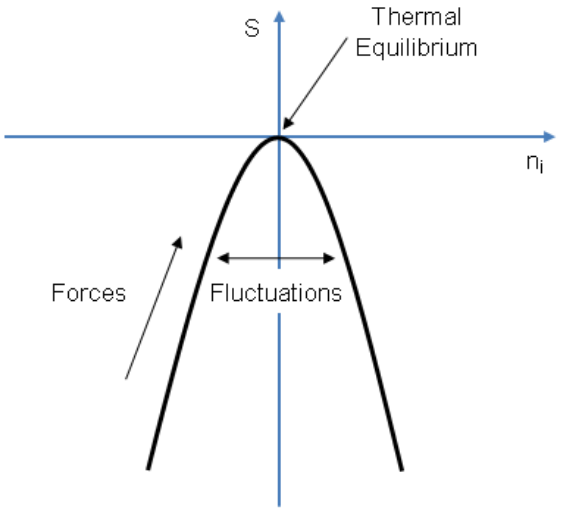

Figure 1.1: Entropy potential. If the system is in thermal equilibrium it is found in a region of states close to the maximum. First and second order derivatives indicate thermodynamic forces and fluctuations.

circular integral over the entropy vanishes:

$$\oint dS = \oint \frac{dQ}{T} = 0 \tag{1.3}$$

Therefore the entropy is an analytical potential:

$$S = S(n_1, n_2, n_3, ...) \tag{1.4}$$

n are the thermodynamic observables like area, particle number, chemical potential, internal energy or the reaction coordinate of chemical reactions.

Since the entropy is in a maximum it can be developed as a function of the variables, n_i [35, 75, 70, 57]:

$$S = S_0 + \underbrace{\sum_i \left(\frac{\partial S}{\partial n_i}\right)_{n_0}}_{\text{Forces}} (n_i - n_i^0) + \underbrace{\frac{1}{2}\sum_i \sum_j \left(\frac{\partial^2 S}{\partial n_i \partial n_j}\right)_{n_i^0, n_j^0}}_{\text{Fluctuations}} (n_i - n_i^0)(n_j - n_j^0) + ... \tag{1.5}$$

The first derivatives represent thermodynamic forces. They describe processes that drive the system back to $\frac{\partial S}{\partial n_i} = 0$. The second derivatives represent thermodynamic fluctuations (Fig. 1.1).

In the region of maximum entropy the forces (slopes) vanish:

$$S \approx S_0 + \frac{1}{2}\sum_i \sum_j \left(\frac{\partial^2 S}{\partial n_i \partial n_j}\right)_{n_i^0, n_j^0} (n_i - n_i^0)(n_j - n_j^0) \tag{1.6}$$

The fluctuations of a system reflect the inverse curvature of the entropy potential

$$\langle \delta n_i \delta n_j \rangle = -k_B \left(\frac{\partial^2 S}{\partial n_i \partial n_j}\right)^{-1} \tag{1.7}$$

As will be seen in the next section, the fluctuations are related to general susceptibilities.

According to Boltzmann [15] S can be interpreted as a probability (Ω):

$$S = k_\mathrm{B} \ln \Omega \tag{1.8}$$

were k_B is today denoted as the Boltzmann constant. Further

$$\Omega = \exp \frac{S}{k_B}. \tag{1.9}$$

A system in equilibrium will most probably be found in a region around maximum probability. This implies that most likely the states in a region around the maximum entropy are occupied. Along the same line, a system observed in a state of low probability will very likely evolve in time to a state of higher probability (see also [75]). In other words, if one can define an entropy potential for a system one can predict that it very probably will evolve to states of higher probability which are identical to higher values of entropy. This finding is consistent with the observation that the entropy of such a system never decreases. In the maximum of the entropy, using eq. 1.6, this relation becomes:

$$\Omega = \exp\left(\frac{1}{k_B}\left(S_0 + \frac{1}{2}\sum_i \sum_j \left(\frac{\partial^2 S}{\partial n_i \partial n_j}\right)_{n_i^0, n_j^0} (n_i - n_i^0)(n_j - n_j^0)\right)\right) \tag{1.10}$$

Therefore the states of a thermodynamic system follow a Gaussian distribution.

The interpretation of an entropy potential may be as follows: Irreversibel processes are processes that move a system of given entropy potential from a state of low to a state of higher probability. In experiments the initial state of relatively low probability is usually prepared by the experimentalist, e.g. by preparing an unlikely initial condition [70]. For example, a droplet of ink put into a volume of water defines a new system with low probability and therefore low entropy. Diffusion leads to an

equilibrated distribution of ink with much higher entropy.

Generally spoken, the law of entropy is time independent [70]. Time therefore is always introduced by an observer, which for example is an experimentalist who measures enzyme activity *in time.* Keeping this in mind, if the system is not in thermal equilibrium, the value of entropy of a state changes spontaneously with time:

$$\sigma := \frac{dS}{dt} > 0 \tag{1.11}$$

σ is called entropy production. Considering several variables, n_i, one can write:

$$\frac{dS}{dt} = \sum_i \underbrace{\frac{\partial S}{\partial n_i}}_{\text{Forces}} \cdot \underbrace{\frac{\partial n_i}{\partial t}}_{\text{Fluxes}} \equiv \sum_i X_i J_i \tag{1.12}$$

where X_i are the thermodynamic forces from above and J_i are the thermodynamic fluxes. These relations have been introduced by Onsager [107]. In case of diffusion, fluxes are changes of density in time.

1.1.2 The Entropy of Interfaces

Kaufmann [70] was the first who applied eq. 1.6 to soft interfaces. Such interfaces occur in lipid membranes, the hydration shell of enzymes, etc. He evaluated thereby the consequences of the 2^{nd}law for such biological systems. However, it was Albert Einstein who pointed out that interfaces (e.g. of a water droplet) have their own entropy [36]. As a consequence interfaces in biological systems exhibit fluctuations in every observable.

The "proper" entropy of lipid membranes and enzymes allows a novel description of nerve pulse propagation and enzyme catalysis [70]. Only the interplay of all thermodynamic variables of such systems within an entropic potential explains the appearance of temperature changes and potential changes in nerve pulse propagation as well as fluctuations of enzyme structure and reaction coordinate.

1.2 Susceptibilities

Generally, the interplay of thermodynamic variables has been well known through the Maxwell relations [20]. In case of the entropy potential they are:

$$\frac{\partial^2 S}{\partial n_i \partial n_j} = \frac{\partial^2 S}{\partial n_j \partial n_i} \tag{1.13}$$

For 2-dimensional interfaces the variables n_i, for instance are the area and a number of particles.

The second derivative of entropy is related to the generalized susceptibilities χ [75, 52, 146]:

$$k_{\mathrm{B}}\chi \equiv k_{\mathrm{B}}\left(\frac{\partial^2 S}{\partial n_i^2}\right)^{-1} \equiv -k_{\mathrm{B}}\left(\frac{\partial n_i}{\partial N_i}\right)_{N_{j\neq i}} = k_{\mathrm{B}}\left(\frac{\partial n_i}{\partial X_i}\right)_{X_{j\neq i}} \tag{1.14}$$

where N_i is defined as the conjugated term of the n_i, e.g., $N_i = \frac{\pi}{T}, \frac{\mu}{T}, ...$

For a 2-dimensional lipid monolayer system with constant temperature $n_i = A$. Then equation (1.14) results in

$$k_{\mathrm{B}}\left(\frac{\partial^2 S}{\partial A^2}\right)_T^{-1} = -k_{\mathrm{B}}T\overline{A}\kappa_T \tag{1.15}$$

where κ_T is the isothermal lateral compressibility of the monolayer:

$$\kappa_T = -\frac{1}{\overline{A}}\frac{\partial A}{\partial \pi} \tag{1.16}$$

It is clear, that the mechanical properties of lipid monolayers represent a measure of susceptibility and therefore a measure of the inverse curvature of the entropy potential. The compressibilities are strongly elevated in the phase transition of lipid monolayers (next section). Therefore phase transitions correspond to high fluctuations.

In bulk experiments the heat capacity c_p can relatively easy be determined as a measure of the uptake of heat. Since $dH = \delta Q + V dp$, at constant pressure c_p is also directly related to the enthalpy H and also to the entropy S:

$$c_p = \left(\frac{dH}{dT}\right)_p = T\left(\frac{dS}{dT}\right)_p \tag{1.17}$$

2 Lipids and Lipid Membranes

The major roles of membranes are their function as a barrier and as carrier for nerve signals. But it also is the place where a whole variety of chemical reactions, catalysed by enzymes, is restricted to a 2-dimensional environment. In the sense of an interfacial description, biological membranes consist of a membrane-protein-hydration layer [70]. The main components of the hydration layers are water, salts and glycerols. From the viewpoint of an interfacial entropy potential, the physical dimensions of the biological membrane are defined by the realization of processes. In other words, the interface is not given by its steric dimension, but through the definition of its potential.

For readings on the physics of membranes the books of Heimburg [57] and Lipowsky & Sackmann [84] are recommended. In the following a short overview on membranes is given. The main focus is going to be a clarification of the thermodynamic perspective on this subject. The section is restricted to pure lipid membranes.

2.1 Lipid Structure and Membranes

2.1.1 Phospholipids

Phospholipids are the most abundant type of lipids determined in biological systems. They are also prevailing in the physical investigation of model systems. The majority of them consist of a phosphate containing headgroup and two hydrophobic fatty acid chains. Usually the head groups belong to the group of phosphoglycerides. This means that the head group and the fatty acid chains are each linked to a hydroxyl group of a glycerol backbone (Fig. 2.1). The various kinds of phospholipids differ in head group, chain length and degree of saturation of their fatty acid chains.

2.1.2 Membrane Phases

Membranes are composed of lipid molecules. Their characteristic nature is the formation of aggregates if they are exposed to water. This behaviour is understood through the hydrophobic effect and the amphiphilic structure of lipids. If the concentration of lipids is very low they form micelles. If concentrations of lipids are

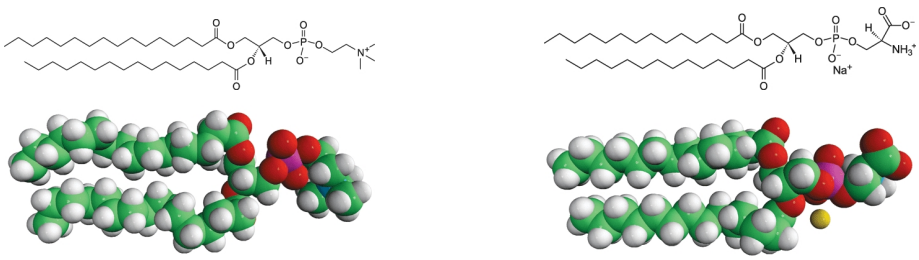

Figure 2.1: Schematic drawings of two phospholipids. DPPC has a chain length of 16 carbon atoms. DMPS has a negative charged head group. The chain length is 14 carbon atoms.

of middle value they form lipid bilayers. This is the most abundant form in biological systems. In high concentrations they build up 3-dimensional structures. At air/water interfaces monolayers are constituted.

In water, lipid bilayers aggregate to spherical shells which are commonly called vesicles. They show distinct phase behaviour, i.e. at low temperatures lipids aggregate to phases with high order and low degree of rotational freedom of the chains. This main phase is called the solid ordered (so) or gel phase (also $L_{\beta'}$) (Fig. 2.2). At high temperatures lipids are disordered with an increased degree of rotational freedom and neglectable lattice structure. The phase is denoted liquid disordered or fluid phase (also L_α).

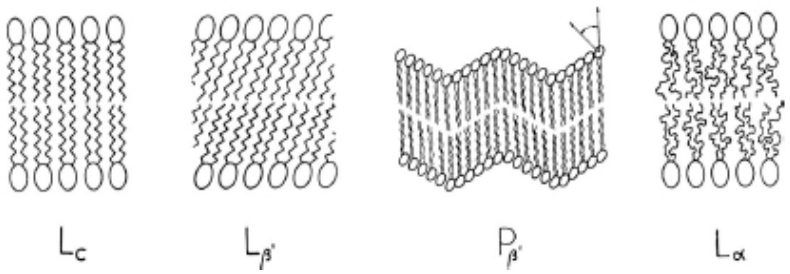

Figure 2.2: Thermotropic phases of phospholipids [84].

At very low temperatures a liquid condensed phase (L_c) has been observed. Between the gel and the fluid phase a ripple phase ($P_{\beta'}$) is found. Both L_c and $P_{\beta'}$ phases exhibit an order behaviour which is comparable to the gel phase. Gel and fluid phases are easy to identify and studied in most times. The transition between these two phases is the main transition of membranes.

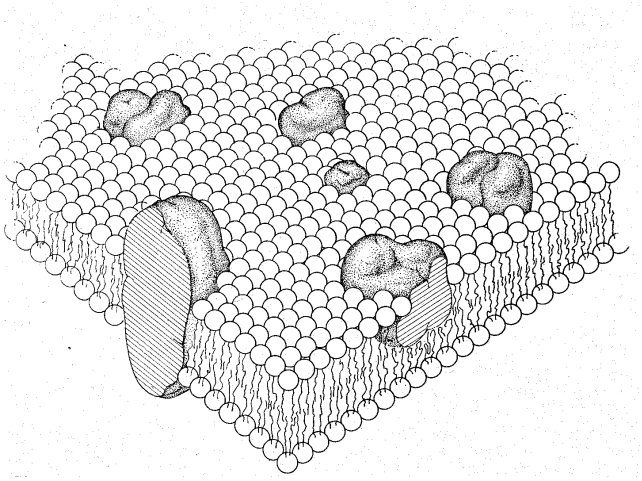

Figure 2.3: Scheme of the fluid mosaic model. Proteins are embedded in a homogeneous see of lipids. The figure was taken from [143].

2.1.3 Head Groups and Charges

The physical difference in head groups is commonly conveyed by their classification in charged and uncharged lipids. In the first case, in nature, only lipids that carry a negative charge are found. Because of this charge their phase behaviour is strongly influenced by any electrical charged compound. In the second case, the uncharged lipids does not carry a netto charge at pH 7. However, the lipids are polarized between the negative pole at the phosphate group and the positive pole at the amino groups. The latter depends on the kind of lipid. Due to the polarization, uncharged lipids are also affected by protonation or shielding through ions [22]. Yet, to a less extend than charged lipids are. This in turn means, that if the pH of the membrane interface is varied strong enough the measured main transition temperature of all lipids is shifted. Changes in the amount of protons within bulk and hydration layer dramatically changes the phase state of lipids. The physical properties of such interfaces are understood much easier if the interfacial parts are considered as one system. Here, this means that pH is implicated as a thermodynamic variable.

2.2 Biological Membranes

According to the famous fluid mosaic model of Singer & Nicholson [143] biological membranes consist of lipid double layers which serve as passive hydrophobic solvent for proteins (Fig. 2.3). This quite simple picture has been redeveloped in several ways: from a physical point of view in numerous studies it has become clear that mechanical properties of membranes, like elasticity and compressibility, strongly

depend on their lipid composition [57, 84]. Moreover, it was found that the lipid compostion is adapted when cells are subject to altered growth conditions. A detailed review on the literature on the latter will be given in section 6.1.

2.2.1 Phospholipid Distribution

Mammalian membranes contain a high portion of phospholipids (40-80% of dried weight) with a very diverse disposition [22]. Thereby, content and composition of phospholipids are highly regulated in cellular membranes. Both properties also differ from cell type to cell type and also within a cell in the different components. Furthermore, lipids are asymmetrically distributed within the two sheets of a bilayer [22]. The most common lipids are those featuring chain lengths of 12 - 24 carbon atomes, where fatty acids with 16 and 18 long chains predominate.

2.2.2 Further Membrane Compounds

Besides phospholipids, a significant amount of sphingolipids is found in most cells. Large concentrations of these lipids are especially occuring in neuron tissue and in membranes of plant chloroplasts [22]. Sphingolipids are build by a sphingosine and a fatty acid.

Out of the class of non-lipids, cholesterol can account for up to 50 mol% of the molecular composition of membranes. It has the tendency to incorporate into the hydrophobic part of the membranes. This characteristic is the reason why cholesterol influences the phase behaviour of membranes in many ways, depending on the lipid system and the concentration of cholesterol (e.g. [22, 29, 64, 87, 159, 97]). For example, at high concentrations it has a dual effect: it condenses and orders the fluid phase and disorders the gel phase leading to some kind of intermediate phase. If biological membranes are studied these molecules need to be regarded

2.2.3 Domains and Rafts

In lipid membranes with only few components, lipids tend to phase separate. In the more complex biological membranes a detailed information on lipid configurations has not been gained yet. However, aspects of ordering and functionality of lipids have been discussed much more intensive through the last years. In particular the possibility of lipid rafts as functional islands in membranes has been taken into account [139, 140]. Rafts are expected to be gel-like lipid structures that float in the fluid phase and accumulate proteins. If so, then the lipid composition defines two phases which could be be identified. Additionally, order parameters can be

defined allowing a physical descriptions of local membrane enviroinments. However, microdomains are supposed to be smaller than 100 nm [139]. Therefore, they are subject to much higher fluctuations and in terms of their size stability interact much stronger with the environment than large domains do.

In the discussion on rafts, also domain-protein structures need do be mentioned. The first who introduced this idea were Mouritsen and Bloom in 1984 [96]. As an extension to the fluid mosaic model they invented the mattress model. Membrane bound proteins were assumpted to attract those lipids in vicinity to their hydrophobic anchor whose fatty acids match best to the protein.

2.3 Critical States of Membranes

In this thesis critical behaviour denominates states of systems in which fluctuations of thermodynamic variables are strongly enhanced. In the following sections a small overview on critical states within single component and biological membranes will be given.

2.3.1 Phase Transitions

The thermodynamic classification of phase transitions is commonly established through types of order. Considering a thermodynamic potential, e.g. the Gibbs Free Energy G, the following properties of transitions were defined: Since a phase transition leads to a change in order, an order parameter η is introduced as an extensive variable. For a phase transition of first order, the first derivative of G resulting in

$$\eta = -\left(\frac{\partial G}{\partial h}\right)_T \tag{2.1}$$

is discontinuous. h is the complementary intensive variable to η. First order transitions are the only transitions that exhibit a latent heat and only here the susceptibilities diverge (next section).

According to the Ehrenfest classification, in a transition of second order, the first derivatives of G are continuous. Here, the second derivatives, presenting the susceptibilits (see 1.14),

$$\chi = -\left(\frac{\partial^2 G}{\partial h^2}\right)_T \tag{2.2}$$

are discontinuous [50]. Phase transitions of higher order are defined analogously.

Since phase transitions points do not represent analytical states, a mathematical description is very difficult. An in part satisfiying theory is the Landau theory of

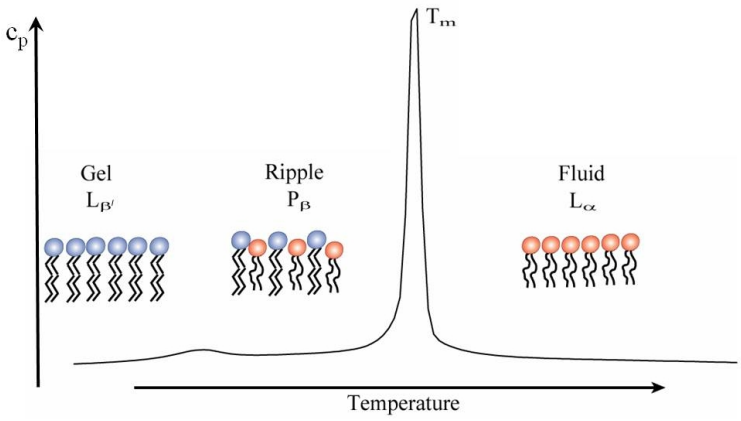

Figure 2.4: Heat capacity (c_p) profile of a single component membrane. The transition is very sharp, indicating a high cooperativity of the melting. Depicted are the main transition as well as the pre-transition to the ripple phase.

phase transition. It is based on the development at the minimum of a thermodynamic potential. The developed parameter is the order parameter η [75]. Landau's theory provides good approximative descriptions of phase transitions. However, it is delimitated to a region outlying to the very near transition range. Within this region fluctuations of the order parameter $\langle \eta \cdot \eta \rangle$ increase strongly. In the product

$$\eta^2 = \langle \eta \rangle \cdot \langle \eta \rangle \tag{2.3}$$

of the developed potential these fluctuations are not included. Therefore, the theory is limited in terms of the characterization of dynamic processes within phase transitions.

2.3.2 Transitions in Single Component Membranes

Phase transitions can be induced by the change of any of the thermodynamic parameters and by varying the lipid compositions. For example, the higher the saturation of fatty acids in lipid membranes the higher are their transitions temperatures. Similarly an increase is observed for longer fatty acid chains. Both mechanisms are especially relevant in cell adaptation.

The main transition of membranes is characterised by the melting from the $L_{\beta'}$ to the L_α phase. In this state an increase of enthalpy and entropy of the lipid bilayer system is observed. One component systems display transitions with high cooperativity (Fig. 2.4), which is demonstrated by a small half width ΔT_h of the heat capacity profile. ΔT_h can be as small as 0.05°C. In the transition region the heat capacity c_p exhibits a distinct maximum which according to equation (1.14) corresponds to high

fluctuations in enthalpy. Through the increase in enthalpy first order transition of vesicles are accompanied by latent heat.

Because of the finite size of vesicles, height and half width of the melting curve are finite. However, being in good accordance with phase transitions classifications, these transitions of real systems can be considered as being of first order. The cooperativity of the transition depends on several factors: the kind of head group, the length of the lipid chains, the degree of saturation, the pH, the ionic strength, the outer pressure and the kind of lipid vesicle. Multilamellar vesicels show higher cooperativity than unilamellar vesicles do.

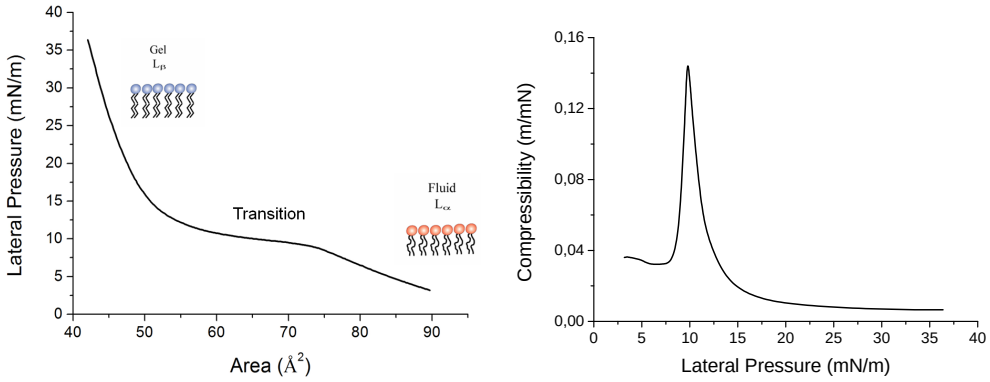

Figure 2.5: Monolayer isotherm (left) and corresponding compressibility κ_T (right) of DPPC measured at 24 °C. κ_T is strongly increased in the transition range. This means that the monolayer is very soft in this region.

Besides vesicles, lipid monolayers are a common tool to study membranes. Such layers go through distinct transitions between liquid condensed and liquid expanded states when the films are compressed (Fig. 2.5). Similar to vesicles the transitions can be very narrow and can lie within a pressure range of few mN. In the transition range the compressibility κ_T is strongly increased corresponding to high fluctuations in the monolayer area (see equation 1.14 and [146]). However, it is necessary to mention that the transition plateau has its theoretical origin in the maxwell construction [20]. Essentially, the measured transition is macroscopic averaged on a large number of monolayer lipids.

Melting of lipids results in an increase of the membrane volume of about 4 %. In parallel the area is increased as much as 25 %.

2.3.3 Critical Behaviour of Biological Membranes

Biological cell membranes show interesting critical phase states which are comparable to those measured in synthetic lipid mixtures.

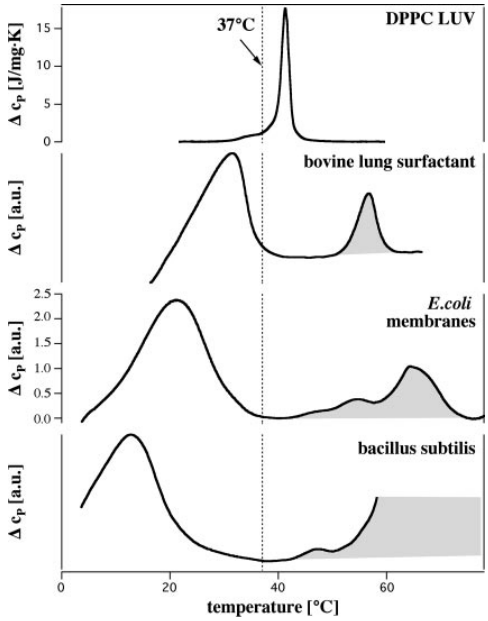

Figure 2.6: Several heat capacity profiles are compared: artificial unilamellar DPPC vesicles, bovine lung surfactant extract, E. coli membranes and B. subtilis membranes. The dotted line indicates the growth temperature at which cells were grown and it represents also the body temperature of bovine of 37°C. Grey shaded regions indicate irreversibel dentauration of proteins. The figure was taken from [58].

As aforementioned, bacteria and yeast change their lipid composition when environmental parameters have been changed. An elegant way to measure this effect is calorimetry where it has been found that whole cells as well as their purified lipid membranes exhibit a maximum in the heat capacitiy [58, 17, 145]. In Fig. 2.6 several heat capacity profiles of biological membranes are compared. Contrary to one component systems (here DPPC) these maxima are broadened and exhibit a total width of 5 -25 °C. As measured for bacterial cells, the growth temperature is usually above but close to the transition peak. If the cells are grown at lower temperatures the peak is also measured at lower temperatures. Examples will be given in chapter 6.

Water and other fluids exhibit a critical point T_c. At and beyond T_c two once separated phases are indistinguishable and become the same. High termally driven fluctuations occur in this region and lead to the phenomenon of opalescence. Interestingly, comparable critical points have also been found in giant plasma membrane vesicles (GPMVs) of rat cells [158, 60, 7]. The authors detected critical transition in GPMVs with temperatures in the range of 15 to 25 °C. The critical states superimpose well with those from synthetic membranes of multiple lipid components [60, 157, 8]. A single liquid phase at high temperatures was observed which separates into two

coexisting liquid phases below a transition temperature. Within this critical range the line tension approaches zero. Consequently steric correlation lengths of fluctuations increase to high values of > 1 μm within ~ 0.5 °C around the transition point. The importance of these results is the fact that although plasma membranes consist of a big variety of lipids they do show distinct phase behaviour.

Both adaptation of the membrane phase transitions and the occurance of critical points indicate a crucial role of membrane phase states and fluctuations in biological functioning.

3 Enzymes

Biological enzymes are proteins that accelerate chemical reactions while not changing the equilibrium of the reaction. Repeatedly Nobel prizes have been awarded for important steps in the understanding of catalysis. However, although being a well known and thoroughly studied phenomenon the underlying mechanisms of catalysis have remained mysterious. In particular, paradox effects are not understood. One of those apparently paradoxal effects is that high substrate specific enzymes belong to the fastest enzymes.

van't Hoff (1884) and Arrhenius (1889) found a relationship that gives the exponential dependence of the rate constant k of chemical reactions on the temperature T and on the activation energy E_a:

$$k = F \cdot \exp(-\frac{E_\mathrm{a}}{k_\mathrm{B}T}) \tag{3.1}$$

F is a pre-exponential factor that shows a weak temperature dependence and that covers the number or frequency of collisions that take place between the reactants. E_a is termed as the potential barrier that has to be overcome to start the chemical reaction (Fig. 3.1). E_a can hardly be specified in detail. It is the parameter that decreases when enzymes catalyse reactions. E_a can be gained by the arrhenius plot of E_a from eq. 3.1.

The goal of the chapter is a small survey on the basics of catalysis followed by the presentation of the novel theory of catalysis of Konrad Kaufmann. Finally the effect of membranes on enzymatic reactions is shortly reviewed.

3.1 Kinetics and Single Enzyme Fluctuations

3.1.1 Michaelis-Menten Kinetics [40]

In 1913 Michaelis and Menten published a kinetic theory of enzyme catalysis which has been validified in unnumerable experiments. One assumption in the theory is that the concentration of enzyme [E] is neglible compared with that of the substrate. Experimentally, it has been found that the reaction rate ν is linear in time as long as

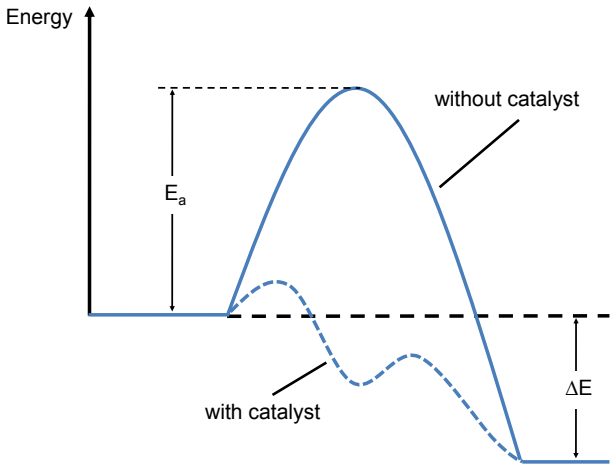

Figure 3.1: Energy diagram of the progress of a chemical reaction. A catalyst decreases the activitation energy E_a leading to an increase in the reaction rate.

the substrate concentration [S] is small. At high substrate levels the kinetic saturates to a maximal value $V_{\max}$ (Fig. 3.2). This is expressed in the Michaelis-Menten equation:

$$\nu = \frac{[E]_0[S]k_{\text{cat}}}{K_{\text{m}}} \tag{3.2}$$

where K_{m} is the Michaelis constant, with $K_{\text{m}} = \frac{1}{2}V_{\max}$.

For the simpliest reaction of a substrate S into a product P the underlying mechanism was described by introducing a transition state ES:

$$E + S \overset{K_{\text{s}}}{\rightleftharpoons} ES \overset{k_{\text{cat}}}{\longrightarrow} E + P \tag{3.3}$$

As indicated in the scheme, two processes are distinguished. First, the enzyme and the substrate combine to a noncovalently bound enzyme-substrate complex, ES, which is also termed the Michaelis complex. The combining step takes place rapid and reversibel. Schematically the ES complex is depicted through the local minimum in the dotted line of Fig. (3.1). The chemical processes then occur in a second step with the turn over number k_{cat}. This second step usually is the rate limiting step of the reaction and is considered as being irreversibel. However, of course their is also an enzyme-product complex, EP, which is necessary for the reverse reaction. But the dissociation of EP takes place very fast and therefore causes slow overall reverse processes. EP and the reverse reactions are ignored in most reactions.

The concept of an ES complex is fundamental in the modern understanding of the mechanism of enzyme catalysis.

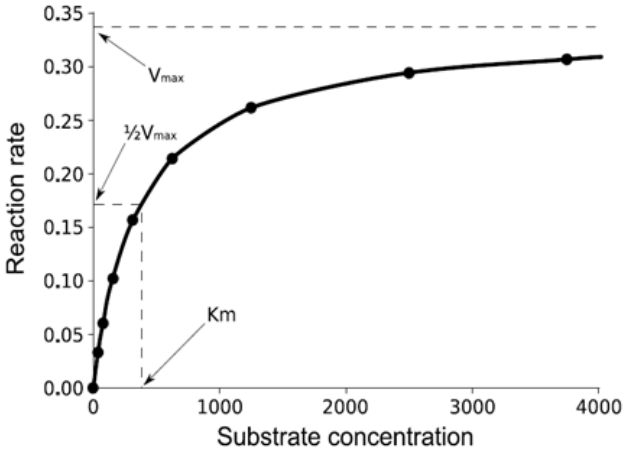

Figure 3.2: Characteristic substrate dependence of the reaction rate ν in the Michaelis-Menten kinetics. ν saturates at high values of [S]. The Michaelis constant K_{m} is defined as the substrate concentration at which ν is half the maximum value V_{max}.

3.1.2 Single Enzyme Fluctuations

Different approaches are supposed to gain more insight into catalysis. One is to determine the three dimensional structure of the enzymes. Usually this is established by x-ray and neutron diffraction of crystalline molecules [40]. The methods allow a very detailed insight into the steric structures of proteins down to sub-nanometer resolutions. However, through crystallization there is no possibility to get information on the dynamics of protein folding or catalysis.

A milestone in enzyme studies was set when in the 1990s technical development has lead to single enzymes measurements [33]. Using fluorescent correlation spectroscopy the group of Rigler [162] observed conformational fluctuations of single DNA molecules. The authors emphazised that the detected conformational fluctuations are very similar to the current fluctuations seen in single ion channel molecules.

Not much later fluctuations in enzymatic turnovers of single molecules were detected (Fig. 3.3) [31, 85]. The authors detected statistical distributed on- and off-times at which the enzymes catalyze or not. The duration of single on times were shown to decay exponentially (more short than long on-times). Changes in substrate concentration showed that single enzymes exhibit Michaelis-Menten behaviour. The results indicate a crucial role of statistical processes in catalytic reactions.

Despite the appearance of a variety of explanations, the role of fluctuations in catalysis is one of the hot topics in current research [30, 91, 92, 116]. For further readings on enzyme catalysis several nobel prize lectures are recommended (www.nobelprize.org),

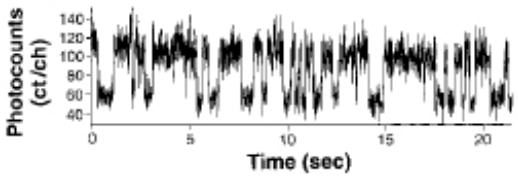

Figure 3.3: Fotocounts of fluorescent light emitted from the active site of cholesterol oxidase. The signal corrsponds to the enzyme activity. Fluctuations in on- and off-times are clearly detected [85].

e.g. the lecture of Gerhard Ertl 2007.

3.2 On Konrad Kaufmann's Theory of Catalysis

The following short summary of the theory of catalysis of Konrad Kaufmann is mainly derived from personal communication with him and with Matthias Schneider. Briefly it is tried to outline Konrad Kaufmann's theory as far as it was understood. It must be emphasized that it is the authors representation and that the interested reader should contact Dr. Kaufmann directly or consult his published work [70].

Konrad Kaufmann has perpetuated Einsteins Entropy formulation and applied it to the interface itself. He coined the term "the proper entropy", to point out that choosing the correct system, here the entropy of the interface, is a crucial step in thermodynamics. To consider the interface as an independent system goes back to Einsteins first publication in 1901, where he showed, that a water droplet has its own heat and entropy [36]. In Konrad Kaufmann's theory the second law in Einsteins entropy potential formulation [35] stands at the beginning and every system has to obey it. The observers viewpoint, e.g. the course of the process in space and time, is irrelevant and can indeed easily induce misleading conclusions.

3.2.1 Proper Entropy

It is crucial to first choose the proper entropy of the interface (section 1.1.2). Equivalent to lipid membranes also proteins represent interfaces: the interfacial (sometimes called surface bound) hydration layer. Importingly, also the reactive adsorbant (A), which is commonly named the substrate, is a crucial part of the interface. Only together do they define the state of the system $S(n_i)$. $n_i = n_{\mathrm{ad}}$ represents the interfacial reaction coordinate of the adsorbant-surface interface.

When A (the substrate) adsorbes to the surface (enzyme) it becomes part of it and in general will accommodate a state different from the state prior to adsorption.

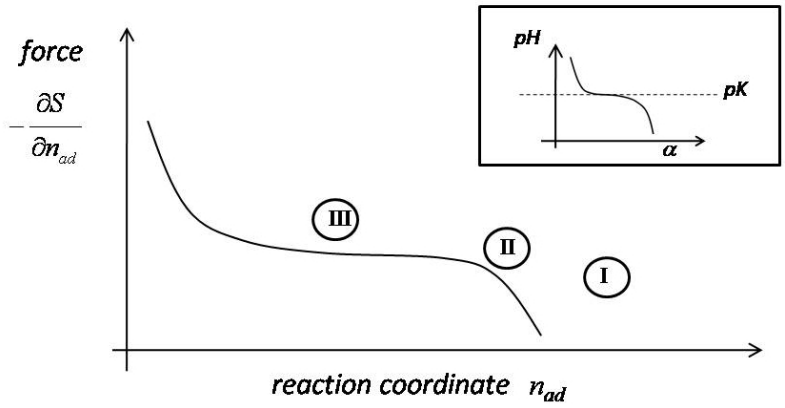

Figure 3.4: State diagram of a molecule-adsorbant interface. Some adsorbants lead to critical states (III) with high fluctuations. In the case of pH the critical state is at the pK of an interface (inlet). At $pH = pK$ protons fluctuate maximal. This is commonly also expressed as the state at which the protonation α is half established. See also text.

Only in some cases the reactive adsorbant A will induce a "near-critical" state of the interface. It will be seen that it is this induction of a critical state, what justifies the term "catalysis". In Fig. 3.4 this state is indicated with III. In general, thoses states (III) correspond to a flat entropy potential with high fluctuations (Fig. 3.5). Marked with I and II are noncritical states which represent e.g. the binding of inhibitors or less specific substrates to the protein.

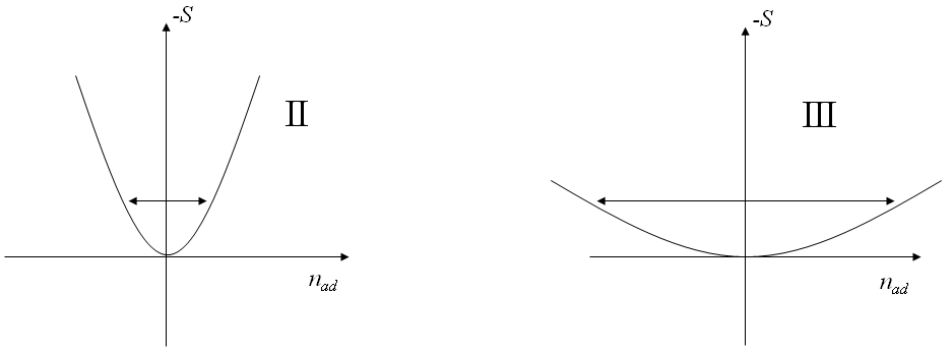

Figure 3.5: Entropy potential at different regions of the state diagramm from Fig.3.4. Without adsorbant the entropy potential is rather steep (left), whereas in critical states, induced e.g. by an adsorbant, the entropy potential exhibits a low curvature corresponding to high fluctuations (right).

A nice example of this abstract concept is the protonation of molecules (Fig. 3.4), for instance of a protein site or a lipid head group. At $pH = pK$ the highest amount

of protons is found to be distributed between being bound and being not bound to the interfacial molecules. This means that fluctuations in interface protonation are maximal (critical). Walking along the titration curve (Fig. 3.4) indicates this behaviour.

3.2.2 Diffusion Analog

The depicted scenario is perfectly in line with the origin of diffusion in the fluctuation-dissipation-theorem (FDT) formulated in 1905 by Albert Einstein [34]. There, Einstein states that fluctuations in displacement x are proportional to the diffusion constant D and the time t:

$$\left\langle (\delta x)^2 \right\rangle \propto Dt \tag{3.4}$$

This result is transferred to enzyme catalysis where now the rate constant k is equivalent to the diffusion constant D. The fluctuations in the interfacial reaction coordinate are proportional to the rate and the time:

$$\left\langle (\delta n_{\mathrm{ad}})^2 \right\rangle \propto kt \tag{3.5}$$

Since the fluctuations are directly proportional to the inverse in the second derivatives of $S(n_i)$, both D and k increase when the curvature of S decreases. Note that time in Einsteins paper [35] was introduced after the implementation of the entropy. Time is not a priori and does not affect the entropy potential. It is the observers choice to count the time it takes until the distribution of particles is homogeneous or until a certain concentration of products are formed. The origin, however, of these rates are fluctuations given by the 2^{nd} derivative of the entropy potential and when these are critical the process is named *catalysis*.

The "pseudo"-irreversible character of the process in 3D, mentioned above, is well-known and for the case of diffusion resolved as follows: Imagine a little drop of ink in a large swimming pool. Although the fluctuations in displacement x (eq. 3.4) are completely reversible, there is a net flux of particles away from the center of the ink-drop. The reason is, that the moment where the ink and the water (or the adsorbant and the surface) "combined", a very unlikely state of the 3D -ink/water or 2D-surface/adsorbant system, respectively, was created. In the language of the entropy potential, all states "collapsed" into one (e.g. the droplet) far away from the centre, where $\frac{\partial S_{3D}}{\partial x} = \frac{\partial S}{\partial n_{ad}} = 0$. In time the system simply adapts the more likely states. The lower the curvature of S, the more rapidly the system adapts to the final distribution of states (equivalent to a higher D or k, respectively). Until now, intentionally the common terminology of catalysis has been avoided, as it was the intention to "derive" it from the theory presented. In this respect, the reactive

adsorbant A is what is called the substrate, while the interface, when exhibiting large fluctuations, is the catalyst. The rate constant decreases as a consequence of the FDT (eq. 3.5) and does not require any additional assumptions or the lowering of any energy barriers.

The reversibel transitions in an enzymatic reaction are summarized as follows:

$$\begin{array}{ccc} EA & \longleftrightarrow & EP \\ \updownarrow & & \updownarrow \\ A & & P \end{array} \tag{3.6}$$

3.2.3 Specificity [70]

The paradox correlation, between high substrate specificity and rate disappears in the theory of Kaufmann: It originates in the bare fact that the critical state of the interface is specific in itself. Theoretically speaking, it is just one point when two variables span the phase diagram, i.e. only one individual combination of the two variables will “induce” this state exactly. The situation becomes increasingly more specific as the number of variables increases (e.g. π, T, pH, μ_{ions} etc.). From a practical perspective, it seems indeed only reasonable to talk about a certain regime near a critical point (or phase transition) rather than “the" point. The picture of a n-dimenional phase diagram also implies that catalysis can be optimized. Varying e.g. the pH, salt concentration or temperatures should change the catalytic activity, with, for instance, different maxima at different temperatures.

3.3 Membrane-Enzyme-Interaction

Membrane bound enzymes are commonly classified in integral bound and peripheral bound proteins [57]. The first class of proteins contains a large amount of hydrophobic regions. The regions enable it to span through the lipid membrane and structures the membrane by hydrophobic matching. The latter means that proteins are surrounded by those lipids that match best with the hydrophobic chains of the protein [79]. The second class describe the peripheral proteins. They are attached to the surface of the membrane. This binding generally involves electrostatical interactions. In both classes the proteins can influence lipid membranes. Experimentally, shifts in the heat capacity profile to lower or higher temperatures are observed.

A crucial question is, wether not only proteins do influence membranes but also membranes impact proteins and enzymes in their functionality?

It is well-established that various membrane-bound enzymes function only if they are embedded in an adequate lipid environment [49, 67, 74, 124, 129, 130]. Activities of

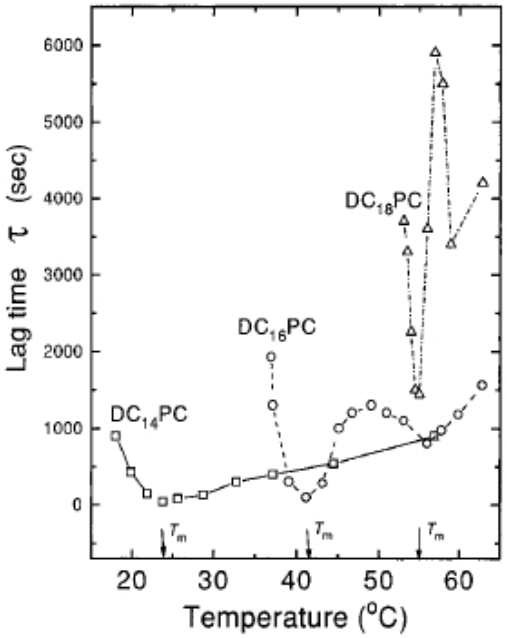

Figure 3.6: Lag time τ of Phospholipase A2 activity as a function of the reaction temperature in the hydrolysis of large unilamellar vesicles of several phospholipids. τ exhibits a minimum when the membrane is in the phase transition regime [61].

several enzymes exhibit a kink in the Arrhenius plot at temperatures which are at or close to the transition temperature of the surrounding membrane matrix [17, 74, 124]. The kink denotes a change in the activation energy E_a (see also eq. 3.1) of the enzmye. For further readings see also the books of Kates & Kuksis as well as Poste & Nicolson [69, 115].

The most striking results were found in the ubiquitous Phospholipase A2 (PLA2) which hydrolyses phospholipids into 1-acyllysophospholipids and fatty acids. The activity of PLA2 exhibits a distinct maximum and a minimal lag time is observed when the surrounding membrane is in its phase transition regime (Fig. 3.6) [3, 61, 109, 110]. Up to now this correlation has been drawn back to the necessity of lipid phase boundaries at which PLA2 is active [61, 68, 80, 141].

4 Methods

A comprehensive picture on the topic of membrane adaptation and membrane-enzyme interaction was gained by measuring the relevant thermodynamic parameters. For this purpose mainly quality standard methods were applied, including calorimetry and black lipid membranes as well as the detection of enzyme activity in lipid monolayers. For the latter, a langmuir-trough-photometer setup was constructed. In addition, several extraction methods were tested to get lipids from cells. Cell adaptation studies were performed in a temperature regulated microscope-cell chamber.

4.1 Differential Scanning Calorimetry

4.1.1 Calorimeter

All substances possess susceptibilities such as heat capacity. In order to detect the heat capacity of lipid systems Differential Scanning Calorimetry (DSC) is one of the most powerful tools. It allows the measure of endothermic as well as exothermic processes in liquid environmens.

In principle, the device consists of two identical chambers. A reference cell is usually filled with water or buffer and the a sample cell is filled with the biological sample/buffer solution. The temperature of the chambers is changed at a constant rate. The temperature difference is kept zero. By measuring the power difference between reference and sample substance one gets a direct reading of the excess heat capacity Δc_p.

Experiments were performed in a VP-DSC from Microcal (USA). In the case of extracted lipid membranes a sample/buffer solution was measured and substracted by a buffer/buffer curve.

4.1.2 Vesicle Preparation

In order to obtain small unilamellar vesicles (SUVs) the following procedure was applied: Chloroform was evapurated from lipid chloroform solutions and subsequently kept in an excicator for at least 3 hours. Afterwards, water or buffer was added in

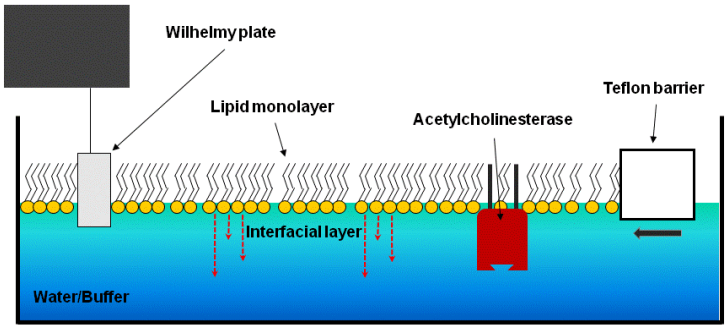

Figure 4.1: Scheme of a Langmuir trough film balance. Lipids are spread on a water or buffer surface. An interfacial layer is formed by the lipid monolayer and adjacent water or buffer, respectively. The surface pressure is detected via a Wilhelmy plate and the area is controlled by a barrier made of teflon or delrin®. AChE was incorporated in the monolayer by dropping a small buffer dissolved amount of it onto the surface.

a proper amount and samples were kept in a waterbath for 2 hours. The adjusted temperature should be above the main transition temperature of the lipid membrane. During this process the solution was shaken vigorously several times to detach lipids from the glass wall. In order to achieve uniform vesicles of size of 50 nm - 100 nm, the suspension was ultrasonicated for 10 minutes in a tip sonicator (e.g. [102]).

4.2 Langmuir Trough - Photometer Hybrid

Langmuir monolayers are lipid films spread on a surface of water or buffer. Due to the amphiphilic nature of lipids the hydrophobic lipid tails are exposed to the air and the hydrophilic headgroups are directed into the subphase. The area of such monolayers is controlled by moving a barrier. In order to parallely detect state diagramms of lipid-enzyme monolayers and activity of AChE parallely, the Langmuir trough (film balance) was extended with a photometric setup (Fig. 4.2 and 4.1).

4.2.1 Monolayers

All experiments were performed on filmbalances from Nima [103]. The trough used in the enzymes studies features a maximum area of 289 cm^2. In some experiments the measurements were performed on a second Langmuir trough of 545 cm^2. The barriers to compress the films were made of teflon or delrin® (polyoxymethylene). Due to its hydrophilicity, delrin decreases the loss of drowning lipid compared to teflon barriers. In addition, in order to prevent contaminations of the monolayer by air flow and dust particles a plexiglas chamber was constructed around the apparatus.

As a monotonic function of area the lateral pressure increases when the film is compressed. The surface pressure of a monolayer, π, is defined as the change in surface tension of the interface [103]:

$$\pi = \gamma_0 - \gamma \tag{4.1}$$

where γ_0 is the surface tension of the subphase without lipid. This value is 72.8 mN/m, corresponding to a clean and pure water surface. γ is the value of surface tension in the presence of a film of molecules and exhibits a value lower than γ_0.

The lateral surface pressure π is recorded by weighing a filter paper (Wilhelmy plate) which penetrates into the water. Since in all experiments the pressure was set to zero before spreading the films, the surface tension is $-\gamma = \pi$. In this case

$$\gamma = \frac{F}{2(w+t)}, \tag{4.2}$$

derived from full wetting considerations of the Wilhelmy Plate [103]. F is the force acting on the paper and the denominator describes the size of the front and the back areas of the Wilhelmy Plate.

The preparation of monolayers was accomplished as follows: lipids dissolved in chloroform solution were spread onto the surface. In single component lipid monolayers a typical amount of about 3 μl from a 10 mg/ml solution was used. The volume of extracted lipids from cells varied depending on the extraction protocol and will be given in the results part. After spreading the chloroform was allowed to evaporate for at least 15 min prior to any further treatment or the start of experiment. All commercially purchased lipids were from Avanti Polar Lipids [4] and were used without further purification.

Determination of both area and lateral pressure yields the isothermal state diagrams of the monolayers at constant temperature. The compressibility of the monolayers was calculated following eq. 1.16:

$$\kappa_T = -\frac{1}{\overline{A}} \left(\frac{\partial A}{\partial \pi} \right)_T \tag{4.3}$$

While performing the experiments, the measured raw data were stored on a computer. Excepting, when additionally the pH was measured, the values were noted manually. The setup also allow the control over temperature by connecting a waterbath to the filmbalance: Three metal plates were fixed at the bottom of the trough to establish a homogeneous heat flow.

Everytime, before and after experiments the Langmuir trough was thoroughly cleaned with isopropanol or ethanol. Subsequently, it was rinsed with clean water at least 4

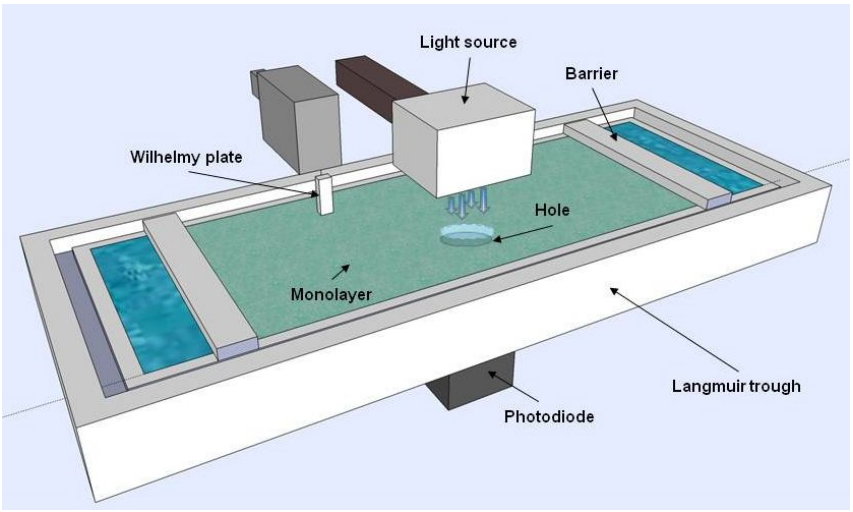

Figure 4.2: Scheme of a Langmuir trough with additional photometer. The activity of AChE was measured by absorption through the central hole

times. The syringe for spreading lipids on the water surface was cleaned at least 10 times with pure chloroform.

4.2.2 Detection of Enzyme Activity

AChE-activity was measured using Ellman's solution [37]. This assay consisted of a dye turning yellow when product was formed. The formation of dye was detected by using a blue light source (412 nm) which was mounted above the Langmuir trough. Subsequently absorbtion was detected through a hole in its central part. Transmitting light was recorded using an amplified photodiode which was installed underneath the central hole. The signal from the amplifier is proportional to the intensity of the light and is read out and transferred to a computer. Using the basic law of absorption

$$E = \epsilon cd, \tag{4.4}$$

where E = Absorbtion, ϵ = coefficient of extinction, c = concentration of dye in solution and d = thickness of dye layer and also $E = log(I_0/I)$, the rate of activity equals the concentration per time unit. For the Ellman's solution (TNB), $\epsilon = 13600$ cml·Mol^{-1} at 412 nm [37].

The incorporation of Acetylcholinesterase took place as following: enzyme dissolved in buffer (20 mM Tris or phosphate buffer, 100 mM NaCl, varying pH) was dropped onto the monolayer surface. A volume of the order of 1 μl including $\sim \frac{1unit}{1\mu l}$ Acetylcholinesterase was used. Several slightly altered procedures were applied and

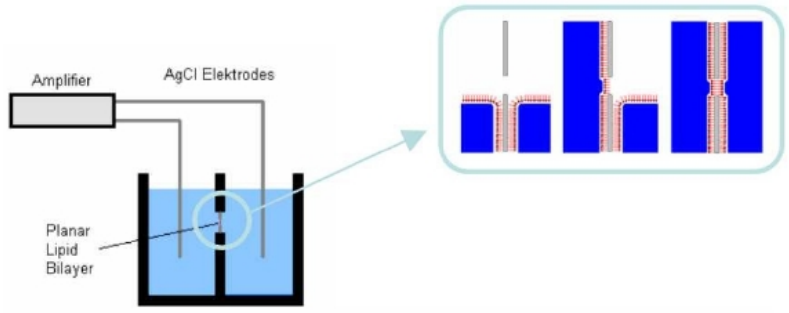

Figure 4.3: Scheme of a BLM setup. Lipids are added to the water surface. By raising and lowering the water levels a bilayer is formed.

will be stated in the relevant sections.

4.3 Black Lipid Membranes

Black Lipid Membranes (BLMs) are free standing bilayers. The method exhibits a very useful tool to study permeabilites of lipid bilayers.

The setup consists of two cells which are separated by a teflon film of about 25 μm thickness. These two cells are connected by a small hole with a diameter of approximately 100 μm. Each of both cells features tiny paths bridging into side chambers that enable external access in order to smoothely fill and empty the main chambers with liquid. Ag-electrodes for current measurements are placed in the side compartements as well. The current is detected, amplified and recorded on a PC. The whole chamber is embedded into a copper block which is connected to a temperature regulated waterbath.

The following protocol to obtain free standing bilayers was applied: The teflon chambers were cleaned with isopropanol and then rinsed by ultrapure water. 5% Hexadecane dissolved in Pentane was prepainted around the hole in the center. Due to its hydrophobicity, Hexadacane supports formation of lipid bilayers. After Pentane has evaporated, the electrolyte (usually NaCl, c = 200mM) was filled into the chambers below the hole. Subsequently, lipids dissolved in Chloroform were spread onto the water surface. An volume of the order of 10 μl from a 10 mg/ml solution was used. The amount of spread lipid leads to a calculated area which is in the order of 500 times larger than necessary to cover the water surface, yielding a highly multilamellar stack of lipid layers in the trough. Before experiments were started the Chloroform was allowed to evaporate for 15-30 min. The described method is also called the Montal-Müller-technique [95].

A low voltage of 5 mV was applied between both chambers and in parallel the current was detected. Then, the water level in the compartements was raised and lowered across the hole. The existence of a bilayer membrane is indicated by a strong decrease in the measured current. If a bilayer is formed then a triangular potential applied to the electrodes leads to a rectangular current curve. The latter shows a proportionality to the capacity of the membrane.

Using the well known relation of charge Q_B, capacity C and voltage U

$$Q_B = CU, \tag{4.5}$$

and $\frac{d}{dt}U = const.$ The capacitiy does not change in time, thus the measured current (I) directly leads to the capacity:

$$I = \frac{d}{dt}Q_B = U\frac{d}{dt}C + C\frac{d}{dt}U = C\frac{d}{dt}U \tag{4.6}$$

4.4 Cell Growth

4.4.1 Human Cells

Human cells were cultivated using standard protocols including an atmosphere of 37 °C and 5% CO_2. For adaptation studies the temperature of the incubator was set to lower or higher values in the range of 28.5 °C - 39 °C. Five different human cell lines were used: HaCat and MV3 [156] cells, which were provided from Prof. S.W. Schneider, University of Manheim. MCF-7, Hep G2 and HEK-293 cells, which were provided from Prof. Ntambi, University of Madison Wisconsin, USA. A short summary of the characteristics of the cells is given in table 4.1. The culturing protocols are similar for all cell lines: HaCat cells were trypsinized for 20 min, all other cells were trypsinized for 5 minutes. Subsequently, cells were seeded in concentrations of 1:3 - 1:10 and grown in cell incubators of the Galaxy class from Brunswick [18].

4.4.2 Bacterias

Pseudoalteromonas Haloplanktis (PH) are arctic sea water bacterias (e.g. [147]) and are known for their distinct ability of chemotaxis. The cells grow in bulk media (Tryptic Soy Broth) and do not adhere to walls. In order to prevent sedimentation PH were grown on a shaker.

Celline	Origin	Culture medium	Further comments
HaCat	skin	RPM1 1640	robust cells
MV3	melanoma	MEM	mechanically soft cells
MCF-7	breast cancer	RPM1 1640	high expression of SCD
Hep G2	liver	RPM1 1640	medium expression of SCD
HEK-293	embrionic Kidney	RPM1 1640	low expression of SCD
PH	bacteria	Tryptic Soy Broth	chemotactic activity

Table 4.1: List of cells used in the experiments. Standard media were used, whereby all media for human cell lines were supplemented with Fetal Bovine Serum (FBS, 10%) and penicilline/streptomyzin (1%). SCD = Stearoyl-CoA-desaturase.

4.4.3 Stage Top Incubator

Cell growth was long time monitored optically in a stage top incubator from Ibidi [63]. The incubator chamber consists of two independent heating plates and contains a temperature sensor. The lower plate in the setup is adjusted to the growth temperature, eg. 37 °C, the upper plate is regulated to about 4 °C higher temperatures. The measure of temperature took place prior to each experiments by an external thermometer. The chamber is connected to a gas flow mixer in which air is enriched by 5% CO_2. Temperature as well as CO_2 enriched air flow are regulated from a controler device. The incubator was mounted onto an inverted microscope from Hund [59]. Cells were seeded and grown in μ-Dishes from Ibidi. Pictures were taken automatically every few minutes and stored on a PC. The number of cells in each flask was counted manually on a PC.

While performing experiments, it was found that the purchased setup featured inhomogenities in the temperature distribution within the μ-dishes. Central parts of the chamber are more exposed to the environment and feature a 1-2 °C lower temperature than the boundary regions do. Furthermore, the microsope lamp accounted for temporal slightly irregular heating of the chamber. The setup was modified by inserting isolating teflon stripes on the bottom of the chamber and by replacing the lamp by a diode. All detected properties were regarded in the analysis.

4.5 Extraction of Membranes and Desaturase

4.5.1 Extraction of Membranes

Several methods were tested in order to extract lipids from cells. Out of the standard protocol the Bligh & Dyer method [13] as well as the similar Folch method [43] gave best results in terms of reproducibility. The Folch method was applied as published in the original paper, the Bligh & Dyer method was slightly modified: 7 cell culture flasks of 175 cm^2 capacity (T175) where grown to confluence. 3.75 ml of Chloroform and Methanol were added to the cells with a ratio of 1:2 (v/v) for each 1 ml of concentrated cell solution and vortexed. The samples were centrifuged at 14000 RPM for 10 min leading to a separation in a two phase system. The upper liquid phase was withdrawn before 1.25 ml of chloroform was added. The mixture was vortexed and 1.25 ml of deionized water was added and vortexed again. Then the sample was centrifuged at 14000 RPM for 30 min to separate liquid and aqueous phases. Only the lower phase which contains chloroform dissolved lipids was withdrawn.

4.5.2 Extraction of Microsomal Desaturase

Desaturase (see section 6.5) is strongly bound to its lipid environment. Therefore, a purification of the enzyme has not been established yet. However, Desaturase bound to lipid vesicles can be separated from cells by differential scanning centrifugation:

Cells were trypsinized and washed in a 0.1 M phosphate buffer (pH 7.2). After the last washing step, the centrifuged pellets were suspended in buffer to a ratio of about 1:10. The cell suspension was cooled on ice and homogenized in a mincer. Subsequently the solution was centrifuged at 10000 g for 15 minutes at 4 °C. The supernatant was withdrawn and protease inhibitors were added to prevent denaturation of the Desaturase. After centrifugation at 100000 g for 60 minutes, the pellet was again suspended in 1 ml of phosphate buffer. It is important to keep the temperature low to prevent degrading reactions.

The concentration of protein in the microsomes was determined by means of the Bradford assay [16]. The amount of Desaturase was set proportional to the amount of all microsomal proteins. The solutions were subdivided into small aliquots and shock frozen in liquid nitrogen. Long time storage took place at -80 °C.

Part III

Results

5 Phase State Dependent Activity of Acetylcholinesterase

One of the most important findings in the research of membrane-enzyme interaction was the decrease of the activation energy in several membrane bound enzymes when the lipid membrane was heated through the phase transition.

In the present part of the thesis membrane phase state dependent enzyme activity was studied on Langmuir monolayers. A thoroughly investigation of the thermodynamic properties of Acetylcholinesterase-membrane systems was performed and for the first time revealed that the activity of this enzyme correlates to the phase state of the monolayer. The activity exhibited a maximum when the monolayer was in the transition region. The only theory capable to explain the results appears to be the one from KK presented in section 3.2.

After an introduction to the Acetylcholinesterase, a short recapitulation of its properties in the presence of membranes is given. The experimental results are then evolved starting from binding and pH considerations which are then followed by the presentation of invariant maximum activity of AChE in lipid monolayers. The new findings are discussed within the theory of Konrad Kaufmann.

5.1 The Enzyme Acetylcholinesterase (AChE)

Acetylcholinesterase is one of the fastest enzymes known in biological systems where it features a crucial function in the propagation of nerve signals.

5.1.1 Biochemistry of Acetylcholinesterase

Acetylcholinesterase (AChE) is mainly found found in neuromuscular junctions and in cholinergic synapses (e.g. [86, 46, 150, 121]), but also in erythrocytes (were its function is not understood yet) [45, 25, 111, 112, 1, 6]. According to the present model of nerve propagation, its function is to terminate the synaptic transmission of nerve propagation signals by hydrolising the neurotransmitter Acetylcholine (ACh) into an acetate and a choline within the synaptic cleft [101]:

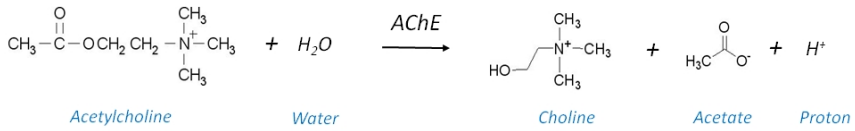

Importingly, the reaction also requires a water molecule on the substrate side and a proton is released on the product side. Since this process takes place with a turn over number $\gtrsim 14000\text{s}^{-1}$ [125], AChE is one of the fastest enzymes known in biology. Depending on the particular type of the enzyme, an AChE monomer exhibits a huge molecular weight of $M_{AChE} \sim 60$ - 80 kDa [46, 122, 86]. The acitive site of the enzyme is buried inside the protein and is connected to the outer part by an often so called "gorge" [138]. The site contains the "catalytic triad" residues Ser 200, Glu 327 and His 440.

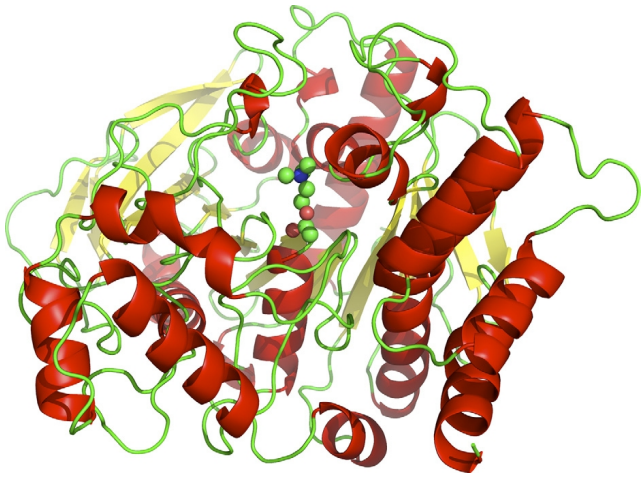

Figure 5.1: Ribbon diagram of the active subunit of AChE from *Torpedo californica*. Balls and sticks represent ACh which is docked in the active site. The picture was taken from [138].

AChE occurs in multiple molecular forms differing in their quaternary structure and mode of anchoring to membranes [137]. These forms are generally subdivided into A and G forms. The A (asymmetric) forms contain an up to 500 nm long anchor at which the enzyme is attached to membranes, whereas the G forms (globular) lack this anchor. Both types occur with one, two or four catalytic subunits, with dimers being the most abundant forms. All types can differ in their hydrophobicity causing varying solubilities of the enzymes. However, despite the variations in structure, no differences in their catalytic subunits have been detected illustrating that the catalytic subunit is highly conserved.

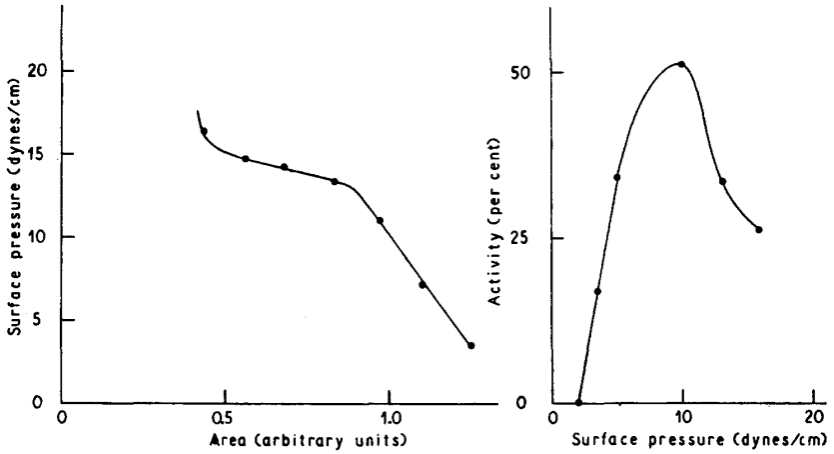

Figure 5.2: Pure AChE-monolayer experiments performed by Skou [26]. Left: Relation between surface pressure and area of the purified protein. A plateau similar to lipid isotherms was observed. Right: Ache activity of the surface-spread protein at varying surface pressures. Skou detected a maximum in activity close to the transition pressure. The figure was taken from [26].

5.1.2 AChE-Membrane Interaction up to now

Already in 1959 Jens Skou has investigated the activity of AChE-monolayers [26]. Studying monolayers of purified AChE from *Electrophorus Electricus* [126], he detected a transition plateau of the protein and a maximum in activity at a pressure close to the transition (Fig. 5.2). The author accounted for the measured effect a partial denaturation of the protein (It can be at least argued about, whether the purified enzyme was entirely free of lipid). In another study, Verger and Pattus [160, 114, 161] found a local acitivity maximum of the enzyme at a certain applied lateral pressure of erythrocytes monolayers. Other groups recorded kinks in the Arrhenius plot of AChE activity in erythrocyte vesicles as well as in DMPC vesicles [45, 111]. Further, studies on AChE-containing vesicles also revealed a maximum of AChE activity at certain concentrations of small molecules like ethanol [24].

In a very different approach Konrad Kaufmann showed that fast hydrolysis of ACh by AChE can induce quantized current fluctuations in lipid membranes by the release of protons [71, 72, 73, 70]. In this sense one may denote the AChE a proton pump rather than “only” an ACh splitting enzyme.

5.1.3 Types of AChE used in the Present Thesis

Three different types of AChE derived from fish were used for the studies. Two of them where derived from the *Torpedo* electric organ differing in the presence and

absence of hydrophobic anchors (with courtesy Prof. Silman, Weizmann-Institute, Israel) [47]. The anchor AChE from *Torpedo* electric organ was the enzyme used in most of the studied. It is a G_2 dimer which is supposed to anchor via two hydrophobic phosphatidylinositol hydrophobic chains to lipid membranes. In the second form the enzyme has been treated with a phosphatidylinositol specific Phospholipase C. It is named the PIPLC form and due to the lack of the hydrophobic chains was not expected to bind to membranes. The third type used was a commercially purchased form originating from *Electrophorus electricus*, type V-S [135]. Here, a detailed information on the detailed extraction ptotocol or the actual structure of the protein was not supplied by the company.

5.2 Prestudies on Membrane-Bound AChE

The aformentioned results in literature already imply a possible crucial role of membranes in AChE activity. However, these results were commonly obtained from experiments in lipid vesicle solutions. Although such vesicle solutions are accurately controlable in total lipid composition and temperature, only few more information on membrane-enzyme interaction can be obtained from such bulk measurements. In contrast, due to the possibility to record thermodynamic state diagrams, lipid monolayers represent a superior method to overcome these restrictions.

In the following, after a short investigation on the binding properties of AChE to membranes, results from vesicle bound AChE will be reported. Then, in a simple but intriguing experiment the activity of monolayer-bound AChE will be demonstrated. Subsequently, the effect of changes in pH on enzyme-lpid monolayers are investigated before the general experimental challenges in the determination of enzymes bound to monolayers will be specified.

5.2.1 Binding of AChE to Membranes

The various types of AChE differ mainly in their membrane binding behaviour (see previous section). In the present section the binding behaviour of two types of AChE to both DMPC multilamellar vesicles (MLVs) and to monolayers are presented. One of the best ways to do this is to compare the melting profiles of pure lipid vesicles with the profile of enzyme-vesicle mixtures. An even better way to observe binding properties was utilized by direct incorporation of the eznyme into monolayers on a Langmuir trough.

Binding to DMPC vesicles The experiments were performed on multilamellar vesicles (MLVs) which were prepared in the same way as small unilamellar vesicles

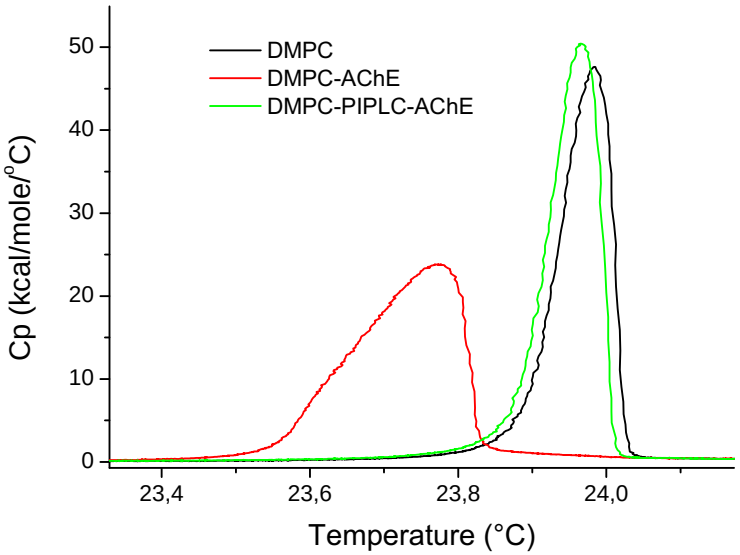

Figure 5.3: Heat capacity profiles of AChE-vesicle solutions. While PIPLC-AChE (green) caused a minor shift in the melting transition, the AChE which contains a hydrophobic anchor caused a significant downshift of the transition temperature (red). Black curves indicate pure DMPC vesicles.

(section 4.1.2), excepting that the sonification step was omitted. In order to prevent denaturation of the enzyme, DMPC vesicles were used as they exhibit a low phase transition temperature of 24 °C. An amount of anchor AChE from *Torpedo* electric organ was used for insertion into these vesicles of a ratio of $\sim 0.5x10^{-6}\,\frac{AChE(dimers)}{DPPC}$ which was comparable to the concentrations used in the monolayer studies further below. For a more detailed description of the binding properties of AChE to vesicles see also [41].

Anchored AChE

The addition of AChE lead to a downshift of the phase transition of the vesicles demonstrating the insertion of this protein into the membrane (Fig. 5.3). In a first approach to understanding the downshift, solution theory was applied to system. In the case of small molecules that are incorporated into membranes the following relation can be used to determine the melting point depression of the vesicle system [57]:

$$\Delta T_m = \left(\frac{R T_{m,A}^2}{\Delta H_{A,0}} \right) x_B \tag{5.1}$$

where ΔT_m is the shift of the phase transition temperature of DMPC, $T_{m,A}$ denotes the measured transition temperature of the mixture, $\Delta H_{A,o}$ is the melting enthalpy of the transitions of the mixture and x_B is the concentration of the molecules (In

the calculations $x_B = 5x10^{-6}$ was used).

Since AChE is a huge molecule it does not fulfill the requirement of eq. 5.1 which is valid for low concentrations of small molecules that only dissolve in the fluid phase of the membrane. However, the enzyme is supposed to bind to the membrane only by the hydrophobic phosphatidylinositol (PS) anchor (PS is a multiple unsaturated lipid with two 18:0-20:4 chains). The formula should therefore provide at least an good order of magnitude estimation of the binding process: for the anchored AChE the calculated shift was $\Delta T \approx 0.15$ mK which is much less than the measured value of $\Delta T \approx 0.2$ K. This finding demonstrates that the interaction of AChE and membranes involves also other contribution to the binding than the anchor. Beside the disturbing effect of the PS chains to the DMPC order, AChE probably also interacts with the head groups of the lipids which leads to a further disturbance of the lipid order. The hydrophobic PS chains are longer than the DMPC chains (14:0) and therefore protrude one lipid layer in the bilayer system causing further disturbances of the lipid order.

PIPLC-AChE

The PIPLC AChE lead to a much smaller decrease of the transition temperature of DMPC. Here, $\Delta T \approx 15$ mK which is close to the resolution and reproducibility limit of the DSC scans. Since the protein lacks the hydrophobic anchor, no insertion of parts of the molecule into the membrane was assumed. However, instead of binding, the detected small shift in the transition might originate from agglomeration of enzyme to the vesicles, which then electrostatically interact with the head groups of the lipids.

Although the melting point depression could not explain the shifts in detail, both findings demonstrate that the enzyme most likely does not insert into the membrane as a whole protein but only with the hydrophobic anchor. From studies in literature it is known that the binding of AChE to DMPC vesicles leads to an inactivation of the enzyme by folding of AChE into a molten globule state [134]. Such an inactivation could be verified in the vesicle studies performed further below and might also contribute to the measured binding properties.

Binding to monolayers In close context with the experiments in the following sections, anchored AChE was accordingly verified to incorporate into lipid monolayers. For this purpose a volume of 5 μl AChE-solution ($\sim$ 2 units) was dropped onto a DPPC monolayer at $\pi = 3.65$ mN/m and $T = 20$ °C (20 mM Tris, 100 mM NaCl, 0.1 mM DTNB, pH 7.5). After an initial strong increase, the pressure decayed to a higher value than before of $\pi = 5.25$ mN/M ($\Delta\pi = 1.6$ mN/m). The exponential fit revealed a small decay constant after the initial jump of only $\tau_{decay} = 7$ s, indicating

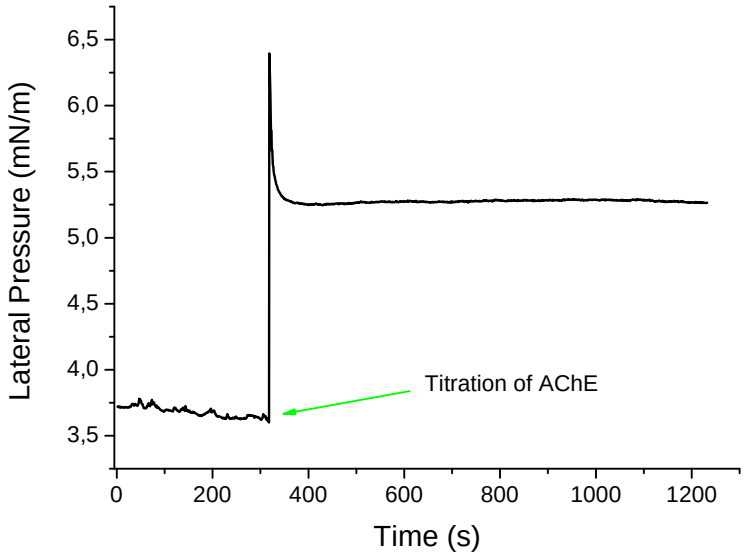

Figure 5.4: Incorporation of AChE into DPPC monolayers. A small volume (5 μl, corresponding to $\sim$ 2 units) of buffer dissolved AChE was dropped onto the monolayer. After a rapid increase, the pressure stayed at an higher value.

a very fast process of insertion of AChE into the membrane.

The pressure increase clearly demonstrates the incorporation of AChE into DPPC-monolayers. Since the pressure stayed constant after the binding of AChE it can be concluded that successive drowning of the enzyme does not occur. However, an uncertainty is given concerning the amount of enzyme distributing into the subphase. Additionally performed experiments demonstrated that after incorporation of AChE had taken place also the bulk exhibited significant activity in a degree of comparable order as was detected in the monolayer bound AChE. This result was gained by transferring the whole monolayer across barriers into a separated region of the trough.

The adding of PIPLC-AChE to the monolayer did not cause any pressure increase of the membrane, displaying that no insertion of the enzyme has taken place. This finding is consistent with the results gained from the vesicle studies.

5.2.2 Activity of Vesicle-Bound AChE

In several series of experiments the activity of AChE incorporated into vesicles was studied in both the anchored AChE as well as the purchased AChE from Sigma. Further, the studies were verified with both manual pH titration of buffer free solutions and by using the Ellman assay (section 4.2.2, [37]). A detailed describtion on the following summary is found in [41].

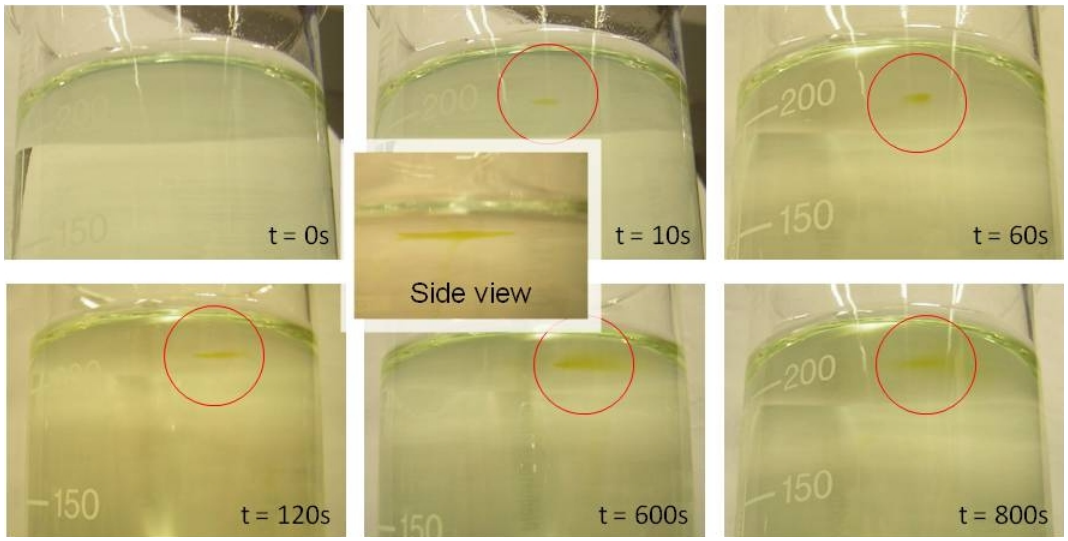

Figure 5.5: Foto sequence of AChE dropped onto a lipid monolayer in a glass. At the beginning the reaction takes only place in a small spot at the surface and with increasing time distributes to a larger area.

In accordance with the literature the activity of AChE exhibited a kink in the Arrhenius plot at the temperature of the phase transition of the vesicles used (DMPC, $T_m = 24$ °C). Due to the Arrhenius equation (section 1.1)

$$k = F \cdot \exp(-\frac{E_\mathrm{a}}{k_\mathrm{B}T}) \tag{5.2}$$

such a kink is refered to a change in the activitation energy E_a. This result already indicates that the enzyme is sensitive to the membrane phase state. In further experminents it was also shown that Cholesterol abolishes the kink [41]. Both types of used AChE from fish showed similar results and are therefore conform with the findings from erythrocyte AChE[45]. Due to this similarity it is supposed that the different membrane bound forms of the enzyme exhibit a similar membrane sensitivity.

Compared to the activity of pure AChE (0.42 μMol/min at 25 °C), the activity in vesicles was only 50% the value (0.22 μmol/min).

5.2.3 Visualisation of Monolayer-Bound AChE Activity

Beside calorimetry and pressure responses of monolayers, the incorporation as well as the activity of AChE in monolayers is visible by the naked eye. For this purpose, a rather simple experiment one can do is to drop a small amount of the enzyme (0.1

units) onto a lipid monolayer in a glass and observe the reaction optically by using the reactive dye of the Ellman assay (pH 7) [37]. In a setup like this, an amount of lipid was spread on the bufffer in a glass corresponding to the fluid phase of the monolayer. In Fig. 5.5 the evolution of a small spot of product (displayed in yellow dye) after the incorporation of AChE into a DPPC monolayer is envisualized in increasing time steps. The location of the spot at the surface of the water volume clearly indicates the restriction of the enzymatic reaction to the monolayer. The high catalytic power of AChE is impressingly demonstrated by the fact that the very small amount of enzyme caused the total bulk volume to turn yellow after two hours. The experiment also demonstrates that the dye distributes from the monolayer region into the subphase:

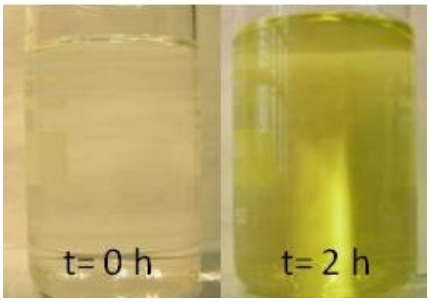

5.2.4 Methododical Aspects

The standard Langmuir-trough-photometer setup which was used in the experiments below has already been introduced in section 4.2. The big advantage of this setup is the possibility of recording both isotherms and AChE activity at the same time. However, a challenge in the studies was the occurance of convection-diffusion of dye in the subphase of the Langmuir trough because as displayed in the previous section, the reaction takes place in the interface/monolayer and subsequently the dye convectively distributes into the bulk. The fluidity profile of this process varied in each of the performed experiment. This in turn lead to difficulties in the determination of the enzyme acitivty which was detected optically through the bulk volume (section 4.2.2, [37]). To account for this issue, several variations in the experimental procedures were implemented:

1. A desired volume (usually $\sim$1 μl) of AChE was dropped onto a prepared lipid monolayer using the total trough volume (Fig. 5.6A). In a standard procedere a pressure of $\pi \approx 4$ mN/m, representing the fluid phase, was adjusted in the monolayer prior to enzyme dropping. After AChE was allowed to incorporate for several minutes, isotherms were recorded by compressing barriers a and c parallely (barrier b was not installed). Simultaneously, the absorbtion was

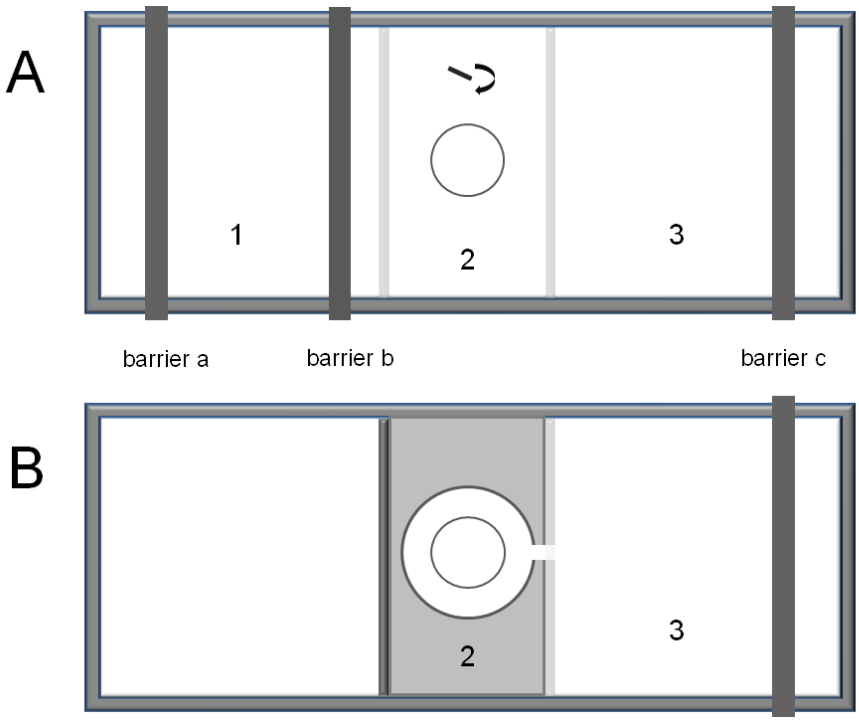

Figure 5.6: Scheme of top down views on the Langmuir trough. The trough is subdivided into 3 chambers, which were also used as one trough when the water level was increased above the barrages. See also text.

detected. Proper progress of the measurements was controlled visually. In cases where convection caused a movement of the active region away from the center transmission path, isotherms were not analysed.

2. AChE was dropped onto region 1 of the trough between barriers a and b, c was not implemented (Fig. 5.6A). Subsequently, the enzyme was carefully dispersed manually by using a pipette. Then the monolayer was transfered at constant pressure by parallely moving the barriers to region 2 and 3 across a separating teflon barrier. The teflon barrier separated subphase 1 from 2 and 3. A second barrier which was inserted in several cases and separated one additional region, lead to a even higher reproducibility. Subsequently, using one barrier (c) the monolayer was compressed and data were recorded as in 1. In parallel a magnetic stirrer was implemented to mix the subphase below the monolayer.

3. Only regions 2 and 3 were used (Fig. 5.6B), whereby region 2 was shrank to a circular region. This setup prevented diffusion of AChE away from the central part. The enzyme was dropped onto the monolayer and after several minutes waiting time barrier 3 was compressed and data were recorded as in 1.

Procedere 1 is the "cleanest" method, since the environment of the enzyme is a free monolayer surface without nearby teflon borders or subphase mixing. However, convection within the monolayer lead to a movement of the relevant areas in the center of the trough. Therefore, it was difficult to obtain exact absolute numbers of activities. Since those effects were prevented in method 2, this procedere gave highest reproducibility in terms of absolute values of activity. The same holds for method 3. All procederes were with 1-3 mM ACh, 0.1 - 0.5 mM DTNB, 100 mM NaCl in Tris buffer (20 mM, for $pH \geq 7.5$) or phosphate buffer (12 mM, for $pH \leq 7.5$) (see also section 4.2.2).

In contrast to convection, non-convective Einstein diffusion in the monolayer plays a minor role in the scenarios described above. The average displacement r of a small partikel can be estimated to:

$$< r^2 >= kDt \tag{5.3}$$

were D is the diffusion constant. $k = 4$ in 2-d systems and k = 6 in 3-d. For lipids, D $\sim 5 \cdot 10^{-10}$ cm^{2}s^{-1} [22]. Considering a standard experiments which e.g. lasts one hour, the lateral 2-d displacement of a lipid within the monolayer is $r \approx 25$ μm. Which is much less than the diameter of the central adorbtion hole of the trough ($d = 1.5$ cm).

5.3 The Role of Protons in Monolayer-Enzyme Systems

Due to the very high turn over number of AChE the enzyme can be considered as a rather fast proton releaser, which for lipid monolayer studies might be of high relevance: The standard amount of AChE used in all activity experiments was 0.1-10 units of AChE, yielding $n \sim 10^{-13}$ - 10^{-11} Mols of monomers (activie sites) which means that in a lipid monolayer with homogenuously distributed AChE each enzyme is surrounded by 1000 - 100000 lipids. However, in the case when enzyme was dropped onto the monolayer the proteins were spread within an area of several cm^2 yielding to 10 - 1000 lipids in the vicinity of the enzyme. This means that, given a sufficient amount of ACh substrate, the local lipid monolayer around the enzyme will be protonated within seconds. Although the majority of protons will dissociate into the bulk, it is obvious that the release of protons in AChE-catalysed reactions might have strong influences in the local environment of those reactions. Such a role of local pH in AChE kinetics was already mentioned in 1967, when Silman [136] showed that the pH dependence of the AChE activity varies significantly when not in buffer but an lipid vesicle-bound form was investigated (Fig. 5.7): The authors found that the activity of AChE in buffer exhibits maxima at $pH \approx 7.5$ - 8 whereas in membrane-bound AChE which were studied in pure water the maximum was at $pH \gtrsim 9$. The reason for this result was proposed to be in a pH gradient between the

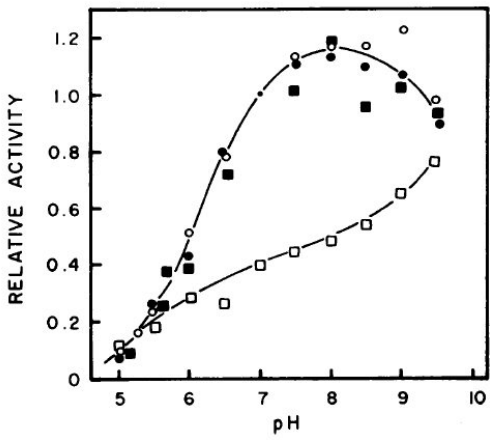

Figure 5.7: *pH* dependent activity of AChE. Several types of AChE are depicted. The curves indicated by filled and open circles and filled squares represent AChE which was dissolved in membranes or in buffer. The activity of membrane bound AChE in the absence of buffer (pure water) differs from the other data by a shift of the maximum activity to higher *pH* (open squares). The figure was taken from [136].

local membrane-enzyme surface and the bulk. Due to strong proton buffering this effect is hidden in experiments were buffer is used. In the cited paper a local *pH* in vicinity of the enzyme surface (taken at the activity maximum) of $pH \sim 6.3$ was concluded.

5.3.1 Determination of the Local pH Maximum in AChE

In this section a simple method will be presented that allows an approach of the determination of the local enzyme *pH*. In the performed experiments, 10 units of AChE were incorporated into a DMPA monolayer in its liquid disordered phase ($\pi \approx 6$ mN/m). The subphase consisted of pure water (*pH* 8) and 100 mM NaCl. After 2 hours the reaction was started by injecting and mixing a final concentration of 10 mM ACh into the subphase. Subsequently, the bulk *pH* was recorded in a distance of $d \approx 0.7$ cm apart from the monolayer.

Immediately after the reaction was started, the recorded *pH* began to decrease indicating a very fast transfer of protons (in form of H_3O^+ ions) from the monolayer to the electrode. Due to the high turn over number of AChE the bulk *pH* decreased rapidly and finally lead to a cease in AChE activity at a low *pH* of 4.9 (Fig. 5.8). The decrease in *pH* reflects an increase in bulk protons, which is also displayed in Fig. 5.8 (green curve). This increase in protons was used to calculate the *pH*-dependent activity of AChE in units of detected protons per time. For this purpose the sigmoidal

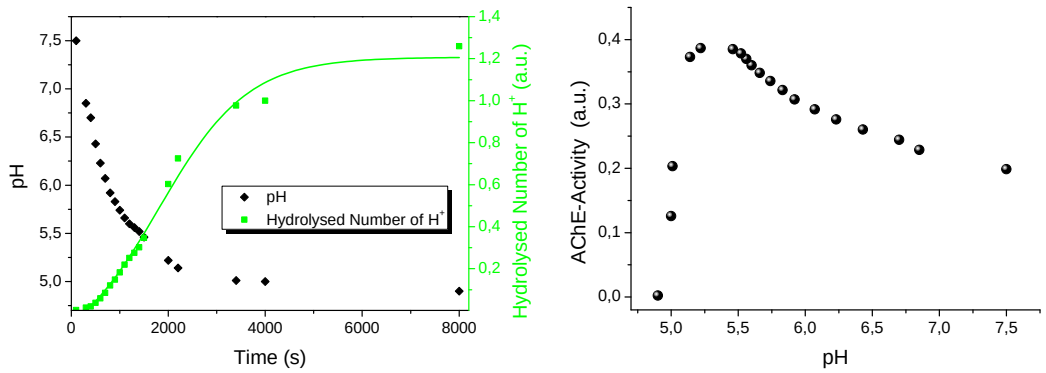

Figure 5.8: Left: pH-time evolution in the subphase below a DMPA-monolayer-bound AChE in the absence of buffer (black curve) and the release of protons through the catalytic reaction (green curve). Right: AChE-activity calculated from the the amount of released protons from the left graph. A maximum activity occurs at $pH \sim 5.3$ - 5.5.

fit of the proton number curve was differentiated (Fig. 5.8). The obtained curve revealed that the maximum of AChE activity occured at $pH \approx 5.3$. The actual value is considered to be slightly higher because of the following reason: At the beginning of the experiment a lag time of ≈ 6 minutes occured at which the pH decrease was small compared to the remaining time. Accounting for this time shift, a value of $pH \approx 5.5$ was found.

The presented simple method displays a good experimental measure of an upper limit of the local pH of AChE. Though, there is a small uncertainty because of the time shift between the release of protons and the detection through the electrode, the found value of $pH \approx 5.3$-5.5 is in accordance to the pK of the active site of AChE which was estimated to be significantly below a $pH \sim 6.3$ [121] but above pH 5.2. The low pH of the detected activity maximum, compared to the value of pH 7.5 - 8 obtained in buffered solutions, implies that in the presence of buffer (and also in the case of pH titration in buffer free experiments) there is a permanent proton gradient between the enzymes (were protons are released) and the bulk concentration (of H_3O^+).

5.3.2 Phase State Dependent Bulk pH

Since enzymatic reactions and monolayer state diagrams obey a strong pH dependence it was of interest wether the monolayer-interface itself exerts measurable responses in the bulk medium while its state is altered. It will be demonstrated that the bulk pH in close vicinity to the lipid monolayer is dramatically decreased when the membrane is in its phase transition.

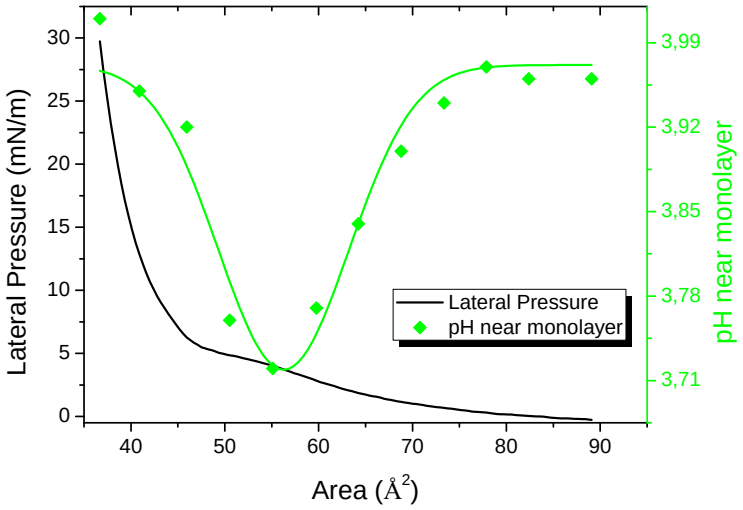

Figure 5.9: Lateral pressure and corresponding pH near the monolayer. The monolayer was expanded and the pH was recorded in a distance of l $\approx$ 3 mm to the surface. A distinct minimum pH close to the phase transition of the monolayer occured. The continuous green line depicts a Gauss fit.

In order to investigate this issue a DPPG monolayer was spread onto a pure water subphase (T = 26 °C) which included 5 μMols Hepes buffer ensuring correctly masured values of the pH electrode (personal communication Prof. Silman, Israel). Then a low pH of 4, which was supposed to be in the order of the pK_a of PG lipids (pK_a 3-4 [32]), was adjusted carefully by the following procedere: In order to mimick the local proton release through the AChE activity small amounts of HCl were dropped onto the monolayer, beginning from a $pH \approx 5.7$. The pK resembles the pH at which half of the lipids are protonated and the second half of proton occurs in H_3O^+ ions. This displays the pH of highest proton fluctuations [70]. The pH electrode was placed in close distance of l $\approx$ 3 mm to the monolayer.

A strong decrease in pH was detected when the monolayer was driven through the phase transition (Fig. 5.9) resulting in a minimum pH value close to the transition. The pH minimum (green curve in Fig. 5.9) of the expanded monolayer was detected slightly right shifted from the transition region to lower pressures, whereas the minimum detected at compressed isotherm was shifted to the left to higher presssures (not shown). This finding indicates a time shift between measured monolayer state and corresponding pH value. This in turn leads to the assumption that the minimum pH occurs exactly at the phase transition of the monolayer.

Since the distance of the electrode from the monolayer (l $\approx$ 3 mm) is small but macroscopic, the recorded pH is considered to resemble "near" bulk pH. This means that in the phase transition regime of the monolayer the lipids appear less protonated

than in the other phases because the low pH in the bulk indicates the presence of a higher number of H_3O^+ there. Thermodynamically this might reflect a strong decrease in the value of the chemical potetial μ_{H^+} of the protons and also might indicate a variable long range interfacial layer in such systems (an ordering of pure water in around cahrged lipid membranes has already been suggested in e.g. [57]).

5.4 Maximum Activity of AChE in Monolayer Phase Transition

Beside the scientific interest in the function of biological processes, one of the main goals in the study of enzymes is the question of how enzyme activity can be optimized or inhibited. The higher the degree of external control of enzyme activity, the more it enables the control of biological processes, which in turn is of high interest in medical research. In the following a distinct dependence of AChE activity on the membrane phase state will be presented.

5.4.1 Maximum Activity Detected on Langmuir Trough

The previously described Langmuir-photometer setup was applied to all following experiments. In order to obtain results with a minimum of external mechanical disturbances, if not otherwise stated, procedere 1 described in section 5.2.4 was applied. Following this protocol, AChE was dropped onto a DPPC monolayer (assay buffer, pH 7.5) and subsequently isotherms and light intensitiy were recorded at constant compression velocitiy. According to section 1.2 the compressibility was calculated using:

$$\kappa_T = -\frac{1}{\overline{A}}\frac{\partial A}{\partial \pi} \tag{5.4}$$

AChE exhibits a maximum in the phase transition region The transmission signal of the light decreased dramatically (Fig. 5.10) when the monolayer was driven through the transition plateau between the liquid disordered and liquid ordered state, indicating a very high acitivity of AChE in this region. The derivative of the transmission curve directly leads to the activity of AChE (section 4.2.2). A combined plot of compressibility and activity demonstrates the strong correlation of both parameters (Fig. 5.11) where both curves clearly exhibit a distinct maximum when the monolayer is in the transition range. This implies that that the activity ξ

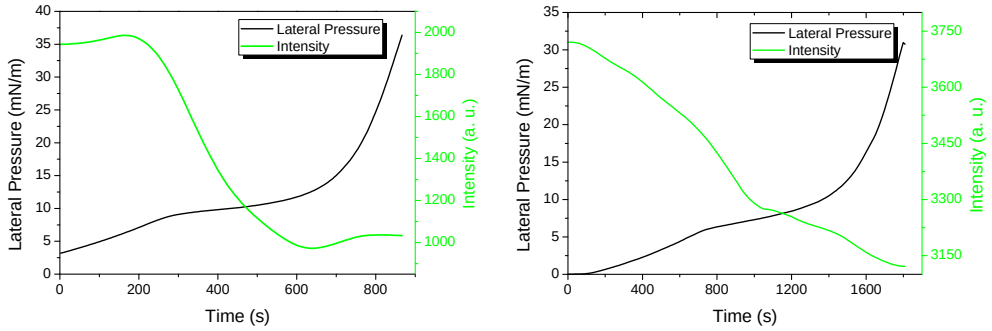

Figure 5.10: Two examples of transmission signals of AChE in a DPPC monolayer. The monolayers were compressed with constant barrier velocities. The transmissions of 310 nm light (Intensitiy, green), indicating the amount of product related dye, decreases dramatically within the transition region of the monolayer (black). Left: curve obtained through procedere 1. Right: Similar behaviour, whereby curve was obtained from procedere 3 (see previous section).

is proportional to the compressiblitiy:

$$\xi \propto \kappa_T \tag{5.5}$$

And since, from a thermodymanic point of view, κ_T is related to fluctuations in area by

$$\left\langle (\delta A)^2 \right\rangle = k_{\mathrm{B}} T \overline{A} \kappa_T, \tag{5.6}$$

the activity ξ appears to be maximal when the fluctutations in area are maximal.

Quantification of the phase state dependent activity The quantification of the maximum activity in the transition compared to the liquid ordered and disordered phases took place by building the ratio

$$\Delta\xi_{lo/ld} \equiv \frac{\xi_{transition} - \xi_{lo/ld}}{\xi_{lo/ld}} \tag{5.7}$$

where $\xi_{transition}$ is the activity in the phase transition and $\xi_{lo/ld}$ is the activity in the liquid ordered or disordered phase of the monolayer. Statistics on 15 curves lead to $\Delta\xi_{lo} \approx 3 \pm 1.5$ (standard deviation) and $\Delta\xi_{ld} \approx 2 \pm 0.7$. The activity in the lipid phase transition was 3 times higher than it was in the liquid ordered phase and 2 times higher than in the liquid disordered phase. Only those curves served as a basis for the quantifaction in which AChE activity was detected in all three main phases of the monolayer allowing for a determination of $\Delta\xi_{lo/ld}$, e.g. only data from curves like shown in Fig. 5.10 (right) were used. The reason for this was that such curves were often obtained with procedure 1 which included strong convection disturbances.

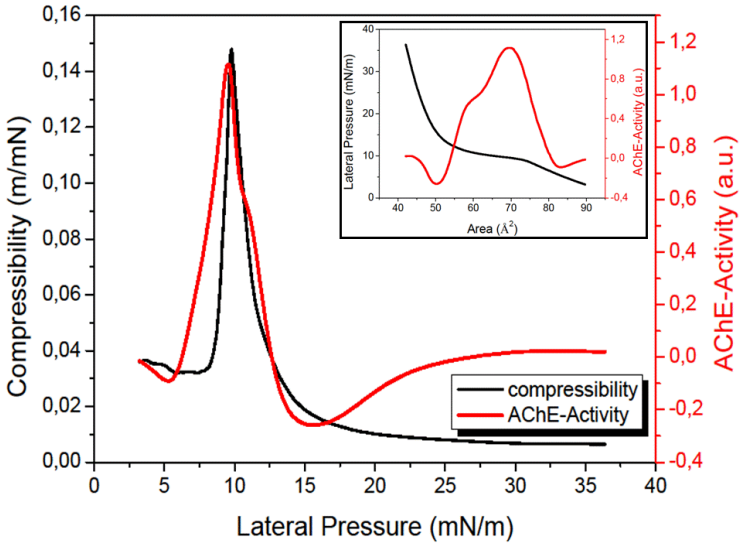

Figure 5.11: Activity of AChE ($m \approx 0.2$ μg protein) and compressibility of the DPPC monolayer superimpose demonstrating highest activity of the enzyme in the transition region of the lipid. Inlet: Activity and pressure plotted against the area per lipid. The monolayer was compressed with 5 cm^2/min, the subphase consisted of: 20 mM Tris-buffer, 100 mM NaCl, 0.1 mM DTNB, 2 mM ACh, $pH7$.

Control experiments The obtained results were confirmed with UV-WIS experiments [41]. In such experiments setup 2 from above was used differing in the use of a magnetic stirrer in the central hole of the trough to accomplish a more symmetrical mixing of the subphase. The activity was measured indirectly by frequently taking small volumes (≈ 50 μl) of dye from the subphase of the central part from which subsequently transmission was detected in an UV-WIS spectrometer. Despite leading to similar results this method is limited in terms of the number of obtained data points which was restricted to a value of 5-8. If too much assay buffer is withdrawn from the subphase, depletion of dye and ACh might take place which in turn changes the conditions in the experimental system.

A course of further experiments was performed to exclude methododical errors in the experiments: In order to eliminate activity artefacts occuring in time, the compression velocity of the barrier was varied in the range from $v = 2$ cm^2/min to $v = 30$ cm^2/min. Since the maxima were detected in the transition range of all velocities, the above results were found to be independent of such effects. Measurements with both compressing cycles and expanding cycles to the proportionality of activity and compressibility. Reference experiments performed without lipid and without enzyme didn't lead to the maxima. Moreover, the enzyme independent autocatalysis was detected and could usually be observed with the naked eye through the gradually

increasing degree of yellow dye. Below $\sim pH$ 7 this effect is unsignificant within the accurancy of the measurement. At higher pH values the autocatalysis needs to be taken into account if exact values of the absolute activity are required.

The impact of the individual components of the reaction buffer on pure lipid monolayers was investigated. ACh at a concentration of 1 mM did not cause any detectable effects on DPPC isotherms. In contrast, DTNB (0.1 mM) shifted the transition plateau of the isotherm to higher values ($\sim$1 mN/m) when water was used as subphase, whereas in buffer solution the upshift was only about 10 - 30 % of the value in water (see also [41]). The main reason for the difference between pure water curves and buffer curves is considerd to lie in the acidic nature of DTNB. In contrast to water, the acid is buffered in the aother case rather than agglomerated to the membrane. However, these substances did not lead to measurable effects in the shape of the transition plateaus and of the isotherms.

Lipid requirement of the detected AChE maximum In the case of anchored AChE, lipids are a natural environment of the enzyme which is rather insoluble in water because of the hydrophobic tails in this case . However, small amounts of additional hydrophobic cholate lead to water soluble forms of AChE [46]. Such lipid free enzymes accumulated to monolayers at the air/water interface giving the opportunity to record isotherms of pure enzyme monolayers.

Although a pressure increase was detected in pure enzyme monolayers when the area was compressed no transition regime was detected at any pressure. In a next step, the same volume of enzyme that was used for the pure AChE monolayers was also incorporated into lipid monolayers. It was found that the lipid incorporated enzyme was more active than the pure enzyme was (see [41] for detailes). Therefore, lipids display a highly defined environment for AChE in monolayers not only in solubility but also in terms of activity. Similar experiments that were performed with PIPLC-AChE revealed no detectable pressure indicating that this type of the enzyme does not assemble monolayers at the air water interface.

Activity of the PIPLC-AChE After detecting the maximum activity in anchored AChE it was of general interest wether the PIPLC-AChE, which lacks the hydrophobic anchor, shows similar activity behaviour or not. From the binding experiments in section 5.2.1 it was already known that PIPLC-AChE can be assumed to not incorporate into the membrane. Following the same procedures as with anchored AChE, the activity of PIPLC was studied in dependence of the monolayer phase state. The following results were obtained with both lipids DPPC and DPPG.

In contrast to the anchored AChE, PIPLC-AChE didn't show any increase of activity

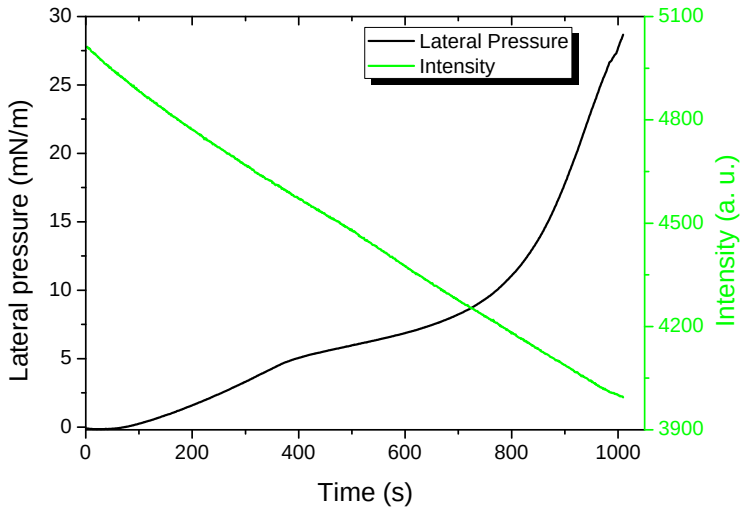

Figure 5.12: Transmission signal of anchor free PIPLC-AChE in a DPPG monolayer. The monolayer was compressed with constant barrier velocity. The transmission of 310 nm light (Intensitiy, green) indicating the amount of product related dye, exhibits a constant decrease. The decrease results from bulk enzyme, but no distinct dip in the curve representing the monolayer bound enzyme was recorded. Therefore, no higher activity occured for this non binding type of AChE in the phase transition of the monolayer.

in the phase transition region of the monolayer which was indicated by a lack of the signal decrease within the transition (Fig. 5.12). This finding displays an excellent negative control for the above findings of the proportionality of both compressibility and activity. Obviously, PIPLC does not incorporate into the monolayer in a significant manner and therefore tending to be less sensitive to the membrane phase state. The result is consistent with the binding studies that displayed no significant binding of PIPLC-AChE to membranes.

Experimental details In the majority of the detected activity curves a minimum at a pressure slightly above the maximum activity occured. In part, this is supposed to originate from a temporary depletion of substrate near the monolayer region. Furthermore, beginning, ending and height as well as the shape of the activity maximum slightly varied in each experiment, e.g. the width of the activity maxima in different measurements was subject to variations ranging from widths of $w \approx 3$ mN/m - $w \approx 8$ mN/m. Nevertheless, the maximum in AChE acitivity repeatedly was observed only in the phase transition region of the monolyer.

The observed slightly increasing transimission signal in the low pressure range and in the high pressure range when procedure 1 was used (Fig. 5.10 left) were found to originate from the following effects: Firstly, in the case of low pressures (liquid

disordered phase) immediately after dropping the enzyme, activity was recorded through the detection of the yellow dye intensitiy. However, due to dye distribution into the bulk and away from the center of the transmission path a decrease in dye concentration within the transmission volume caused a net apparent decrease in activity in the subsequent minutes. Though the enzyme was still active:

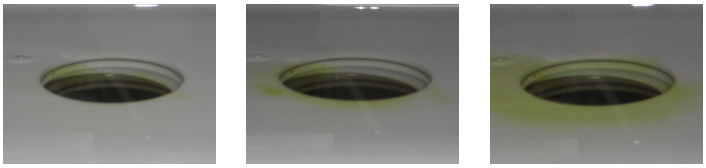

1 min 5 min 15 min

Secondly, in the same way as for low pressures, a cease in the decrease of the signal at high pressures in the liquid ordered phase was observed. This is explained by the same effect as before. Large amounts of dye produced within the phase transition region now distributed into the bulk and by parallely increasing the central lateral region of dye causing a change in the light intensity. As mentioned further above, the use of stir bars and smaller volumes lead to a disapearance of such effects in most of the measurements.

5.4.2 Lipid Titration as Alternative Method

Another method to detect phase state dependent activity of AChE in monolayers is presented in the following. Beside stirring of the subphase of the monolayer, by scaling down the dimensions of the setup convection effects can be reduced. Since the control of pressure through the barriers is limited in the case of small volumes, the technique was changed and now titration of lipids onto a small volume of assay buffer was performed. For this purpose a volume of 2 ml of assay buffer was placed in the central hole of the teflon trough as depicted in the pictures:

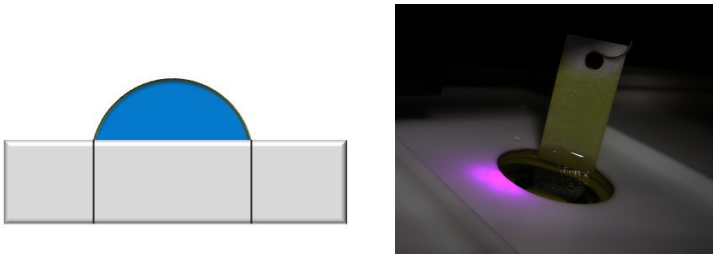

Chlorofom dissolved DPPC was dropped successively in small volumes ($\sim$ 0.2 - 0.4 μl) onto the surface of the reaction buffer (T = 19 °C). In parallel the pressure as

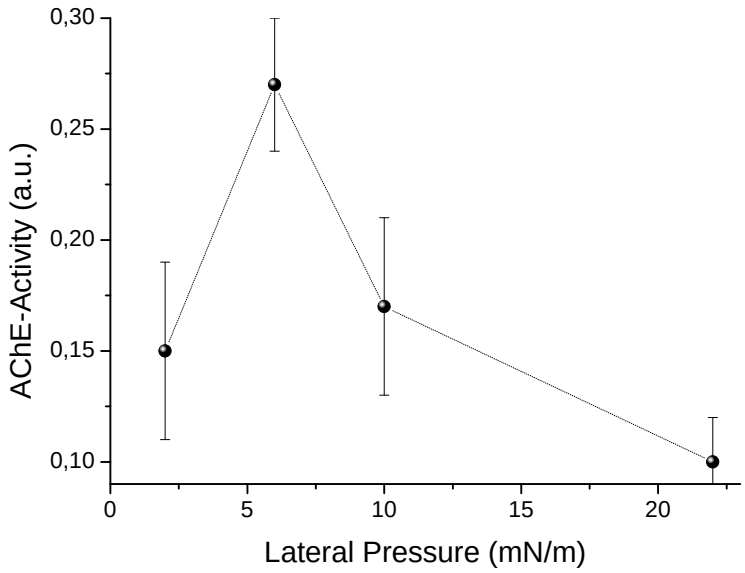

Figure 5.13: AChE activities gained from lipid titration to a small volume of assay buffer. A maximum occurs in the pressure range ($\pi \approx 5$ mN/m) which corresponds to the transition region in Langmuir layers.

well as the transmission were recorded. Again, a maximum in activity occured at a pressure were DPPC was in its transition (Fig. 5.13). The maxima were detected in more than half of the experiments. The reason for that may be found in the fact, that despite diffusion effects of the dye can be excluded this time, the inaccuracy in setting especially a phase transition pressure, may lead to this inreproducabilites. Nevertheless, this way of detecting membrane-bound AChE activity is a fast and simple method.

5.5 Invarianz of the Maximum Activity

In order to find out wether the maximum of activity in the lipid transition was of universal character, the thermodynamic variables of the system were altered. Such thermodynamic properties of lipid monolayers depend on the variables that account for changes in lipid phase behaviour (eg. area, pH, temperature) and of course on the type of lipid (chapter 2). In this section it is shown that the maximum activity of AChE also changes when the monolayer transition is changed through variations in thermodynamic variables.

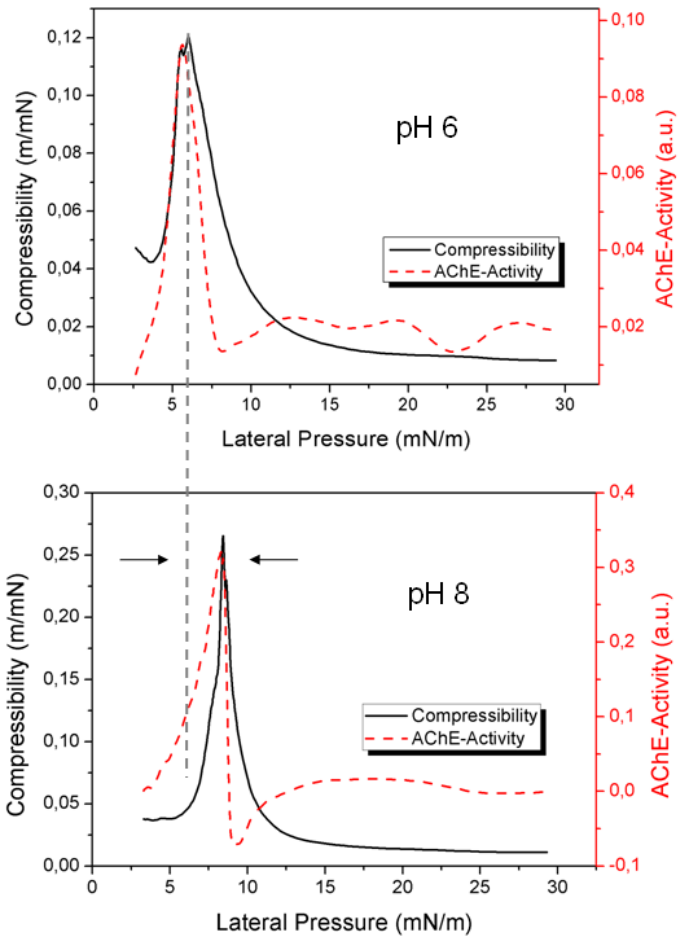

Figure 5.14: Comparison of compressibilites and AChE activites at varying pH. The compressibility maximum of DPPS is shifted to lower pressures when the pH is decreased. The activity of AChE follows the lipid shift and establishes maximum activity in the transition of DPPS.

5.5.1 Invarianz in pH and Lipid

Charged lipids like DPPS are very sensitive to protonation. If the pH of the solvent is decreased the transition of charged lipid monolayers is also decreased to lower pressures [153, 152]. In the following, all monolayer experiments were performed in the same way as explained in the previous section, with the difference being, that the charged DPPS was used and the measurements took place at a temperature of 32 °C.

When the pH of the buffer was decreased by a value of 2 a downshift of the transition of DPPS of 2 mN/m was observed (Fig. 5.14). This downshift also appeared in the maximum activity of AChE which also had moved down 2 mN/m. Hence, in the same

way as shown above, the correlation of compressibility and activity was detected, clearly indicating that the proportionality of the two paramters is maintained after the *pH* was changed. Moreover, a decrease in activity to about 1/3 was observed when the *pH* was altered from *pH* 8 to *pH* 6 being in agreement with own *pH* measuements and with those of former authors (e.g. [136]). Not only could this finding be proved for DPPS but also measurements performed with DMPS, DPPG and Cardiolipin lead to similar results. These results impressingly demonstrate the lipid independent character of the correlation of compressibility and activity.

In the depicted experiment the temperature was 8 °C higher as it was in the DPPC measurements in the last section. This already demonstrates that the correlation of the maxima might also be shifted by changes in temperature.

5.5.2 Invarianz in Temperature and Lipid

When the temperature of the monolayer is decreased then also the pressure at which the transition occurs decreases. This is known for all one component lipids. In the present case Cardiolipin [123, 83] was used which was also found to be a natural lipid environment of erythrocyte AChE [10, 9]. Cardiolipin is negatively charged and consists of four fatty acid chains which are connected by a double phosphate group (appendix B.2) and exhibits a distinct transitions in monolayers below room temperature.

In the same way as alterations in *pH* did change the occurance of the activity maximum it was observed for changes in temperatures and further types of lipids. When the temperature was alterd both the maximum of the compressibility as well as the maximum of activity shifted towards lower pressures. Also in this case an activity maximum was observed that occurs at the pressure where the compressibility is maximal. The findings demonstrate that the proportionality of AChE activity and compressibility is temperature independent. Concerning the shape of the maxima, a characteristic feature of Cardiolipin was the slightly shifted maximum of activity to lower pressures compared to the maximum of compressibility. Furthermore, the peaks by trend occured more narrow (width $\lesssim$ 2. 5 mN/m) in Cardiolipin compared to common phospolipids. The presented shift of Cardiolipin activity to changes in temperature was also proven for the lipids DMPS, DPPS and DPPC.

5.6 Theory and Discussion

The presented data clearly demonstrate the dependence of AChE activity on the monolayer phase state. A maxium of activity was found in the transition regime of the monolayer indicating strong correlations of enzyme activity and area fluc-

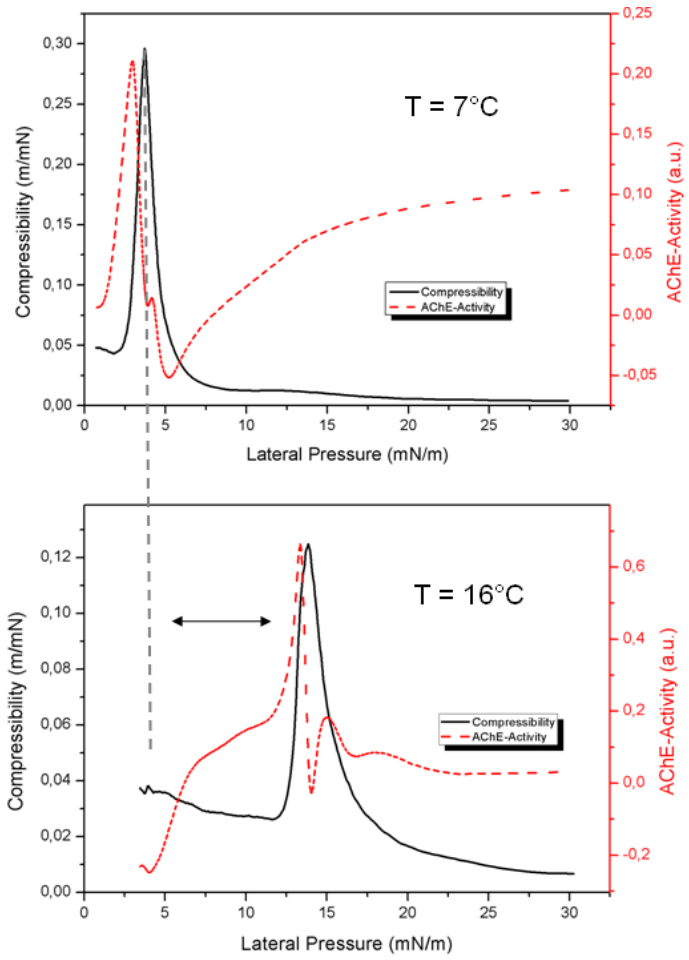

Figure 5.15: Comparison of compressibilites and AChE activites at varying temperatures. The compressibility maximum is lower at lower temperature. The activity of AChE follows the lipid shift and establishes maximum activity in the transition of Cardiolipin.

tuations within the lipid-AChE-hydration layers. The correlation was detected to be qualitatively independent of changes in thermodynamic parameters. Can this proportionality of compressibility and AChE activity be explained?

Area fluctuations and activity When the enzyme incorporates or adsorbs to the membrane it becomes part of the membrane interface. As water is the driving force for membrane formation, both lipids and enzymes are covered by the same water layer ("shell"). It is therefore assumpted that processes that originate from the membrane interface also influence the local surface of the enzyme via the hydration layer. When the monolayer is driven through the phase transition, fluctuations

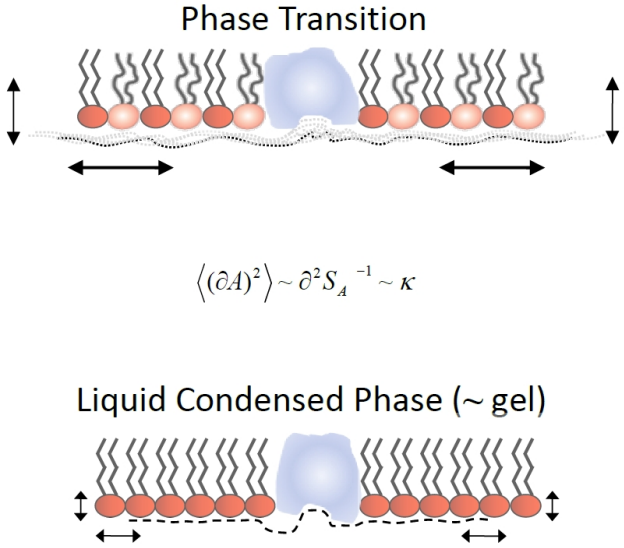

Figure 5.16: Visualisation of the lipid-AChE-hydration layer. In the liquid ordered ("gel") and in the liquid disordered ("fluid") phases fluctuations are comparatively small (lower picture), whereas in the phase transition of the monolayer (upper picture) the area fluctuations are strongly enhanced. The fluctuations are indicated through the grey dotted lines. Since enzymes, lipids and hydration layer define one system, the fluctuations also occur in AChE and is directly affected by the fluctuations of the lipids. The compressibility κ displays a measure of the fluctuations.

in area are maximal (section 1.2). Therefore, it is supposed that the influence of membrane area fluctuations on the hydration layer of the enzyme is also enhanced in the transitions, suggesting that the catalytic process is also maximal influenced in these cases. The correlation is summarized in Fig. 5.16. However, this of course does not explain why these fluctuations magnify the catalysis. At present, the only theory that allows to explain fluctuation dependent enzyme activity is the theory of excitable hydration layers of Konrad Kaufmann (see below).

In the present thesis the maxima in the activity of AChE were detected to occur at *pH* 7.5 - 8 as well as in the phase transitions of the monolayers. As a consequence of these two detected maxima an overall maximum of activity is proposed for AChE (Fig. 5.17). In a region around the phase transition of the monolayer and at *pH* 7.5 - 8 the activity of AChE exhibits a maximum.

The theory of Kaufmann Kaufmann's theory of catalysis was introduced in the theoretical part of the thesis (section 3.2 and [70]) and is applied to the observed phenomena above: When a substrate binds to the enzyme a critical state is induced

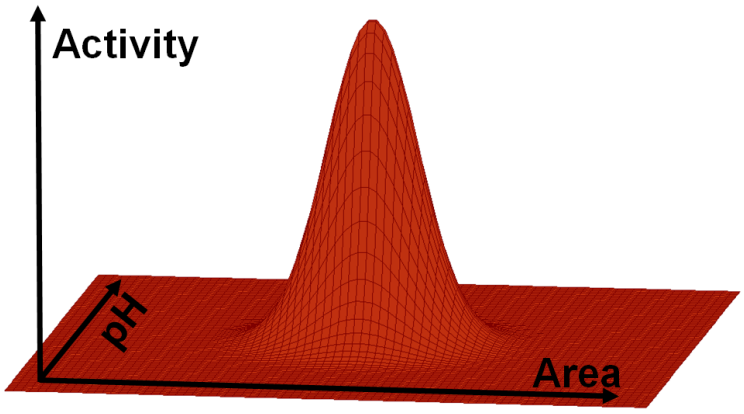

Figure 5.17: Proposed optimum of the AChE activity. Due to the activity maxima in pH as well as in the monolayer transition, where fluctuations in area are maximal, a region of states exists which represents an overall maximum in activity.

leading to enhanced fluctuations in the reaction coordinate, which then causes a magnification of the activity. Enhanced fluctuations in this parameter, according to Kaufmann [70], lead to higher turn over numbers. This is in analogy to the fluctuation dissipation theorem of Einstein [34] (for further discussion it is strongly adviced to contact to Dr. Kaufmann personally).

Coupling of fluctuations? A "near" critical state is refered to, when any of the systems extensive variables (volume, area, protonation, charge, etc) exhibit maximal fluctuations. For the enzyme in solution this would be the pK near which the protonation "jumps" between two values. I.e. the protonation exhibts maximum fluctuations at the pK. At least if protons are involved, any catalytic reaction should therefore have a pK, which corresponds to the pK of the catalytic site. A local maximum $pH \sim 5.3$ of AChE activity was already evalutated in section 5.3 and might differ only little from the pK of the active site.

But how can area fluctuations amplify such critical states in enzymes? In case of the membrane it seems at first more difficult. The reason is supposed to be that the area fluctuations in the membrane are not "alone". Considering for example a constant number of charges at the surface, the charge density will fluctuate along with the area density. An increase in charge density in turn will attract more charged ions (especially multivalent ions like Ca). I.e. the surface potential, the binding of calcium, the degree of protonation, etc. fluctuates as well including also fluctuations that influence the catalytic reaction. Due to the large size of the monolayer the enzyme will not escape from the strong fluctuations of the water layer.

It is expected that this couplings are the origin of the experimental results, which sug-

gest that fluctuations in the thermodynamic variables of area and reaction coordinate are coupled:

$$\left\langle (\delta A)^2 \right\rangle \propto \left\langle (\delta \xi)^2 \right\rangle \tag{5.8}$$

where from section 1.2

$$\left\langle (\delta n_i)^2 \right\rangle \propto -\left(\frac{\partial^2 S}{\partial n_i^2} \right)^{-1} \tag{5.9}$$

was used with $n_i = \xi$ being the reaction coordinate [70] of the enzymatic reaction.

The existence of thermodynamic correlations in the lipid-protein monolayers is underlined by recent results from Steppich et. al. [146] who had revealed a thermal-mechano-electrical coupling in pure lipid monolayers. They verified the existence of fluctuation correlations between area, charge and entropy. These findings in turn arise the question if not only the named but fluctuations in all extensive variables might be coupled?

The entropy potential From experimentally determined correlations in fluctuation one can gain more information on the entropy potential. In the present case of the lipid-protein-hydration layer the potential is certainly rather complex:

$$S = S(A, \xi, n_i) \tag{5.10}$$

The n_i denote further probable contributions to the potential which may involve e.g. the number of protons n_{H^+} and charges q. Another important parameter could be the adsorbtion of a substrate (adsorbant) described by an adsorbation parameter $n_i = n_{ads}$, which could, for instance, be reflected in the substrate concentration. A complete description of the entropy potential would require the knowledge of all variables and states of the system. This, of course, is not possible. Nevertheless, the experimental results from above strongly support the theoretical ansatz of an existing entropy potential of the lipid-enzyme-monolayer.

Contradiction to a folding-unfolding transition As mentioned before, Skou had already observed pressure dependent activities of pure AChE monolayers (section 5.1.2 and [26]). He explained his observations by the degree of folding and unfolding of the proteins at various pressures. However, a lipid independent folding of AChE between various states is considered to not take place because of the following reasons. Since the obtained results from the previous sections were detected in monolayer compression and expansion curves, the proteins would need to unfold and backfold between different distinct states. If one consideres that a maximum activity was

detected at different temperatures, pHs and lipids the requirement of a continuum of states between which the enzyme folds would be needed to explain the observed maxima by folding. This is inconsistent, because in the standard energy landscape for folding proteins usually one dominant minimum is proposed which commonly is assumed to be only altered by the binding and unbinding of e.g. ligands. Although transitions between many different slightly varying structures within the energy minima are detected in single molecules, they are in general assumed to take place only via unstable transient states [19, 106, 30, 31].

6 The Physics of Adaptation in Biological Membranes

In the previous chapter it was demonstrated that the state of the lipid monolayer-interface directly determines the activity of Acetylcholinesterase. In fact, similar results have been reported for Phospholipase A2 studied in vesicles (see also section 3.3). These results strongly support the idea of an integrating interfacial hydration layer. In the following this aspect is elaborated more by extending this idea to lipid "producing" and lipid "digesting" enzymes of the lipid metabolism.

The need of cell adaptation is ubiquitos in life. From single cell organisms up to complex mammalian species cells are exposed to external changes. In case of simple organisms, like bacteria or yeast, these changes include ample variations in temperature, pressure, diet and others. In mammalian cells the changes are less distinct since the body temperature as well as the external atmospheric pressure can be treated as constant. However, also here the distinct organs are subject to changes induced through, e.g. different diets or even substances like nikotin. Surprisingly, few is found in literature on the adaptation of mammalian cell membranes to external changes in physical parameters.

In order to obtain a comprehensive physical description of cell adaptation, in the following experimental sections membrane phase transitions as well as adaptative processes in human cells are proven to be evident. The obtained experimental data as well as the striking results from the previous part of the thesis will then serve as basis of a general thermodynamic model of adaptation. Beforehand, an overview on the widespread literature is given, which will then be followed by an exemplary verification of adaptation of arctic sea water bacterias.

6.1 Crucial Role of Membranes in Cell Function

The physical properties of lipids in biological membranes are sensitive to changes in environmental parameters [28, 149, 76]. From membrane fluidity studies it has become evident that biological membranes establish a phase transition in or below growth temperature, i.e. their physical state of the membrane appears more fluid than gel-

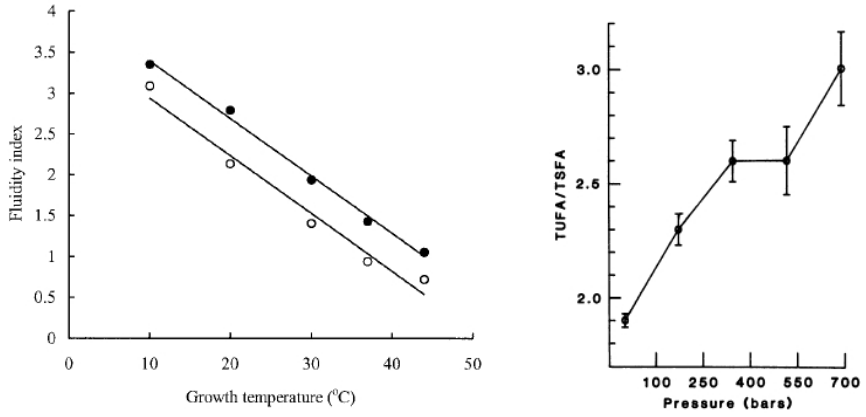

Figure 6.1: The relative amount of unsaturated fatty acids in bacteria increases with higher temperatures as well as with higher pressures. Left: The ratio of saturated/unsaturated fatty acids (fluidity index) of E. Coli. drops with increasing temperature [21]. Open circles depict cells in stationary growth phase, filled circles indicate exponential growth phase. Right: The ratio of unsaturated/saturated fatty acids (TUFA/TSFA) of barophilic marine bacterium CNPT3 increases with pressure [27].

like, but remains in the vicinity of the transition [11, 39, 54, 65, 89, 99, 145, 113, 127]. A shift in growth temperature has been found to lead to a change in the measured phase transition temperature of simple organisms [21, 55, 88, 90]. This adaptation is usually established by a modification of the ratio of saturated to unsaturated fatty acids or by changing the fatty acid chain length of membrane lipids. Lower temperatures cause an increase in the amount of unsaturated and short chain fatty acids and higher temperatures lead to higher saturation and longer chains [21, 88, 155]. This behaviour was also referred to as homeoviscous adaptation [55, 142]. Similarly to changes in temperature, adaptation of fatty acids has also been detected when the hydrostatic pressure was varied [27] (Fig. 6.1). Several authors have summarized those fluidity properties of biological membranes [5, 23, 55, 122, 149].

The regulating mechanisms of these highly self organized adaptation processes have remained unclear. However, the capability of cells to adapt to various types of changes indicates that the underlying mechanisms of adaptation feature a very general character.

It has already been mentioned in section 3.3 that various membrane-bound enzymes function only if they are embedded in an adequate lipid environment [49, 67, 74, 124, 129, 130] and that the activities of several enzymes exhibit a kink in the Arrhenius plot at or close to the transition temperature of the surrounding membrane matrix [17, 74, 124]. In order to understand adaptation the membrane-enzyme interaction of lipolytic enzymes is of special interest. Maximum activity of Phospholipase A2

(PLA2) and a minimal lag time was observed when the surrounding membrane is in the phase transition regime [3, 61, 109, 110, 68, 80, 141].

In adaptation to lower growth temperatures, unsaturation of fatty acids and lipids is established by Desaturases [38, 98, 118, 120]. Several authors found a strong increase of present Desaturase activity right after the environmental temperature was changed [48, 66, 151, 154]. In carp a strong increase in specific activity of carp liver microsomal Desaturase was reported the first days after the animals were subjected to cold shocks [151, 154]. On a single cell level, in Escheria Coli, a large increase in Desaturase activity was detected within the first few minutes after temperature was decreased [48]. Since the activities have increased before enzyme synthesis has started, thermal adaptation was proven to be intrinsic, rather than synthesis.

From a physical perspective it was shown that fluctuations in area and enthalpy are strongly elevated if a membrane is in its phase transition (see section 1.2). Critical fluctuations have been measured in synthetic lipid mixtures as well as in plasma membrane vesicles [158, 60, 7]. It has also been found that the permeability of pure membranes is enhanced in the phase transition regime of lipid membranes [2, 163].

6.2 Adaptation of Bacterial Membranes

In the following, for the first time, membrane phase transition and adaptation were calorimetrically verified for Pseudoalteromonas haloplanktis (PH, with courtesy of Dr. Thomas Franke from the University of Augsburg) (e.g. [147]). In the course of the present study they serve as bacterial model system for the experimental proof of adaptive behaviour of bacterial cells.

Cell growth and calorimetry In order to study adaptation of PH the cells were grown at different temperatures and subsequently the heat capacity profiles of whole bacterias were compared to each other. The following procedure was applied: PH were seeded in capped Ehrlenmeyer flasks (200 ml) and grown at the three temperatures of 21.8 °C, 24.5 °C and 32.6 °C. Growth at the latter two temperatures was established on a heating plate and in an oven, respectively. After 96 hours the cells were washed 2 times in artificial sea water ($T_{seawater} = T_{growth}$) using a centrifuge and 500 g. Subsequently, pellets were resuspended in artificial seawater to a volume of $V \approx$ 0.5 ml. The temperature of the washing solution was adjusted to be equal to the growth temperature to prevent adaptation before the measurements. Then the heat capacitiy profile of the final cell solution was determined in the DSC applying the following settings: after a fast prescan from 1 °C to 40 °C at a scan rate of 90°C/h the main scans were run up and down from 1 °C to 80 °C with a scan rate of 60

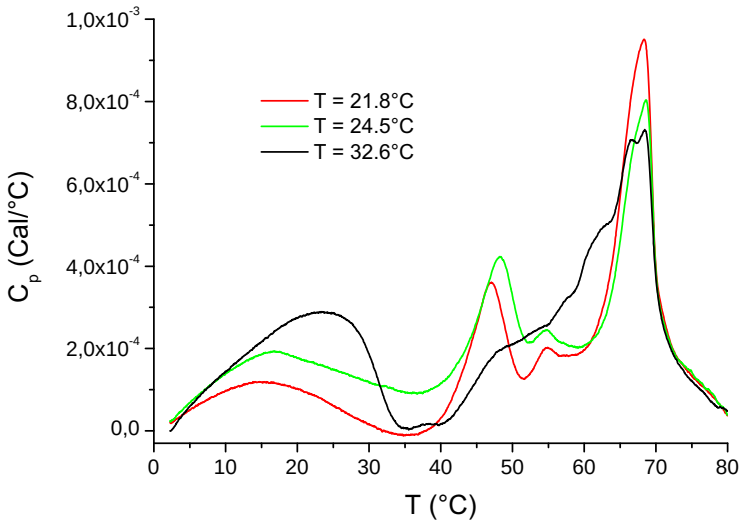

Figure 6.2: Heat capacity profiles of whole cells of Pseudoalteromonas haloplanktis. Curves of cells grown at three different temperatures are compared. The peaks at higher temperatures above 40 °C originate from protein denaturation. Peaks at the lower temperature are from the membrane transition. Higher growth temperatures cause membrane transitions that are shifted to higher temperatures.

°C/h. All further operated runs were 1 °C to 80 °C with scan rates of 20 °C/h. Using the DSC software, baselines were substracted from the profiles.

Shift in membrane maximum Whole cells of PH exhibited several maxima in the heat capacitiy profiles (Fig. 6.2). The peaks in the temperature range above 40 °C indicate protein denaturation peaks since they occur at identical positions at each growth temperature. Since these peaks almost vanished completely in the second run to 80 °C they are regarded as being irreversibel (Fig. 6.3, right). Contrary, the maxima in the temperature range below 40 °C were observed to be almost reversibel and are therefore identified as membrane peaks. These reversibel maxima are shifted to each other when the cells were grown at different temperatures (Fig. 6.3, left). At low temperature maxima start and end nearly at the same temperature with a total peak width of $\Delta T \approx 30$ °C, but differ in the position of their transition maximum temperature ($T_{max,21,8} = 15$ °C, $T_{max,32.6} = 23$ °C). The measured shift of the peak is ≈ 2.6 °C less than the external change in temperature was, but the effect is still in very good agreement to what was expected from the aforementioned literature studies.

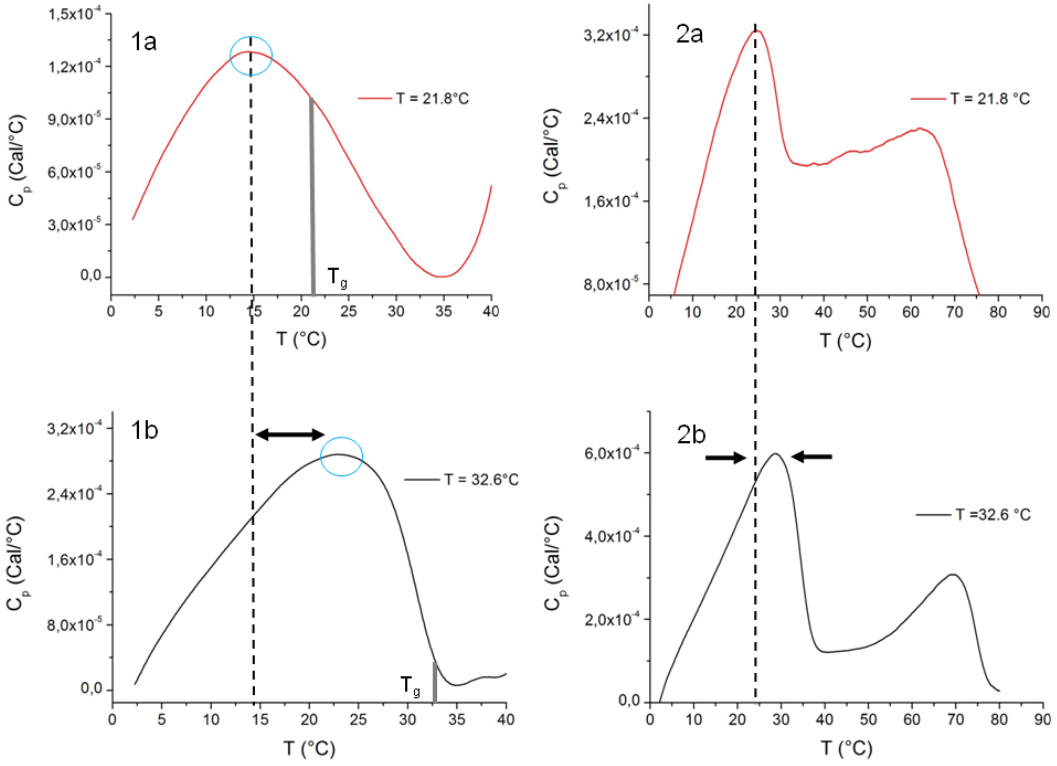

Figure 6.3: Comparison of the heat capacity profiles of Pseudoalteromonas Haloplanktis before (left) and after protein denaturation (right). Two different cell growth temperatures are depicted. Left: The membrane transition peak of whole cells grown at 21.8 °C (1a) is about 8 °C lower than the peak of cells grown at 32.6 °C (1b). Right: heat capacity profile of the same cells as before but from the second upscan to 80 °C. The protein peaks have almost vanished and the membrane peaks have moved to higher temperatures by some degrees. Note the different scales in the two columns.

The transition enthalpy is given through the area below the heat capacitiy maximum

$$H = \int_{\Delta T_{Transition}} c_p dT \tag{6.1}$$

For the two cell samples which were grown at 21.8 °C and at 32.6 °C the enthalpies are $H_{21.8°C} \approx 1$ kJ/mol and $H_{32.6°C} \approx 2.5$ kJ/mol. Compared to the enthalpies of pure lipid membranes, e.g. $H_{DPPC} \approx 36$ kJ/mol [57], the transition enthalpies of PH are smaller but of significant order. The numbers were gained from an estimated average weight of 700 g/mol per lipid and from monolayer area considerations. Whereby the latter were established through the extraction of the membranes of the bacterias with the Bligh & Dyer method (section 4.5.1). From this sample the volume needed

to establish a pressure increase on the Langmuir trough was compared to the average volume needed from the lipid DPPC. Only membranes from cells grown at 21.8 °C were measured on the monolayer and therefore, the higher transition enthalpy of the cells grown at 32.6 °C very probably originates from a larger number of cells.

In case of the second run, where protein peaks have vanished, the membrane maxima depict very similar shapes as were found in the first run. However, compared to the first runs, both peaks exhibit 1.5 - 2 times higher maxima and they are displaced several °C to higher temperatures.

Discussion The heat capacity profile of Pseudoalteromonas haloplanktis clearly reveals a reversible phase transition. Since the observed transitions were below the growth temperature, the presented DSC scans strongly support the aspect that the bacteria "live" in a membrane state which reflects a more fluid phase but is still very close to the phase transition maximum. This finding is consistent with several results reported in literature [58, 88, 99]. The adaptive processes in PH cells are established in such a way that a similar physical state of the membranes is maintained at all growth temperatures:

When the bacterias were subject to changes in temperature the maxima in pre- and post protein denaturation peaks scans shifted towards the direction of the change in growth temperature. More distinct maxima in the post-denaturation scans compared to scans of the whole cells have already been determined in acholeplasma membranes [89]. These differences may originate from the denaturation of proteins which might lead to a higher cooperativity of the transition: Through denaturation, proteins have changed their structure and lost their biological functionality. Therefore, membrane structuring by protein incorporation is expected to differ to the case of intact cells. Consequently, the changes in the maxima are assumed to originate mainly from the denaturation of proteins. However, since the maxima of the first scans are only 5 °C apart from post denaturarion scans, it is concluded that polar lipid-protein interactions are significant but do not cause a vigorous modification in membrane phase behaviour.

The topic will be discussed further in the sections below, in particular in the studies on human adaptation and in the presented model of adaptation at the end of the chapter.

6.3 Experimental Proof of Phase Transitions in Human Cell Membranes

The study is now focused on human cells. Due to the complexity and the diversity of the cells a comprehensive picture of the interfacial properites of human cell membranes has still been missing. However, through experiments on lipid vesicle systems, monolayers and black lipid membranes a better insight has been gained into this topic in the present thesis. By careful determination of heat capacities and of the compressibilites, for the first time, the occurance of phase transitions in extracted human membranes could be verified. In addition, the existence of a critical point will be indicated through monolayer measurments. In addition, data of permeability measurements did strongly indicate enhanced fluctuations in the phase transition regime of the membranes. The obtained results are compared to each other.

6.3.1 Susceptibilities of Human Cell Membranes

Both the isobaric heat capacity c_p and the isothermal compressibility κ_T were obtained from extracted human HaCat cells and MV3 cells. HaCat cells are human keratinocytes which had spontaneously immortalized [133, 144]. These cells are known to be robust in culture. They are not cancerous [133, 144]. MV3 cells are human melanoma cells [156].

Cell lipid extraction In a standard extraction, 3-7 T175 cell culture flasks were grown to confluence at 37 °C with each flask corresponding to about 60 mg of wet tissue. Subsequently, lipids were extracted by applying the Folch method [43] whereby the final volume of the extraction was about 2 ml of lipid-Chloroform solution with a deviation of less than 30% per extraction. The concentration of lipids in the solution was evaluated to be $c \approx 4$ mg/ml. This value is gained through the comparison of monolayer pressure curves of extracted lipids and synthetic lipids of known concentration (see also previous section on bacterias). Extracted lipids were stored at -20 °C and used without further purification. HaCat cells were used from passage 45 to passage 150. These cells are known to not differentiate up to 300 passages. MV3 cells were used from 17 to 40 passages.

Vesicles were prepared according to the protocol explained in section 4.1. A 10 mM Hepes buffer pH 7 containing 1 mM EDTA was used. EDTA features a high binding affinity to calcium and also other ions and therefore prevents experimental variations caused by potentially varying salt concentrations in the different experiments.

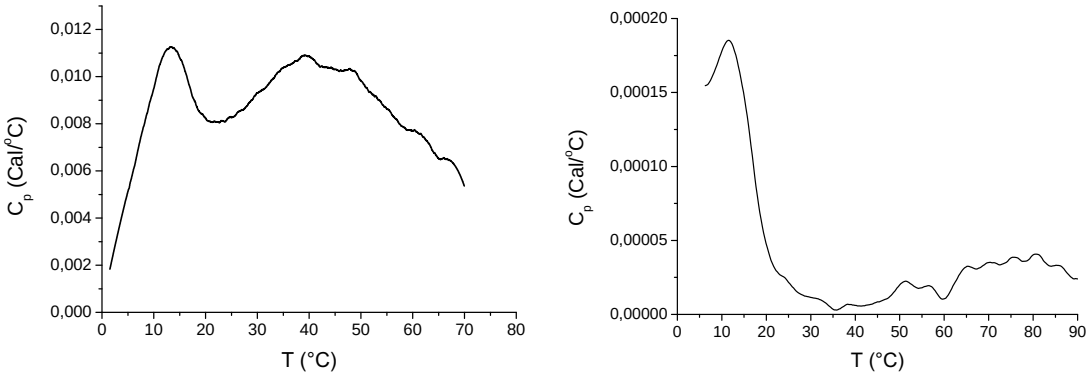

Figure 6.4: Heat capacity profiles of extracted membranes from HaCat cells (left) and MV3 cells (right). Cells were grown at 37 °C. In both cases a *reversibel* maximum at temperatures around 12 °C was recorded.

In both cell membranes of HaCat cells as well as of MV3 cells a clear maximum in the heat capacitiy profiles was detected (Fig. 6.4). The maxima were reversible and therefore they are concluded to be of membranous origin. Moreover, since extracted lipids were used no significant protein peaks were detected. Reproducibility could only be obtained when the extraction protocol in each new experiment was followed identical to the previous extractions.

In case of HaCat cells the center of the transition was found at a temperature of 12 $\pm$1 °C. The transition enthalpies of the maxima in three experiments were ΔH_{HaCat} $\approx$ 4 kJ/mol (see eq. 6.1). Interestingly, in membranes of MV3 cells the transition peak occured also at 12 °C, where the transition enthalpy was $\Delta H_{MV3} \approx 0.9$ kJ/mol. As for the measurements of bacteria, these number was gained from an estimated average weight of 700 g/mol per lipid and monolayer area considerations. Again, as for the bacterial membranes, the obtained enthalpies of human membranes are at least of one order of magnitude smaller than they are for pure lipids, e.g. $H_{DPPC} \approx$ 36 kJ/mol, but closer to the range of two component mixtures like DOPC/D15PC (5:95) with $H_{DOPC-D15PC} \approx 6$ kJ/mol [163]. The width of the maxima is roughly determined to be 10 - 20 °C, where both maxima show strong descents at one side of the peak. Due to the freezing point of water the lower temperature range of the measurements was restricted to a minimum of 1 °C.

In order to test wether cholesterol influences the measurements, β-Cyclodextrin from Sigma [135] was added in a concentration of 1 mM to the sample solution. In all measurements the substance seemed to suppress the phase transitions.

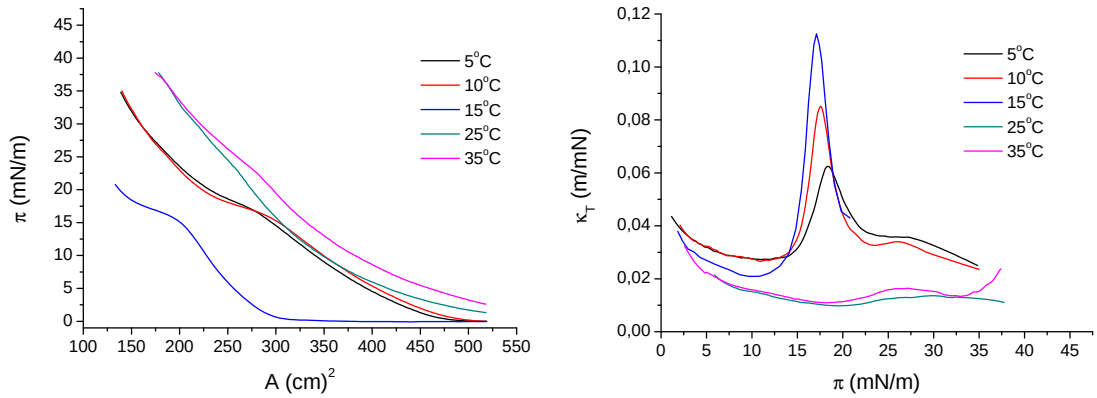

Figure 6.5: Left: Langmuir isotherms of lipid monolayers from MV3 melanoma cells at different temperatures of measurement. Right: Compressibilities κ_T calculated from the isotherms.

Transitions in Monolayers After heat capacity peaks were found in the membranes it was expected that transitions could also be seen in monolayers. Using the extracted lipids from above, a set of experiments measurements at various temperatures were performed. For this purpose chloroform dissolved lipids of both cell lines were spread onto a Langmuir trough (section 4.2) and after evaporation of the solvent the isotherms were recorded. Each curve displays a completely new experiment. Since the drowning of lipids occured, only first compression runs were used for the analysis of the data.

It could be shown that membranes from MV3 cells exhibited distinct phase transition plateaus at varying temperatures (Fig. 6.5). Isotherms detected at the low temperatures of 5 °C and 10 °C featured transition regions at lower pressures compared to the curves gained from higher temperatures of 25 °C and 35 °C. The latter were considered to not display a transition. However, the plateau at lowest pressure was recorded at 15 °C. The occurance of transition plateaus is nicely characterised through maxima in the compressibilities κ_T (Fig. 6.5, right).

Since the plateau vanished above a certain temperature between 15 - 25 °C this finding suggests the occurance of a critical point which marks the distinct state at which two phases become indistinguishable. Critical points are known from one component lipid systems [146]: increasing the temperature in such systems leads to an increase of the thermal energy and therefore the plateau pressure of the transition π_T is expected to shift to higher values. In parallel the transitions become less broad when the temperature is increased and finally converge into the critical point. The

critical points can sytematically be obtained using the Clausius-Clapeyron- equation

$$\Delta Q_T = T \cdot \left(\frac{d\pi_T}{dT} \right) \cdot (A_{LE} - A_{LC})) \tag{6.2}$$

where $\Delta Q_T = T \cdot (S_{LE} - S_{LC})$ is the latent heat of the transitions that vanishes at the critical point, $\Delta Q = 0$. A_{LE} and A_{LC} are the onset areas of the transition plateau in the isotherms [132]. In the present case the equality of both areas takes place between 15-25 °C (whereby here in part $\frac{d\pi_T}{dT} < 0$, which is not understood yet). Although the obtained data from the complex human cell membranes do not allow for a strict application of eq. 6.2 the indication of a critical point is intriguing. The results obtained through monolayer studies strongly support the assumption of the occurance of critical states in cell membranes which have already been detected through the phases transitions in the previously described DSC measurements.

Discussion Despite the complexity of the lipid composition and the necessitiy of a carefully accomplished extraction procedure, the data from both calorimetry and monolayers clearly demonstrate that the native lipids of human MV3 cells exhibit a reversible phase transition. Furthermore, the temperature dependece in the monolayer studies indicates that these lipid system exhibits a critical point around 20 °C and 20 mN/m (Fig. 6.5). This, in turn, suggests the occurance of different phases in the membranes.

Physically, the detected compressibilities and heat capacities of the cell membranes are related to fluctuations in area and in enthalpy (see section 1.2 and [57]):

$$\kappa_T = -\frac{1}{\langle A \rangle} \left(\frac{d \langle A \rangle}{d\pi} \right)_T = \frac{\left\langle A^2 \right\rangle - \langle A \rangle^2}{\langle A \rangle RT} \tag{6.3}$$

$$c_p = \frac{d \langle H \rangle}{dT} = \frac{\left\langle H^2 \right\rangle - \langle H \rangle^2}{RT^2}. \tag{6.4}$$

The comparatively small excess heat capacities of the measured membranes imply smaller fluctuations of the enthalpy compared to one component systems. In addition, the broad width of the peaks ($\sim$ 30 °C) reveals a small cooperativity of the transition. The latter is not very surprising if one consideres the multi-faceted composition of biological membranes.

From a theoretical perspective enhanced fluctuations in biomembranes are the main focus of this work (section 1.1.2). That they exist in living systems is underlied by the above determination of phase transitions in bacterias and in human cell membranes. For rat plasma membrane vesicles the occurance of transitions and critical fluctuations has also been published in literature [158, 60]. The authors in

these papers detected a transition temperature range from 15 - 25 °C which is very close to the observed transitions around 12 °C (DSC) in the human cells of the present thesis.

Both methods the calorimetry and the Langmuir monolayers serve as a valuable means of detecting the thermodynamic properties of extracted lipid membranes from human cells. In case of the DSC measurements the reversible membrane peaks occur at a lower temperature than it was found for most other cell systems in literature [11, 39, 54, 65, 89, 99, 145]. A transition in a similar temperature range of $\sim$ 10 - 15 °C has also been found in membranes of Bacillus Subtilis that were grown at 37 °C [58]. Further, due to the extraction with Chloroform and Methanol all inner cell components have been dissolved. It is obvious that the prepared vesicle solutions contain a rather different assembly of lipids than it is found in living cells. Therefore, the statement of the experiments with extracted lipids to living cell systems will be restricted to the conclusion that phase transition in these membranes occur and might be crucial for cell functions. Nevertheless, the results indicate that phase transitions in biological membranes are not restricted to simple organisms and that the identity or the approximaty of growth temperature and transition peak may be of universal relevance.

6.3.2 Phase State Dependent Permeability

The very useful methods of calorimetry and Langmuir monolayers are restricted to vesicles and air/water interfaces, respectively. By means of black lipid membranes (BLM, section 4.3) it is possible to study the electrical current through free standing bilayers. Using BLMs one obtains access to the crucial study of ion conductivity through membranes. In this context, ion channel proteins have been found to play a major role in the regulation of ionic transport across the membrane [100]. In the literature on ion channels the characteristics of membranes has also been taken into account and it was found that membranes exert strong influences on the function of the channels (e.g. [14]). Later, Antonov has ascertained that quantized ion-conducting channels appear in pure lipid membranes close to the phase transition [2]. This finding was more verified by Wunderlich [163]. In this paper the permeability was detected to be proportional to the heat capacitiy of the membrane.

Based on the observations of Antonov [2] and theoretically more in Wunderlich and Blicher [163, 12] the focus in the present section will be brought on the detection of the permeability of protein-free biological membranes of extracted MV3 cells. In very good accordance with studies on synthetic low component lipid bilayers, the biological membranes will be presented to depict enhanced quantized current fluctuations in the phase transition regime.

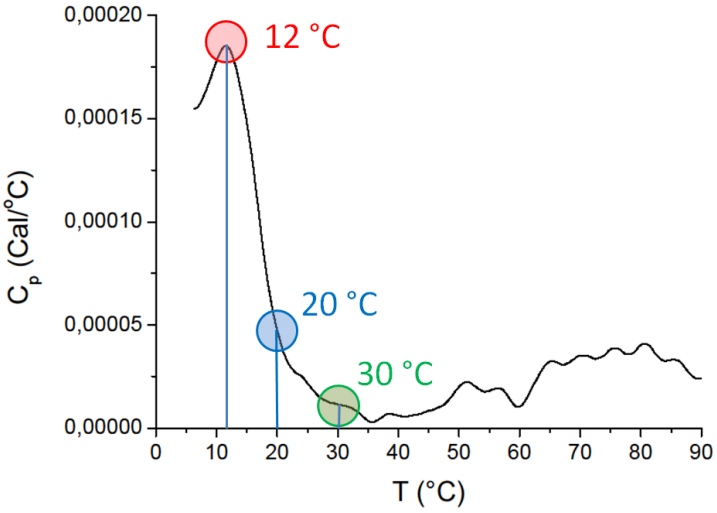

Figure 6.6: Heat capacity profile of the MV3 membranes like already shown in Fig. 6.4. The temperature regime of the performed permeability measurements are marked in colours.

Bilayers of the extracted lipids were formed according to section 4.3. The temperature regime of the experiments included the temperature midpoint of the phase transition (12 °C) and two temperatures in the fluid-like phase (20 °C and 30 °C) of the extracted membrane of MV3 cells (Fig. 6.6). Due to difficulties in forming bilayers below the transition temperature at 5 °C no data were obtained from the gel phase of the membrane. At this place it also should be mentioned that the formation of stable bilayers is a challenge and not arbitrarily reproducable.

Current fluctuations are strongly enhanced in the phase transition A Voltage V was applied and increased successively until current fluctuations were observed. This took place at voltages in the range of 200 - 300 mV. Subsequently V was kept constant over minutes or if desired it was changed to lower or higher values.

In the phase transition at 12 °C the currents were rather stepwise and quantized with long opening times which repeatedly were in the range of seconds. The average value of one current step was determined to $I_m = 2.5$ pA. In contrast, at temperatures of 20 °C and 30 °C the current fluctuations were rather spike like (Fig. 6.7, left).

Opening times are increased in the phase transition The typical timescales of the opening times were analysed. For this purpose the data of each temperature were used and data of two or three different voltages were evaluated. The normalized

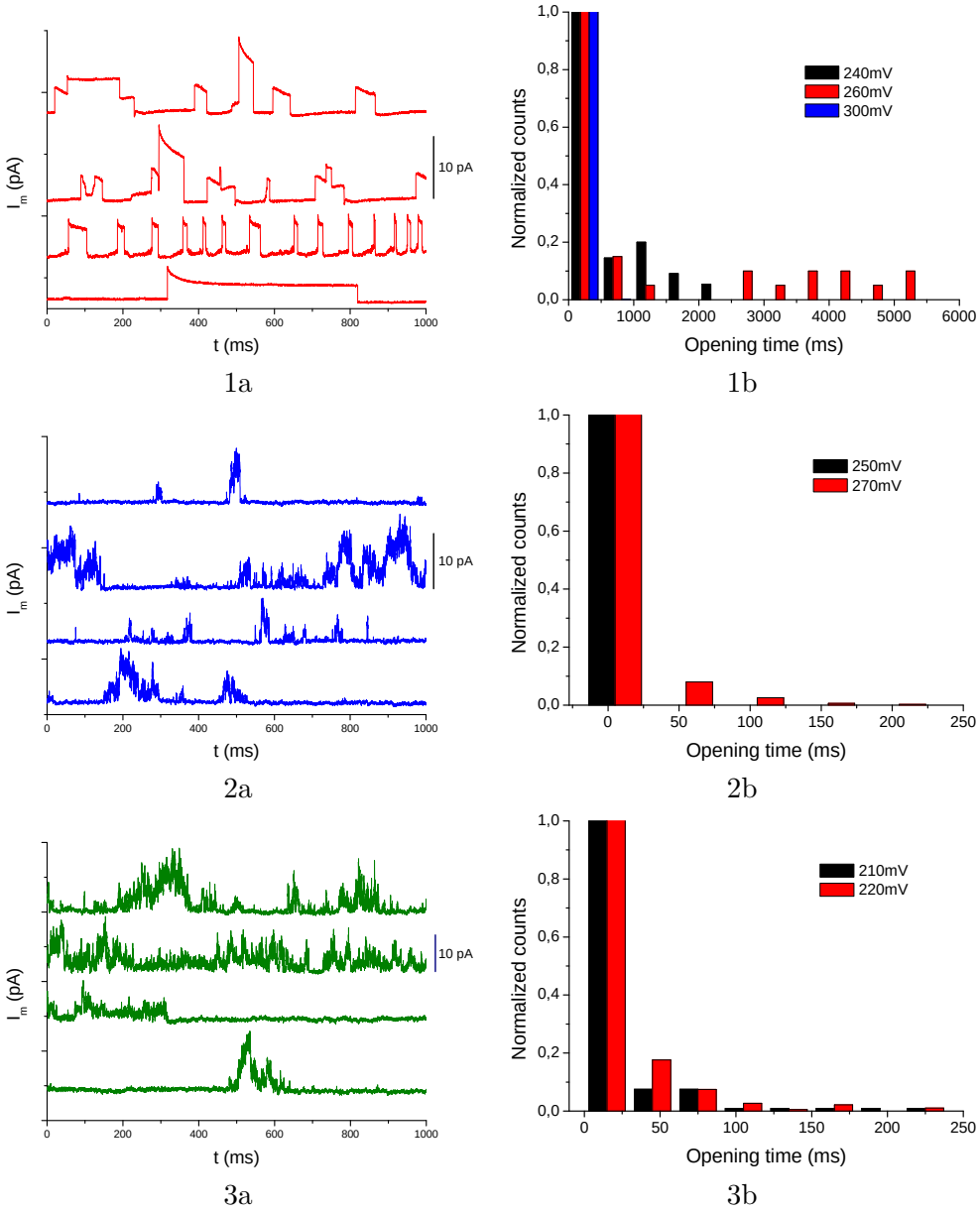

Figure 6.7: Left: Current fluctuations of extracted MV3 lipids at 12 °C (1a), 20 °C (2a) and 30 °C (3a). In the phase transition at 12 °C stepwise quantized current fluctuations are observed. Right: Corresponding timescales of the current fluctuations at 12 °C (1b), 20 °C (2b) and 30 °C (3b). At 20 °C and at 30 °C the currents tend to exhibit spike like forms and the opening times are much smaller compared to the phase transition. Note the different scales at the abscissa.

plots depict that the opening times in the phase transition regime (12 °C) are much longer than they are in the fluid-like phase (20 °C and 30 °C) (Fig. 6.7, right). The mean average opening times are summarized as follows :

Temperature (°C)	12	20	30
Opening times (ms)	92	15	24

In the phase transition at 12 °C they are several times higher than in the fluid phase of the membrane, whereby, the timelengths of the opening times are broadly distributed and in the phase transition span from 40 ms to 1500 m. Compared to the presented opening times, synthetic lipid mixtures (5:95 DOPC/D15PC) exhibit average opening times in the phase transition of $\tau_{synt} \sim 20$ ms [163].

Correlation of opening times and susceptibilities After transitions had been observed in the monolayers further above, the relation of compressibilities and relaxation times can now be evaluated. From the theoretical perspective such a relation has been missing up to now. Matthias Schneider (personal communication) has closed this gap: Based on Onsager's statement, that since perturbations of a system are fluctuations away from the entropy maximum [107, 108] and therefore fluctuations and relaxation lifetimes are the same, a proportionality of the opening times τ to compressibilities κ_A can be derived. In the present case the area A is applied as thermodynamic variable. Further, the entropy potential and the simplest form of the Onsager relations are used (section 1.1.1). For small deviations the first derivative of the entropy is:

$$\frac{\partial S}{\partial A} \approx \frac{1}{2}\left(\frac{\partial^2 S}{\partial A^2}\right)\Delta A \tag{6.5}$$

and from Onsager, if all forces are coupled [51, 57], it is known:

$$\frac{dn_i}{dt} = \sum_j L_{ij}\frac{\partial S}{\partial n_i}. \tag{6.6}$$

Using $n_i = A$, this expression becomes

$$\frac{dA}{dt} = -L'_O\frac{\partial S}{\partial A}. \tag{6.7}$$

In eq. 1.7 it was demonstrated that fluctuations are proportional to the inverse of the second derivative of the entropy, which in the present context is

$$\left\langle (\delta A)^2 \right\rangle = -\left(\frac{\partial^2 S}{\partial A^2}\right)^{-1}. \tag{6.8}$$

Since it is known from section 1.2 that the compressibility is proportional to the fluctuations

$$k_{\mathrm{B}} \left(\frac{\partial^2 S}{\partial A^2} \right)_T^{-1} = -k_{\mathrm{B}} T A \kappa_T, \tag{6.9}$$

the timescales of the area relaxation and therefore of the opening times are proportional to the compressibility

$$\tau \approx L_O \, AT\kappa_T. \tag{6.10}$$

Where L_O denotes a lipid dependent constant which up to now has not been determined.

Using the values obtained for the compressibility of MV3 lipids in the transition plateau ($\kappa_{15°\mathrm{C,max}} \approx 0.1$ m/mN, $A \approx 40$ Å^2, $T = 288$ K) and $\tau \approx 92$ ms, the constant L_O is determined to be $L_O \approx 6.4$ x 10^{12} Ns/Km^3.

From pure lipid bilayers the relation between opening times and heat capacity has been identified as follows [51]:

$$\tau = \frac{T^2}{L} \Delta c_p \tag{6.11}$$

where L is a lipid dependent phenomenological coefficient. For example, for DMPC large unilamellar vesicles (LUV) it is $L = 15.7$ x 10^8 JK/mols and for DMPC multilamellar vesicles (MLV) it is $L = 6.6$ x 10^8 JK/mols [163]. The present measurements allow a determination of L of the MV3 lipids, which is $L \approx 1.9$ x 10^8 JK/mol. Where the following numbers were used: using $\Delta c_p \approx 15$ mCal/K ≈ 220 J/Kmol $= 3.6$ x 10^{-22} J/K. Since this value is close to those obtained in the pure MLV lipid DMPC membranes, it is reasonable to assume that eq. 6.11 also might be valid for transitions in biological membranes.

The tendency of longer τ at higher temperatures is given through $\tau \propto T^2$ (eq. 6.11). However, the values of the temperatures of 20 °C and 30 °C differ to a larger extend than it was expected from this relation. On the other hand, at 20 °C the membrane is still slightly in the phase transition which should cause the opposite effect of longer opening times at 20 °C (Fig. 6.6).

Discussion Current fluctuations occured in the whole measured temperature range, yet the stepwise quantized forms have merely been found in the phase transition regime of the MV3 membranes. The opening times were much longer in the phase transition than they were in the fluid phase. These results underline the existence of critical states in human cell membranes which are here displayed by a distinct slowdown of the realxation times τ and the distinct steplike current shapes. Therefore, the current fluctuations are concluded to be determined by the membrane phase state.

Even though the c_p transition is less distinct in cell lipids than it has been found to be in one or two lipid component systems, the opening times were measured to be longer in cell lipids. This effect may be due to charged lipids which tend to stabilize membranes and amplify current fluctuations [82]. Moreover, the content of Cholesterol in extracted lipids is unknown and might also contribute to fluctuations.

6.3.3 Comparison of the Three Applied Methods

Three methods were applied to study the thermodynamic properties of MV3 cells: DSC, Langmuir trough and BLM. In the following the results of these are shortly compared by employing the data gained in the phase transition regimes at 12 - 15 °C.

The potency of monolayers lies in the possibility to detect thermodynamic parameters over a large range in temperature and lateral pressure. The results from these monolayers measurements revealed that not only do phase transition occur but that also a critical point of the cell membranes exist in a region around 20 °C and 20 mN/m. Moreover, the calorimetric measurements exhibited a distinct heat capacitiy maximum of the used human lipid membranes at temperatures around 12 °C.

The detected high current fluctuations in the BLM studies approve these results in an impressing manner. Concerning the agreement of the results, the obtained numbers are now compared. Heimburg [56] has found an expression which relates the compressibility and the heat capacity of lipid vesicles:

$$\Delta\kappa_T = \frac{\gamma_{area}^2 T}{\overline{A}} \Delta c_p \tag{6.12}$$

Using the c_p data of the MV3 cells the compressibility was calculated, using eq. 6.12, to $\Delta\kappa_T^{calc} \approx 0.2$ m/N. Where $\gamma_{area} = 0.893$ m^2/J was used, which is the constant found for DPPC [56]. The value measured for MV3 monolayer was $\Delta\kappa_T \approx 100$ m/N at $\pi = 17$ mN/m and a lowest value of $\kappa_T \approx 20$ m/N in the fluid phase ($\pi \approx 10$ mN/m). This values are higher by a factor of 50 - 500 times than expected from the DPPC vesicles estimation. Such a difference seems to be too large in number to originate from uncertainties in the data. Of course, due to the lack of curvature, the occurance of an air/water interface and a monolayer system rather than bilayers, the thermodynamical properties of monolayers differ from vesicle/bilayer systems, e.g. monolayers appear softer than bilayers are. In addition, γ_{area} is not exactly known for the extracted lipds and the value for DPPC was used. However, the obtained large discrepancy implies that there might be some additional factors that have to be taken into account when biological membranes are characterised. Possible experimental reasons for the discrepancy involve drowning of lipids in the Langmuir

trough, deviations in the concentrations of the gained lipid solutions and unknown effects caused by the influence of Cholesterol.

The results suggest that the membrane of human MV3 cells adapt near a critical state, where physical properties (e.g. like compressibility, conductivity, electrical capacity, thermal conduction etc.) are "optimized" (or maximized). The system is therefore capable to "switch" its properties quite drastically allowing it to respond rapidly to changing enviromental conditions. The findings therefore represent a self organized responding system. Such reactions of cell systems to environmental changes are in the focus of the following sections.

6.4 Adaptation of Human Cells

After phase transitions have been verified in human cell membranes, adaptation to changes in the external parameters was investigated. In order to keep the theory simple, the performed measurements were restricted to changes in temperature. In this context, the adaptation of HaCat cells to shifts in temperature was also determined by population studies. Afterwards, by using calorimetry and performing fatty acid analysis of mammalian cell membranes it will be shown that adaptive processes of mamalian cell membranes take place.

6.4.1 Cell Growth at Various Temperatures

The distinct natural environment of human cells within an organism is the origin of a more complicated cell culture compared to bacterial culture. Most of the human cell lines grow in in-vitro cultures only when they are cancerous. Once in culture, single cells tend to connect to other cells and the makority of the cell lines grow only in two dimensional monolayers with a minimum reproduction range of 10 hours. The culture of human cells is commonly restricted to 37 °C. The further the culture temperature distinguishes from this value the less cells will survive the change. However, it will be presented that HaCat cells are able to survive for a certain time at temperatures below 37 °C and that cell growth is optimized at 37 °C.

The growth of cells Growth studies were performed by counting the numbers of living cells. In order to enable long time monitoring of the cell growth, a stage top cell chamber was used for the studies (see also section 4.4.3).

Cell growth is divided into 4 different phases which are defined as lag time, exponential growth time, stationary phase and as mortal phase (Fig. 6.8) [131]. The exponential (or logarithmic) growth describes the phase in which cell doubling takes place. The

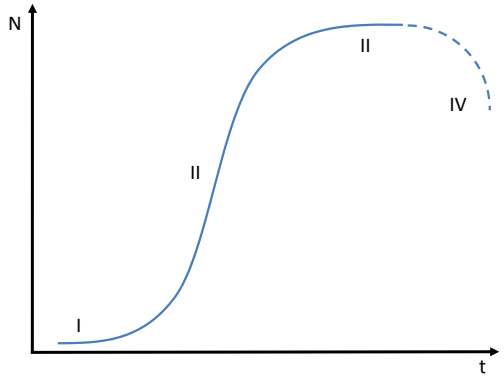

Figure 6.8: The 4 phases of cell growth. The total number of cells (N) is plotted against the growth time. After a lag time (I) cells start to divide leading to an exponential growth (II). When the cells have grown to confluence they reach the stationary phase (III). In phase IV the cells die. This phase is usually prevented by splitting of the culture or by exchanging the growth medium.

growth rate in this phase is set up as a rate equation:

$$\frac{dN}{dt} = \mu N. \tag{6.13}$$

N is the total number of cells and μ is a prefactor that includes the doubling time t_d. $\mu = \frac{\ln 2}{t_d}$ is obtained from the doubling condition of the cells $N(t) = 2N_0$ with the initial number of cells N_0. Through using t_d of the cells the exponential cell growth is

$$N = N_0 \exp(\frac{ln2}{t_d}t), \tag{6.14}$$

where t_d is determined from the cell count experiments.

In a course of experminents HaCat cells were split 1:10 and seeded into μ-dish flasks from Ibidi [63] (Fig. 6.9). Before the dishes were put into the stage top incubator in which the desired temperatures was adjusted, the cells were allowed to adhere for 3 hours at 37 °C. Usually, cells were kept in the incubator for 3-10 days. Long time monitoring was started after the dishes were put into the stage top incubator and pictures were taken every 5 minutes.

The experimentally detected lag time was in the range of 24 h when cells were grown at 35.5 °C and at 37 °C. Beyond this phase the cells started to grow exponentially (Fig. 6.10). According to eq. 6.14 both curves were fitted with a single exponential function which allowed the detection of the doubling time, which was $t_d = 12.5$ hours

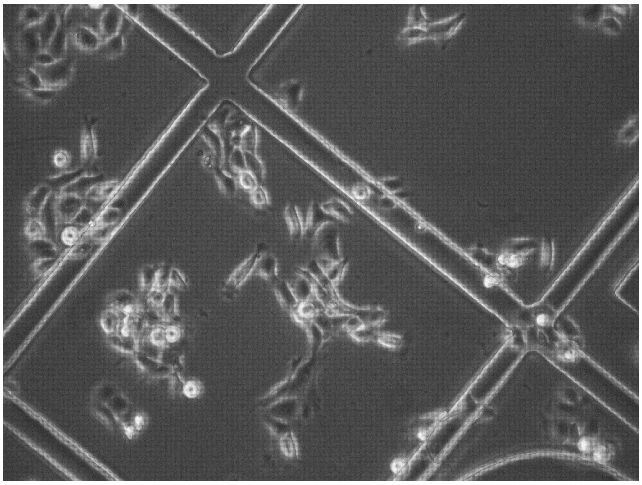

Figure 6.9: Picture of human HaCat cells grown in a gridded μ-dish at 37 °C. The cells adhere to the surface and grow insular. The white spherical cells are currently dividing cells.

at 37 °C. At slightly lower temperatures of 35.5 °C the growth was significantly slowier (t_d = 19 hours).

When the temperature values were set below 35.5 °C, no or only low exponential growth was established within the observed time intervall. In this temperature range the total number of cells increased almost linearly with time rather than exponential. Here, the cell growth slew down with long doubling times of more than 50 hours. After 3-5 days of growth the cells in most cases started to stop dividing. Eventually, after 7-10 days they often started to die gradually. On the other hand, in some cases ($\sim$ 20% of the analysed data) the cells have been monitored to not to die. Several times cells survived 14 days at 32 °C demonstrating acclimation to the harsh environment.

The transition from exponential growth to low exponential growth occurs within a small temperature range of 1.5 °C below 35.5 °C (Fig. 6.11). Below 34 °C the change of t_d with temperature follows a linear trend. This finding enables the prediction of doubling times in the temperature range from 30 °C to 34 °C. In this intervall t_d changes 2 h/°C compared to t_d = 4 h/°C at temperatures above 35.5 °C (of course, the result from the latter was determined from only 2 points).

In addition, despite the cells were allowed to adhere at 37 °C prior to lowering of the temperatures, in half of the experiments they didn't establish any growth. In these cases they died gradually. Then the cell death took place not only irregularly, quickly within several hours, but also slow in more than 100 hours.

At an increased temperature of 39 °C the cells didn't divide (Fig. 6.10). After 84 h

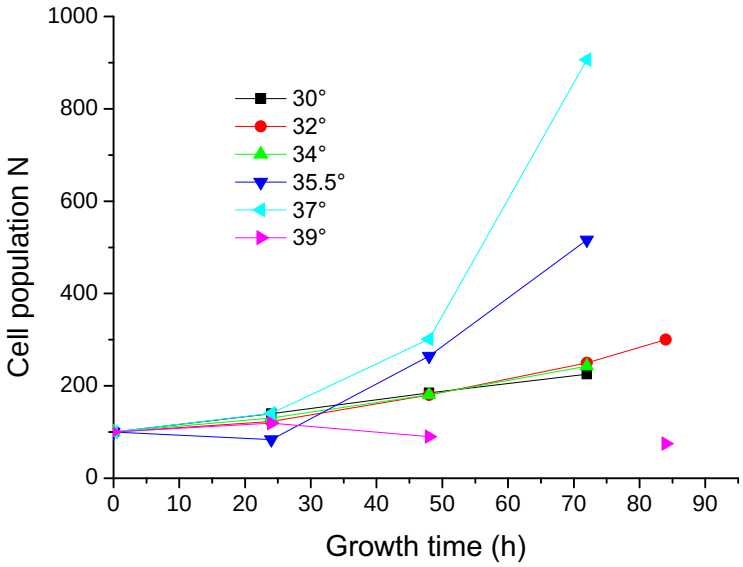

Figure 6.10: Growth pattern of HaCat cells obtained at different temperatures. Two evolutions are distinguishable: At 35.5 °C and at 37 °C the curves start to increase exponentially after 24 hours, resembling exponential growth. At temperatures below 35.5 °C cells establish only a very weak exponential growth. The accurancy of the numbers is within 5 % of each individual cell count. The data display the growth optimization to 37 °C.

of growth only 75 % of the originally seeded number survived.

Generally, the cells tended to form spherical shapes when the temperature was set below 37 °C. Elongated shapes were detected at 39 °C. In cases where cells died, they beforehand usually responded to the stress with blebbing. Moreover, the overall mobility of single cells significantly decreased with decreasing temperature.

Variations in the protocol The cells responded very sensitive to variations in experimental procedures. They rarely attached to the flasks when they were seeded directly at temperatures below 35.5 °C. Only in 2 out of 13 experiments did they adhere in these temperature range. Since in the studied cell lines adhesion is crucial to their survival they eventually died in most of these cases.

Discussion HaCat cell growth was otpimized at 37 °C. At this temperature the growth rate was detected to be maximal. However, the cells survived at low environmental temperatures for at least 1 week. The sharp transition of the growth rate into slow doubling times below a growth temperature of 34 °C indicate that there is a

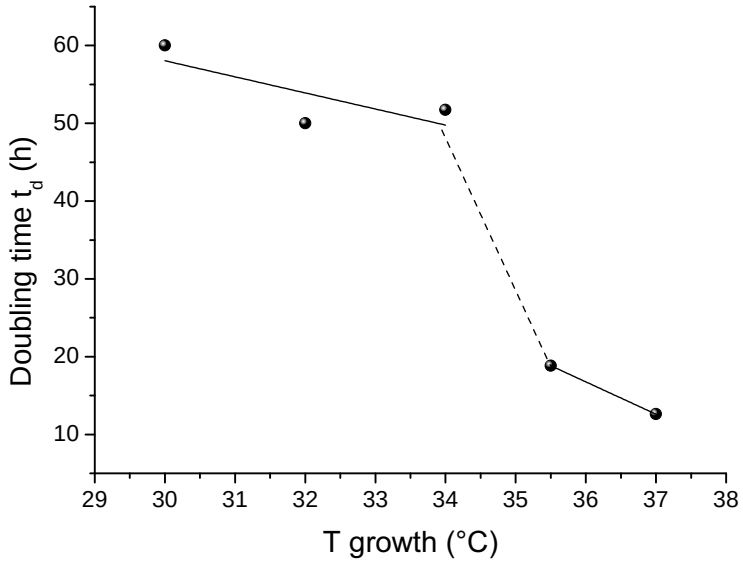

Figure 6.11: Doubling times of human HaCat cells which were grown at different temperatures. Each point represents a separate measure. A transition from fast to slow doubling is observed when the growth temperature was adjusted below 35.5 °C. In the higher temperature regime data were obtained from exponential growth fits. In the lower range a linear growth, approximating very low exponential growth, was taken as a basis (see also Fig. 6.10).

threshold for the establishement of normal exponential growth patterns. Below this threshold cells are able to survive at least for a certain period of time and reproduce very slow. If so, then cell survival is, at least partly, decoupled from cell reproduction in terms of a separation of survival and reproduction. On the other hand, since also at temperatures below 34 °C an increasing cell population was observed, albeit very slow, one can conclude that adaptation of at least few single human cells takes place.

However, the very small growth rate below 34 °C as well as the frequently observed blebbing indicated high stresses for the cells at decreased temperatures. A characterisation of cell death, e.g. wether the frequently observed cell death belongs to apoptosis or nekrosis [131] is not further adressed in the framework of this physically motivated thesis.

6.4.2 Adaptation of Human Membranes

After the adaptation of cell populations was studied the adaptation of human cell membranes to changes in temperature was investigated. First, it will be shown that the phase transition of HaCat membranes is shifted after the growth temperature has been altered. The second part is dedicated to the fatty acid analysis of three

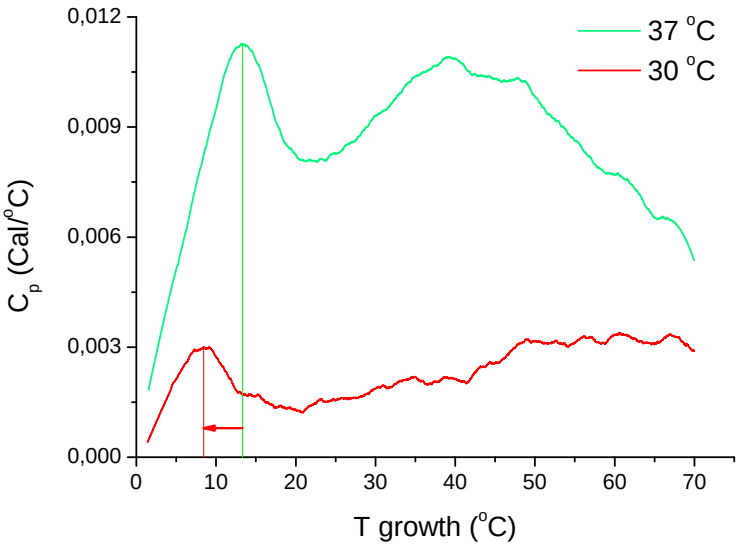

Figure 6.12: Heat capacitiy profile of HaCat cells grown at 37 °C. The green curve was taken from Fig. 6.4. The red curve is from cells that were kept at 30 °C for additional 7 days. The membrane of the latter has adapted and the phase transition has shifted to a lower temperature. The peak at 8.5 °C obtained from the cells at 30 °C was reversibel. Both curves display the second upscans (5 °C/h) in the DSC.

different cell lines that were subject to temperature changes.

Calorimetrically detected adaptation of HaCat membranes After HaCat cells were grown to confluence at 37 °C they were kept at 30 °C for 7 days. Lipid extraction, vesicle preparation and DSC measurements were performed analogous to the procedures before (section 6.3.1).

The c_p-profile of cells kept at 30 °C displays a distinct maximum with the center of the peak being at 8.5 °C and a total width of the peak of $\Delta T \approx 10$ °C (Fig. 6.12). Compared to the cells grown at 37 °C the peak is downshifted, clearly demonstrating that adaptive processes had taken place. Since the maximum occured reversible it was considered to be of membranous origin. Due to the Chloroform extraction no protein peaks were observed. The transition enthalpy was calculated to $\Delta H \approx 1.3$ kJ/mol. These values may include uncertainties since the beginning as well as the ending of the transition are not clearly defined.

The temperature difference between the c_p maxima of 30° C grown cells and the one of 37 °C grown cells is quite dramatic (3.5 °C) and of the same order than the shift in growth temperature (7°C). This finding is crucial because it demonstrates a significant shift of the transition in human cells, which beforehand was only known

from simple organisms.

The smaller shift in the transition maximum compared to the shift in growth temperature has also been observed in the bacterial adaptation of section 6.2. As presented in the previous section, the cells are subject to large stresses at a temperature of 30 °C. Therefore, the ability of adaptation likely is restricted in these cells, which, on the other hand, is reflected in the gap between transition and growth temperature shift. Otherwise, adaptation processes might take place very slow and may be completed after a much longer time intervall than it had been utilized in the study. Compared to the fast adaptation of bacterieas, it can be expected that the time for adaptation increases somewhat with the complexity of the organism.

Further evidence for human cell adaptation through fatty acid analysis In contrast to the thermodynamic properties of membranes which are achieved through calorimetry, one obtains a detailed information of the fatty acid content of membranes from gas chromatography (GC).

In order to study effects of temperature changes on fatty acid compositions, 3 human cell lines were grown at 37 °C to late exponential phase. Subsequently, one half of the flasks was kept at 37 °C while the second half of the flasks was set to 28.5 °C for 24 hours prior to fatty acids analysis. The following cell lines were used: Human Embryonic Kidney (HEK-293), liver cells (Hep G2) and breast cancer cells (MCF-7). Beside the distinct physiological differences, a predominate difference between these cell lines is their content of the enzyme Desaturase [105]. It is highest in MCf-7 followed by Hep G2 and HEK-293. After growth and temperature shift, the cell lipids where extracted and analyzed chromatographically (section A.2).

The analysis of the data reveals that the ratio of unsaturated fatty acids to saturated fatty acid is enhanced in cells kept at 28.5 °C compared to cells from 37 °C (Fig. 6.14). This finding is in particular considerable when one focuses on the 16 and 18 long chains. Both types of chains serve as natural substrate for the Desaturase in human cells (see next section). Evidently, the higher degree of unsaturation at 28.5 °C demonstrates that the transition is shifted towards lower temperatures implying to some extent an increase in fluidity often mentioned before in the context of “homeoviscous adaptation” [55, 142]. In high Desaturase expressing cells like in MCF-7 the observed shift in ratio is more pronounced than it is in low expressing cells like HEK-293. The ratio is enhanced by a factor of 3 in the case of MCF-7 cells and by a factor of 1.2 in the case of Hep G2 cells and HEK-293 cells. Higher levels of Desaturase in trend lead to faster adaptation.

	cells	cells	cells	cells	cells	cells
Fatty acids	MCF-7 28,5°	MCF-7 37°	Hep G2 28,5°	Hep G2 37°	HEK-293 28,5°	HEK-293 37°
12:01	0,00	3,88	33,47	41,03	40,39	66,98
14:00	11,09	7,28	0,42	0,79	0,50	0,72
14:01	2,44	2,86	2,74	2,36	1,07	0,64
15:00	5,66	9,88	0,85	0,75	1,26	1,14
16:00	22,72	24,01	16,24	17,04	13,77	7,88
16:01	0,98	0,35	10,43	7,29	3,28	1,52
17:00		3,55	2,21	1,57	3,64	2,44
18:00	11,49	12,52	2,89	2,97	4,99	3,07
18:1 (n-9)	35,09	8,21	15,38	13,35	19,46	10,26
18:1 (n-7)	3,36	5,06	9,25	8,16	2,22	1,48
18:2 (n-6)	0,00	0,51	2,13	1,47	6,48	2,25
18:3 (n-6)	0,55	0,50	0,12	0,05	0,29	0,13
18:3 (n-3)	1,73	0,19	0,21	0,03	0,05	0,05
20:00	1,60	1,28	0,11	0,09	0,12	0,07
20:1 (11-13)	0,27	28,36				0,05
20:1 (13-15)	0,13	0,66	1,73	1,37	0,26	0,21
20:3 (n-6)	0,11		0,33	0,23	0,11	
20:3 (n-9)	0,42	0,24	0,34	0,24	0,25	0,15
20:04	1,30		1,75	1,28	2,51	1,67
20:05	0,06			0,03	0,06	0,04
22:00	1,23	0,55	0,21	0,07	0,15	0,08
22:01						0,04
22:5 (n-3)	0,25		0,29	0,16	0,26	0,18
22:06	0,20		0,08	0,06	0,15	0,10
24:00:00	0,23					
% of total fatty acid	100,00	100,00	100,00	100,00	100,00	100,00

Figure 6.13: Fatty acid composition of three human cell lines which were grown at 37 °C. Subsequently one half of the flask was kept at 28.5 °C for 24 hours. Grey shaded fields indicate the fatty acid chains that are directly involved in catalytic reactions with Desaturase. The amount of unsaturated fatty acid is higher at 28.5 °C than at 37 °C demonstrating adaptive processes.

Discussion The results gained through gas chromatography are conform to the DSC data and give rise to the conclusion that human cells change their lipid composition to maintain a certain physical state of the membrane when the temperature of growth is shifted. Importingly, these data not only confirm but extend the known adaptation from simple organisms to cultured human cells.

Compared to the experiments on bacterias, the calorimetric results gained with the human cells feature a strong similarity: beginning and ending of the maximum of the adaptated cells are almost equal before and after the temperature was changed (see section 6.2). A smaller shift in this peak maximum compared to the shift in growth temperature has also been observed in both cell types the PH and the HaCat.

All performed experiments on bacterias and human cells strongly indicate that adaptation occurs in both systems. The similarity of the detected adaptation phenomena in both types of cells mentioned above is intriguing. Both bacterial cells (procaryotes) and human cells (eucaryotes) differ to a great extend in terms of their

	Whole cells					
	MCF-7	MCF-7	Hep G2	Hep G2	HEK-293	HEK-293
	28,5°	37°	28,5°	37°	28,5°	37°
ratio 18:1/18:0 (n-9)	3,05	0,66	5,32	4,50	3,90	3,35
ratio 16:1/16:0	0,04	0,01	0,64	0,43	0,24	0,19
ratio 18:1(total)/18:0	3,54	1,16	9,38	7,77	5,71	4,62

	Microsomes	Microsomes
	Hep G2	HEK-293
ratio 18:1/18:0 (n-9)	5,30	3,56
ratio 16:1/16:0	0,44	0,21
ratio 18:1(total)/18:0	9,09	4,66

Figure 6.14: Ratios of unsaturated to saturated fatty acids of 16 and 18 long carbonhydrogen chains (obtained from Fig. 6.13). In all cell lines the ratios have shifted to lower saturation after the temperature was set to 28.5 °C. Additionally the ratios of Desaturase containing microsomes, which were extracted from cells grown at 37 °C, are depicted. The data indicate that the fatty acid ratio of microsomes are representative for the ratios of whole cells.

complexitiy, size, components, processes, natural environments, cooperativity with neighbour, etc. Furthermore, in both cell types very different metabolic processes lead to the modifications in the lipid composition, e.g. in the case of simple organism like bacteria, Desaturase has been found to catalyze the unsaturation of fatty acids and lipids, whereas in the case of human cells unsaturation is restricted to fatty acids (e.g. [98, 44, 53, 119]). All demonstrated facts lead to the conclusion that the underlying processes of cell adaptation are absolutely fundamental and of universal character rather than cell specific.

6.5 The Activity of Membrane Bound Desaturases

The aim for the following section was to find out wether the correlation of enzyme activity and membrane phase state, that was found for Acetylcholinesterase, also holds for Desaturase, which is one of the key enzymes in adaptation. Although due to the strong binding of the enzyme reproducable purification is still an issue, the activity of membrane bound Desaturase will be presented to depend on the lipid phase state.

The familiy of Desaturases is ubiquitos in all organisms and has already been shortly introduced in section 6.1. The enzymes catalyze the insertion of double bonds at various positions of fatty acids chains and lipids (e.g. [98]). Through this function they feature a key role in maintaining membrane fluidity as well as

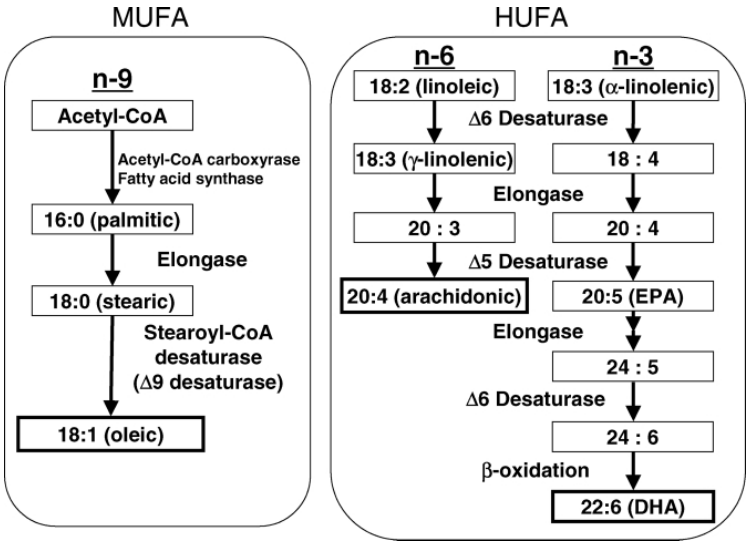

Figure 6.15: Synthesis of unsaturated fatty acids in mammals. Left: monounsaturated fatty acid (MUFA). Right: highly unsaturated fatty acid (HUFA). EPA: eicosapentaenoic acid and DHA: docosahexaenoic acid [98].

in the metabolism of triglycerides (fat tissue) and is also involved in the further synthesis of several important fatty acids like Docosahexaenoic acid (22:6 chain acid) [98, 149, 148, 38, 67, 118, 104, 93, 42, 128, 44, 53]. Fig. 6.15 displays a schematic drawing of the metabolism of unsaturated fatty acids in mammals. In terms of thermodynamic behaviours of Desaturase related systems it was published that the natural lipid environment of Desaturase exhibit a phase transition temperature themselves at about 39 °C [81]. In another study it was shown that the acitivity of the enzyme is enhanced in the order transition of hydrogenated membranes [62].

Within the present thesis, experiments on Desaturase were performed in the lab of Prof. Ntambi [105] by using stearoyl-CoA-Desaturase (SCD). This subspecies of Desaturases catalyzes the insertion of a double bond at the 9th position of the fatty acids in human cells. The reaction displays the last step in fatty acid synthesis.

In a set of experiments human Hep G2 cells and HEK-293 cells (see previous section) were grown to confluence at 37 °C. Subsequently, SCD-containing microsomes were extracted (section 4.5.2) and stored at -80 °C for further applications. The activities were determined through the conversion of radioactive labeled 18:0 fatty acids into 18:1 fatty acids (section A.1).

SCD Activity ceases at high assay temperatures In order to find out wether the phase state of the microsomes influences the function of SCD, activity assays were performed at variaous temperatures. The presented data resemble a mean of three

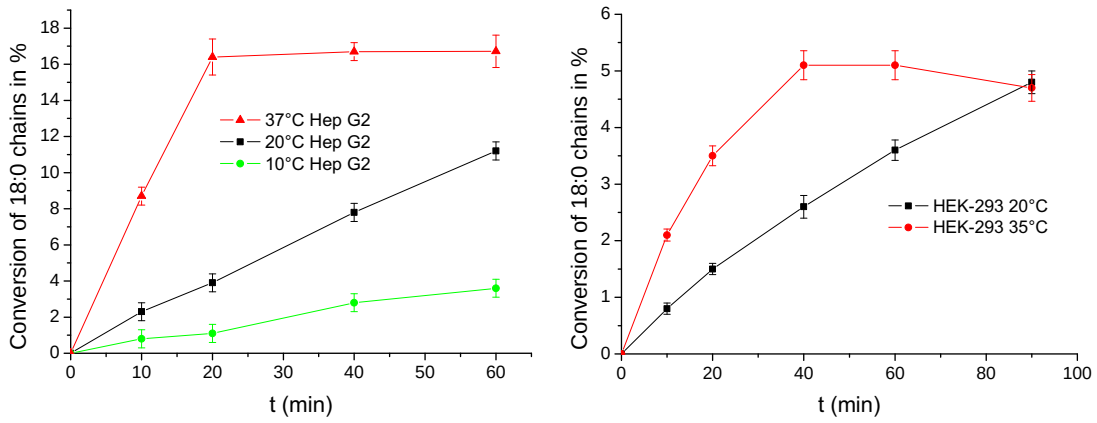

Figure 6.16: Conversion of 18:0 to 18:1 fatty acid chains in Hep G2 cells and in HEK-293 cells, determined at varying temperatures. At 37 °C the conversion ceases. Note that the activity can be obtained from the slope of these curves.

separate experiments. Measurements that were performed by additionally inhibiting the proteases did not affect the activity.

In microsomes of both cell lines the conversion of 18:0 fatty acids increased linear in time for assays performed at 10 °C and 20 °C. Whereas, at 37 °C the kinetics ceased after 20 minutes (Hep G2) and 40 minutes (HEK-293), respectively (Fig. 6.16) (The apparent decrease of the activity after 90 minutes in the case of HEK-293 SCD can be related to further conversion of oleic acid into 18:2 chains). In microsomes of both cell lines the enzyme activity stops after 16.5 % of converted 18:0 in the case of Hep G2 and after 5 % in the case of HEK-293. The obtained results are in good accordance with studies in hen liver microsomal SCD [53, 67], whereby saturation has never been measured in human cell SCDs.

The activities of SCD from both cell lines display a kink in the Arrhenius plot (Fig. 6.17). According to the Arrhenius equation

$$k = F \cdot \exp(-\frac{E_\mathrm{a}}{k_\mathrm{B}T}) \tag{6.15}$$

a kink resembles the change in activation energy E_a. Such kinks have been detected in studies on membrane bound enzymes before [17, 74, 124] and was mentioned for Acetylcholinesterase in the first part of the thesis. In single component lipid systems they occur at the temperature of the main phase transition (e.g. [148]). In the present case they were supposed to mark the phase transition temperature of the local membrane environment of the SCD.

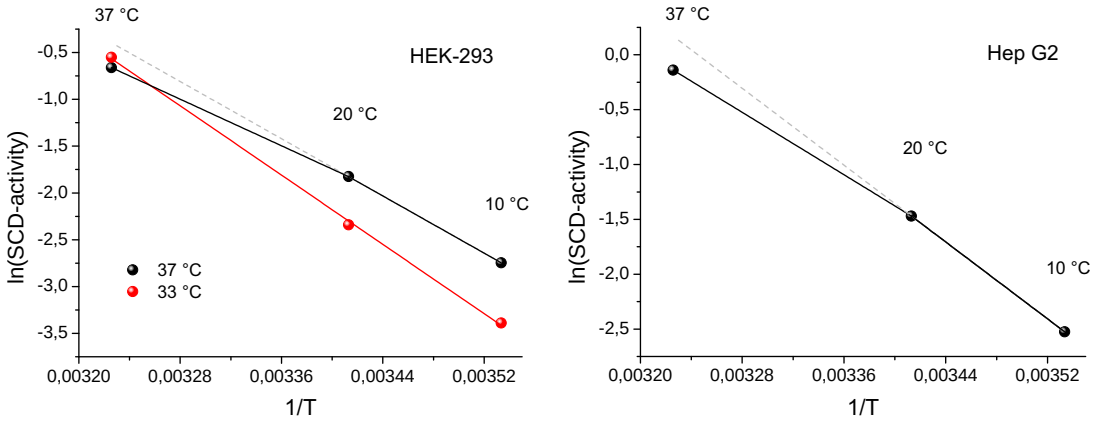

Figure 6.17: Arrhenius plots of SCD activities of HEK-293 cells (left) and Hep G2 cells (right). Activities of SCD from both cell lines display a kink in the plot when they were grown at 37 °C. HEK-293 cells kept at 33 °C for 5 hours do not display a kink. The activity assays took place at 20 °C and data were analyzed after 10 minutes (Hep G2) and 20 minutes (HEK-293), respectively.

Phase transition in human microsomes In order to test wether the microsomes exhibit a membrane phase transition, the heat capacities of extracted microsomes from Hep G2 cells were measured in the DSC (Fig. 6.18). Indeed, a local maximum was found at $T \approx 15$ °C. The detected transition temperature is very close to the 12 °C which were measured for the extracted lipids of whole HaCat cells and MV3 cells. Since the fatty acid ratios of microsomes and whole cells are very similar (see Fig. 6.14) the transition of the whole HEK-293 cells used in the present studies might also take place at 15 °C.

A decrease in growth temperature abolishes kink Since at lower growth temperatures more unsaturated lipids were detected (previous section), in the next step it was tested wether SCD activity increases when cells are subject to a decrease in temperature. For this purpose SCD acitivities from HEK-293 cells that were kept at 33 °C for 5 hours were determined and compared to the SCD activities of cells grown at 37 °C (Fig. 6.17). This time, no kink was observed in the Arrhenius plot of SCD from the cells kept at 33 °C meaning that the activity displays Arrhenius behaviour. This in turn reveales that the phase state of the microsomal membrane has changed.

Influence of fatty acids on the membrane phase transition In the following, the degree of change in membrane phase states through saturated and unsaturated fatty acids will be presented and compared to the concentrations of the real microsome systems. This is especially relevant for the studied SCD system of human cells which establish unsaturation in fatty acids before lipids are generated. For this purpose,

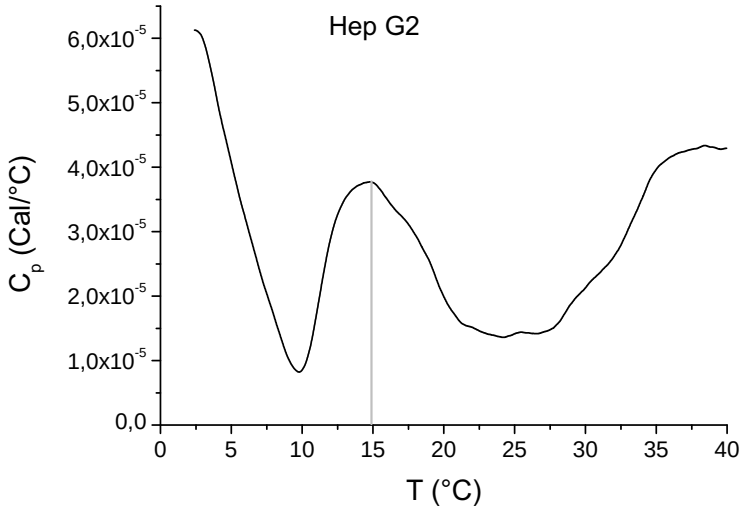

Figure 6.18: Heat capacity profile of Hep G2 microsomes. At 15 °C a (local) maximum occurs. The indicated maximum at higher temperatures originates from protein denaturation.

in two series of experiments, several concentrations of stearic acid (18:0) and oleic acids (18:1) were incorporateed into small unilamellar DMPC vesicles before they had been swelled (the above used stearoyl-CoA differs to stearic acid in the head group and is converted to the latter after the unsaturation has taken place, see also 6.15). Subsequently the heat capacities were determined in the DSC (Fig. 6.19). Fatty acids were of puriss grade and were purchased from Sigma [135].

Stearic acid gradually shifted the phase transition of DMPC to higher temperatures when its concentration was increased, whereas a downshift was observed for oleic acid (Fig. 6.19). In both cases high concentrations of 10% lead to almost abolished transitions. The results demonstrate the incorporation of the fatty acids into the membranes originating in the hydrophobic character of the chains. Because of the strongly differing phase behaviours of the fatty acids, the shifts to higher temperatures through stearic acid (T_m = 69 °C) and to lower temperatures through oleic acid (T_m = 13 °C) were in accordance with the expectations.

SCD features a main role in adaptation These findings are now compared to the concentrations of fatty acids involved in the SCD reactions: The amount of converted stearic acid per SCD experiment was calculated to be in the order of μMol and the total lipid amount in microsomes was in the order of mMol. This means that the ratio of oleic acid to microsomal-lipid is in the small order of 0.1 percent, which is in a range where only small disturbances of the melting profile were observed (Fig. 6.19). However, the analysed data of the experiments originated from short measure

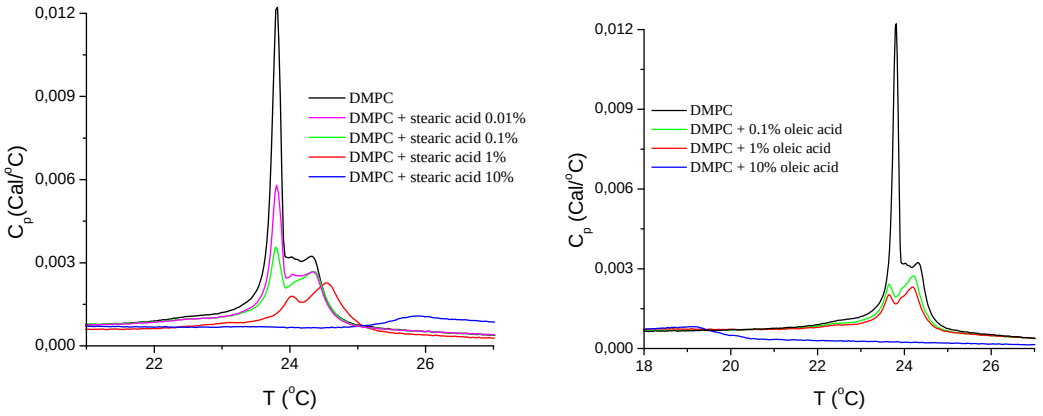

Figure 6.19: Heat capacity profiles of DMPC with various concentrations of fatty acids. Stearic acid (left) increases the maximum of the heat capacity and shifts the peak to higher temperatures, the more the higher the concentration is. In contrast, a shift to lower temperatures is observed for high concentrations of oleic acid (right).

intervalls of 10 and 20 minutes. Therefore, the amount of converted fatty acids has to be extended to the long time ranges that human cells need to adapt to alterd conditions (see also section 6.4) and can be concluded to be in the order of percents within several hours. Moreover, also the metabolic conversion of fatty acids into lipids needs to be taken into account. Such processes take place in parallel to the unsaturation of fatty acids. Hence, from lipids it is well known that unsaturation strongly influence the phase state of the membranes (e.g. [77, 78]).

Discussion The results in this section are a further indication that membrane phase transition might be crucial for cell function and adaptation. Both findings the heat capacitiy maximum as well as the kink in Arrhenius plot demonstrated the existence of transition states in the membranes of HEK-293 cells (At present, the exact temperature at which the Arrhenius kink occurs is only roughly determined to occur between 10 °C and 37 °C). Interestingly, all phase transitions of membranes of human origin that were detected in this thesis so far, were found to be in the range from 11 - 15 °C. The multiple occurance of this temperature range in three different cell lines indicates a general temperature range which seems to be crucial for cell function.

Although, a phase state dependent maximum activity of SCD has not been detected yet, the absence of the kink when HEK-293 were shifted to 33 °C impressingly indicates that a change in the physical state of the microsomal membrane has taken place. This result leads to the conclusion that in the shifted cells the SCD activity might have increased compared to cells kept at 37 °C.

The cease in activity at 37 °C, that was found at the beginning of the section, probably originated from the following: beside SCD, the catalytic reaction requires NADH, oxygen, and an electron transport sequence comprising NADH-cytochrome b5 reductase and cytochrome b5 [98]. The detected cease of activity therefore may be traced back to the depletion of one of these components. In living cells, however, it is expected that these substances are supplied permantently by the cells and therefore a cease in activity will unlikely take place.

Several percent of unsaturated fatty acids within the cell membrane (and therefrom generated lipids) were found to cause a significant phase transition shift of the DMPC membranes. Extrapolating the measured amounts of unsaturated fatty acids to the longer adaptation time spans in living cells, then the values are supposed to account for the observed shifts of a factor 1.2 and 3 found above in the fatty acid analysis (Fig. 6.14).

6.6 A General Model of Cell Adaptation

A general thermodynamic description of cell membrane adaptation is presented. Motivated by the above findings of enzyme-membrane correlation and membrane adaptation, the physical state of membranes and its control over enzyme activity are put at the beginning of the model. It is demonstrated that if processes, which are involved in lipid adaptation, are correlated to fluctuations in the membrane the system will "self organised" evolve towards the lipid phase transition. this explains the observation of homeoviscous adaptation. The explanation is free of further model assumption and can be easily verified.

6.6.1 Theoretical Considerations

Adaptive thermodynamic potentials First, a rather macroscopic description of a system perfectly adapted to its environment at $T_E = T_m$ is considered, where T_E is the growth or environmental temperature and T_m the temperature at which the heat capacity profile (experimentally determined) exhibits a maximum. Adapted in this sense basically means, that the distribution of lipids $W(n_i)$ remains constant over time, where the observable n_i is not further specified, but will in principle determine the degree of fluidity of the lipid (order parameter ζ) and could, for example, reflect the area per molecule, the charge or from a chemical perspective the chain length or degree of saturation of the alkyl chains.

The exact coincidence of T_E and T_m is an idealization of the experiment as in nature the adapted state is slightly above T_m (see previous sections). However, it will be shown below that this idealization captures the major idea of the theory and the

extension to real systems can easily be implemented by accounting for the known asymmetry in fluctuations between gel and fluid-like phase.

The basis of the theory was given in chapter 1.1 and the following experimental sections. Nevertheless, it is shortly recalled: It has been shown that one can attribute an independent thermodynamic potential $S(n_i)$ (interfacial potential) to lipid membranes and monolayers by experimentally demonstrating the existence of both reversible fluctuations and sound propagation over macroscopic distances [52, 163, 57, 70]. This finding is in accordance with the postulation of the lipid interface entropy which was introduced by Kaufmann and is based on Einsteins work [70, 34, 35]. The lipid states of each system (e.g. the plasma membrane) are described by a thermodynamic or entropy potential $S(n_i)$ of the membrane, which according to $S(n_i) = k \cdot lnW$ determines their distribution $W(n_i)$. For small changes in n_i, $S(n_i)$ was expanded in a power series:

$$S \approx S_0 + \sum_i \left(\frac{\partial S}{\partial n_i}\right) n_i + \frac{1}{2} \sum_i \sum_j \left(\frac{\partial^2 S}{\partial n_i \partial n_j}\right) n_i n_j \tag{6.16}$$

Stability in the lipid distribution (Eq. 6.16) requires the vicinity of an extremum (maxima or minima) of the entropy potential [117]. The first derivative is therefore approximately zero and hence:

$$S \approx S_0 + \frac{1}{2} \sum_i \sum_j \left(\frac{\partial^2 S}{\partial n_i^2}\right) n_i n_j. \tag{6.17}$$

Assuming a continous transition, S becomes flat near T_m (Fig 6.20a) which is equivalent to high fluctuations in n_i according to

$$\left\langle (\delta n_i)^2 \right\rangle = -k_\mathrm{B} \left(\frac{\partial^2 S}{\partial n_i^2}\right)^{-1} \tag{6.18}$$

External disturbance Increasing the environmental temperature $T_E \rightarrow T'_E \neq T_m$, will increase the relative number of lipids in the fluid state (Fig. 6.20b). Since the fluctuations are maximal at $T_E = T_m$, they decrease upon any change in T, which in turn requires a steeper thermodynamic potential with higher curvature according to eq. 6.17 and 6.18 (Fig. 6.20a). As it was introduced at the beginning of the thesis, the actual relations between the second derivatives of S or fluctuations and thermodynamic susceptibilities are:

$$\left\langle (\delta A)^2 \right\rangle = -k_\mathrm{B} \left(\frac{\partial^2 S}{\partial A^2}\right)_T^{-1} = k_\mathrm{B} T \overline{A} \kappa_T. \tag{6.19}$$

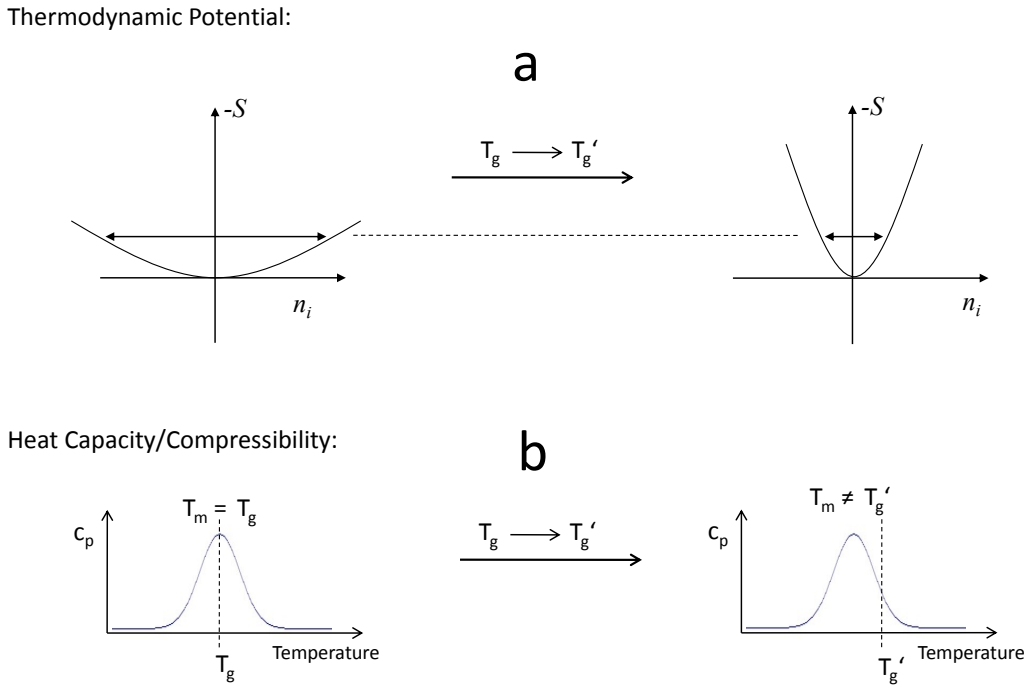

Figure 6.20: Entropy potentials (a) and corresponding heat capacity profiles (b) following a temperature jump $T_E \to T_E'$. From eq. 6.20 it is known that $c_p \propto \left(\frac{\partial^2 S}{\partial H^2}\right)$. (Left) Originally, the system is in the vicinity of the transition. Assuming a continuous transition this corresponds to a flat thermodynamic potential. (Right) Immediately after the temperature increase the system accumulates in a state above the transition, which in turn calls for a more steep thermodynamic potential.

and also

$$\left\langle (\delta H)^2 \right\rangle = -k_\mathrm{B} \left(\frac{\partial^2 S}{\partial H^2} \right)_T^{-1} = k_\mathrm{B} T^2 c_p \tag{6.20}$$

Consequently, a change of curvature in $S(H)$ results in a different heat capacity c_p, consistently with Fig. 6.20.

6.6.2 Fluctuations and Enzyme Activity

An integral part of the model is based on the assumption that interface fluctuations and enzymatic activity (of enzymes attached to or involved in interface synthesis or degradation) are coupled. This is motivated from the experimental observations with

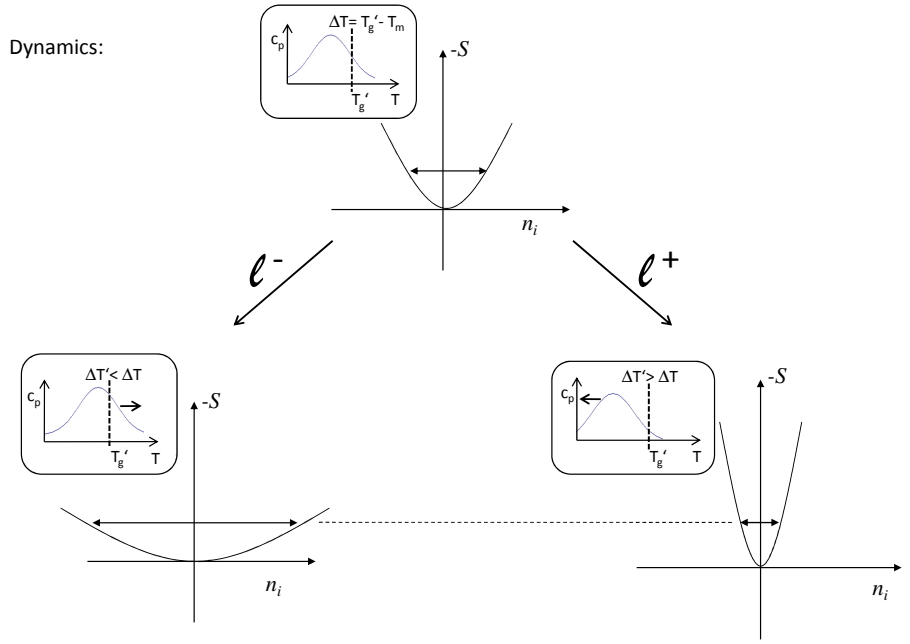

Figure 6.21: Evolution of the thermodynamic potential following a catalytic step. When a lipid is produced or modified, the lipid phase transition of the system can either develop towards (lower left) or away (lower right) from the new environmental temperature T'_E, leading to a decrease or increase in ΔT'. A decrease in ΔT' corresponds to a decrease in curvature, which in turn increases the growth rate g. Effect exaggerated.

Acetylcholinesterase in chapter 5 and from the maximum activity of Phospholipase A2 in the phase transition of the surrounding membranes [3, 61, 109, 110, 68, 80, 141]. Furthermore, experimental data from the previous section proved the occurance of phase state dependent Desaturase activity. It has also been shown that the lipid microenvironment of Desaturases exhibits a distinct phase transition [81]. Though, Desaturases are difficult to purify, their activity has be found to be enhanced in the order transition of membranes [62].

Assuming that this phenomenon is of general character, the working hypothesis states that the rate of lipid synthesis, modification or growth α is simply proportional to the fluctuations $\left\langle (\delta n_i)^2 \right\rangle$:

$$\alpha \propto \left\langle (\delta n_i)^2 \right\rangle \propto - \left(\frac{\partial^2 S}{\partial n_i^2} \right)^{-1} \tag{6.21}$$

A steeper thermodynamic potential S, occurring for example as a consequence of the temperature jump $T_E \rightarrow T'_E$ (Fig. 6.20), implies therefore a reduction in enzyme activity. Near T_m, in the adapted state, the activity is optimized and either shift along the c_p-profile, caused for instance by a variation in temperature will decrease the activity. It will be demonstrated that this represents a stability criteria which "locks" the membrane near T_m. In order to provide for a transparent interpretation between enzymatic activity and adaptation, no further assumptions on the catalytic mechanism are imposed. The a-priori probability for a catalytic step that decreases or increases the phase transition of the membrane are kept equal.

Following the temperature shift $T_E \rightarrow T'_E$, two szenarios can be visualized: i) the production of lipids that shift towards T_m and ii) the production of lipids that shift away from T_m . While the first results in a decrease in both and the curvature of the thermodynamic potential, the second has the opposite effect (Fig. 6.21). In the first case, the system has moved to a potential with smaller curvature and therefore higher fluctuations. This is resembled in a position lying closer to the heat capacity maximum where fluctuations are higher and therefore the enzyme activity is higher (eq. 6.21). In the second case the system has evolved towards a potential of higher curvature and therefore smaller fluctuations resulting in a lower enzyme activity (eq. 6.21), which means an evolution away from the maximum of the heat capacity. Extending the scenario depicted in Fig. 6.21 from one to an entire ensemble of individual systems will lead to the observed adaptation process as described in the next paragraph.

6.6.3 Evolution of the Populations

In the following a system is defined as a multi lipid component membrane with certain distribution. The maximum of the phase transition profile of the heat capacity c_p at $T_E = T_m$ is proposed to resemble the distribution with highest propability. This state of highest probability originates from the fact that highest fluctuations in the phase transition lead to highest enzyme activities and therefore keep the membrane at this region. In the case of $T_E \neq T_m$ this in turn means, that if a catalytic step shifts the phase state of the system at $T_E \neq T_m$ towards T_m (smaller ΔT), this system will grow faster, meaning the next catalytic step will take place "sooner". Even though it appears intuitively clear that over time these systems, which grow faster, will represent the majority of the overall population and dominate the ensemble, briefly the population dynamics is described in analogy with a modified diffusion process.

Diffusion analog In the present case the object of diffusion is virtual and best represented by the maximum of the heat capacity profile, which "diffuses" along

the 1D temperature axis when the lipid composition changes (Note, that while T'_E is essentially a constant boundary condition the transition temperature T_m is a dynamic variable, which changes after each catalytic step). In this picture, the diffusion constant, which is given by the frequency of individual random steps, is represented by the enzyme activity which is reflected in the turn-over rate (This value originates from the degree of fluctuation of the reaction coordinate, see also section 3.2). The higher this rate, the more flickering of T_m will take place. The further away T_m is from the environmental temperature T'_E, that is the larger ΔT is, the smaller is the enzyme activity and therefore the smaller occurs the flickering of T_m. The reason for this behaviour is found in the higher fluctuations at the center of the heat capacity profile than apart from it (see above). In the picture of diffusion this means that also the diffusion constant D becomes the smaller the larger ΔT is, implying that D appears as a variable. The system represents an ensemble of diffusing objects with a spatially varying diffusion constant $D(x)$ or equivalent ΔT dependent activity $\alpha(\Delta T)$):

$$D(x) \rightarrow \alpha(\Delta T) \tag{6.22}$$

always keeping in mind that ΔT is just the representation of the difference of two lipid compositions which establish a phase transition that can be detected e.g. by calorimetry.

The diffusion in one physical variable (e.g. space, or angle) leads to a development towards (-) a certain point (here the phase transition $T_E = T_m$ of the membrane, the region around this point denotes the states with highest overall probability) with each step featuring equal probability $P_+ = P_-$. Although each single state resembles the same propability, regions closer to the transition maximum represent higher fluctuations and lead to the evolution in this direction. In statistics it is shown that the ensemble of all possible sequences becomes overwhelming as the number of steps becomes large.

Consequently a system does not remain at its position but starts to diffuse. Therefore, the particles will migrate towards regions of *higher mobility (or larger D)*. Regions of lower D will become depletion zones. The "diffusing" state of the membrane will eventually reach the point where $\Delta T = 0$, i.e. the maximum of the heat capacity profile coincides with T_E'. In this state either shift of T_m will lead to a decrease of the enzymatic activity $\alpha(\Delta T)$, since it already reached its maximum value α_{max}. Consequently the system is stable and will remain near this state until external perturbations (e.g. temperature changes, pH changes, changes in the chemical or ionic environment) will force it to adapt again.

6.6.4 Discussion

The presented model is certainly an idealization, but fairly robust in its assumption. A few of the assumption are discussed briefly in light of known experiments.

1. Asymmetrical distribution

The most obvious difference between the presented model and the experimental results is the asymmetry between heat capacity and T'_E. I.e., the fact that biological membranes adapt their phase transition maximum (T_m) close to, but always below T'_E (see results from experimental sections). This asymmetry is expected from the model simply by including the fact that the fluctuations are not symmetrically distributed around T_m. Experiments show that heat capacities as well as compressibilites are higher in the fluid state than they are in the gel-like phase (e.g. compressibilites in Fig. 2.5):

$$c_{p,fluid} > c_{p,gel} \tag{6.23}$$

$$\kappa_{T,fluid} > \kappa_{T,gel} \tag{6.24}$$

Therefore, fluctuations are higher in the fluid state than in the gel like state of the membrane as well

$$\left\langle (n_i)^2 \right\rangle_{fluid} > \left\langle (n_i)^2 \right\rangle_{gel}) \tag{6.25}$$

and recalling Eq. 6.21 a higher activity towards the fluid phase is expected. This drives the state of adaptation slightly into the fluid phase, which leads to $T'_E > T_m$ in accordance with the experiment.

2. The equal probability

Also, the assumption of equal probabilities for the (+) and (-) catalytic steps is not critical and any ratio between them will lead to the same qualitative result. The reason is that the "growth" of the population with the higher activity is exponential and will for larger timescales not be affected by the actual ratio of the probabilities P_+/P_-. Only the absolut time of the adaptation will change.

3. The system definition

The same holds for the system definition. If more familiar with the molecular point of view, one may ask for a definition of what exactly is called a system. However, the present approach simply claims that such a cooperative unit or system must exist and can be represented by a small microdomain, a membrane patch or even the whole cell? In principle, one would expect that there is a variety of cooperative size scales in cells, but this will not change the general trend of the results and is a question that will not be addressed further in this thesis.

Conclusion A thermodynamic model for cell adaptation has been presented. Starting from the observation of adaptative shifts in the lipid compositions and phase transitions, the perspective was turned around by putting the phase state of the membrane at the beginning of the model. It was assumed that the entropy potential S can be defined. The applied concept of a correlation of enzyme activity and membrane phase state is strongly supported by the findings of the first part of the thesis as well as from the studies on Phospholipase A2.

Apart from changes in temperature, biological membranes are subject to a variety of external influences leading to changes in fatty acid composition, pH, ethanol or adhesion substrates. If those apply to a cell or a cell population, the latter will adapt its lipid composition in the same manner as it was seen for changes in temperature. For example, fatty acids supplemented to the growth medium incorporate into cell membranes. This incorporation causes a shift in the phase transition of the membrane. In analogy to the adaptation process after changes in temperature, the membrane adjusts its membrane to reach the original physical state of the membrane.

Part IV

Summary and Outlook

The subject of the present thesis was the physical investigation of the influence of biological interfaces on general cell function. The obtained results are now summarized and evaluated.

Membrane phase state dependent activity of Acetylcholinesterase In the first results chapter it was demonstrated that one of the fastest enzymes in biology, Acetylcholinesterase, exhibits a membrane phase state dependent acitivity. Acetylcholinesterase showed highest activity when the surrounding membrane was driven through its phase transition. Most of these measurements were performed on Langmuir monolayers which proved to represent an excellent tool to controling the phase states of monolayer membranes. Regulations of such an extent are not possible with any method which is based on bulk measurements. In order to get a detailed information on the interaction of Acetylcholinesterase with such monolayers, a photometer like apparatus was set up onto the Langmuir trough which enabled a parallel recording of enzyme activity and monolayer phase state.

The experiments revealed that Acetylcholinesterase activity was proportional to the compressibility of the monolayer. In the transition range of the monolayer the enzyme featured a 2-3 times higher activity than it did in the liquid condensed and in the liquid ordered states. In several series of further experiments it was proven that the detected correlation is also valid for different types of lipids, changes in pH and also to variations in temperature. The maximum was found in the lipids DPPC, DPPS, DMPS, DPPG and Cardiolipin. Those findings imply that the effect is invariant to changes in any of the thermodynamical parameters and therefore is considered to be of absolute general character. In the experiments, difficulties concerning convective diffusion within both bulk and membranes could be overcome through a variety of improvements of the setup as well as through a complete series of control measurements.

In every single reaction, catalysed by Acetylcholinesterase, one proton is released within an acetic acid molecule. The effect of such protons was experimentally simulated through various monolayer experiments with and without the enzyme. In both membranes and enzymes protons account for dramatic changes in thermodynamic responses. For instance, the activity of Acetylcholinesterase ceased below pH 5, whereas a maximum activity of the local pH at the enzyme was recorded at $pH \approx$ 5.3-5.5. Studies on pure lipid monolayers suggested a phase state dependent ratio of protons accumulated to the membrane. The near bulk pH of the subphase of the monoloayer exhibited a lower pH in the phase transition than it was found in the other phases. The experiments demonstrated the necessitiy to distinguish between bulk and interface measurments as well as between buffered and unbuffered systems. Accordingly, they might also indicate a long range behaviour of the interfacial layer

in pure water systems.

All results presented so far have clearly demonstrated an exceptional role of the interfacial layer consisting of monolyer and Acetylcholinesterase. Changes in certain thermodynamic states of this system lead to dramatic changes in other states. In critical states, like in the phase transitions of membranes, this fact has become very obvious: The activity of Acetylcholinesterase was strongly enhanced when the monolayer was driven through its phase transition. Such a coupling of thermodynamic variables suggests the existence of own thermodynamic properties of the interface.

None of the established theories up to now were able to explain the recorded effects. However, the theory of interfaces and excitable hydration layers invented by Konrad Kaufmann is able to describe almost all phenomena in a satisfying manner. In his theory he introduced a proper entropy which theoretically allows the derivation of many of the observed phenomenons as long as the interfacial layers obtains its own entropy. Through the above findings such interfaces were proven to very likely exist for monolayer-enzyme-hydration layer systems. Developing the entropy potential directly leads to thermodynamic forces and fluctuations. Fluctuations in area are strongly enhanced when the membrane is in its phase transition regime. Therefore, it was concluded that fluctuations lead to the increased activity of Acetylcholinesterase in the phase transition of the membrane and a coupling of area fluctuations and reaction coordinate fluctuations was proposed.

The physics of cell adaptation In the second results chapter, the above findings of the correlation of enzyme catalysis with membrane phase states as well as the assumption of an interfacial entropy were set as a basis for a series of experiments on the phenomenon of cell adaptation. From simple organisms it was known that cells adapt to environmental alterations. This behaviour was proven to be valid not only for simple bacterias but also for human cells as well and therefore was shown to be of very universal character. In order to describe adaptation physically, a general thermodynamic model of adaption was developed on the basis of the entropy potential.

Both bacterial cells (Pseudoalteromonas Haloplanktis, PH) and different types of human cells were kept in culture and subsequently exposed to alterations in temperature. This was usually established by a decrease in growth temperature for a certain period of time. Afterwards the heat capacitiy profiles of the cell membranes were recorded in a DSC. Whole cells of bacterias exhibited distinct phase transitions revealing both reversibel peaks of membrane origin as well as peaks from protein denaturation.

For the first time such adaptive behaviour was also thoroughly proven to take place in

human cell membranes which were extracted beforehand. When the temperature of growth was changed, also the reversibel phase transitions in the membranes displayed a shift in the melting temperature. The analysis of Langmuir monolayer isotherms of these human cell membranes revealed the existence of phase transition plateaus and of a critical point. Due to the similarity of the transitions found in human cells to transitions found in simple organisms, the presented results strongly suggest a crucial role of membrane phase states in biological functions. This finding also verifies the existences of different phases within these biological membranes.

In order to describe the phenomena of adaptation and phase transitions in cell membranes, a general thermodynamic model of cell adaptation was developed. Here, only the above findings served as a basis: The occurance of phase transitions, adaptation, correlation of enzyme activity with membrane phase state and, most important, the entropy potential were the starting points of the model. When a membrane system is subject to environmental variations our interpretation is that the system has been put into a state further apart from the phase transition midpoint of the membrane. Due to higher fluctuations in critical states and phase transitions the enzyme activity was supposed to be maximal in close vicinity to the transition maximum and smaller apart from it. Based on this statement the system was explained to evolve back to a state in or close to the maximum of the phase transition. The reason for this behaviour and for the variations in fluctuations were described to originate in different curvatures of the entropy potential in the various phase states of the membrane. Because of these reasons the potential evolves in time from a steep potential apart from the transition to a more flat potential within the transition range.

The correlation of enzyme activity and membrane phase state was proven for Acetylcholinesterase on monolayers and was also known beforehand to occur with Phospholipase A2 in vesicles. Therefore, the next step was to investigate if important enzymes involved in adaptation processes exhibit the same behaviour. For this purpose a subspecies of the Desaturases was investigated. Though, it was not possible to purify these tightly membrane bound enzyme, it can be proven that its activity depends on the membrane phase state. It was observed that the phase transition in the microsomes, to which Desaturases was bound, had vanished when the cells were subject to temperature changes before the activities were detected. This finding indicates that the studied Desaturase has altered its lipid environment after the external change had taken place. The results suggest an increased activity of the enzyme in this case.

The experimental findings obtained within this thesis contributed to the prove that membrane based interfaces are crucial for cell functioning. The results superimpose with the theory of Konrad Kaufmann. Therefore, both a theoretical as well as

an experimental fundament have been set that can serve as a basis for numerous following studies on interfacial properties of biological matter. Due to the assumption of the interfacial entropy potential, the present thesis represents a rather systemic and deductive approach to biophysical research. In future research, for instance in medicine, the focus can be directed more on the possibilites of changing membrane properties of membrane bound enzymes rather than only enzymes. In addition, of course, the findings obtained with Acetylcholinesterase will be extended to other membrane bound enzymes, too. At present we already study ATPases in terms of these properties in our lab. Moreover, the treatment of membranes as crucial thermodynamic interfaces for biological systems will be elaborated to a much higher extend within the next years. The increased interest on the role of lipids has already been reflected by a dramatic rise in the number of publications having come out the last decade on this topic.

Part V

Appendix

A Procedures

A.1 Desaturase Activity Assay

The SCD-activity was measured essentially as described in [94]. Beforehand, SCD-containing microsomes were extracted as described in section 4.5.2. To prevent protease reactions, several protease inhibitors were added: Phenylmethanesulfonyl fluoride (0.1 mM), Pepstatin A (1/100 from 5mg/ml), leupeptin (1/1000 from 10 mg/ml) and aprotinin (1/1000 from 2 mg/ml).

For a standard reaction the following procedure was applied:

- Prepare amounts of 100 μg of microsomal protein in 40 μl and 0.1 Mol/l of Tris/HCl buffer (pH 7.2).
- Prepare assay buffer leading to final concentratoins of 0.03 mM stearoyl-CoA, 0.3 μCi 14C-stearoyl-CoA, 20 μl of 2 mM NADH in 0.1 M pK buffer
- Start reaction by adding 160 μl to the microsome solution
- After desired time stop reaction by adding 200 μl of 2.5 M KOH in ethanol:H_2O 3.1
- Incubate at 80 °C for 45 minutes
- Add 280 μl formic acid
- Vortex and add 700 μl hexane
- Vigorously vortex
- Dry hexane under nitrogen
- Resuspend in 50 μl of hexane
- Saturated fatty acid and unsaturated fatty acid methyl esters are now separated by 100 g/L $AgNO_3$-impregnated TLC (thin layer chromatography) using Hexane/Diethyl ether (9:1) as developing solution.
- Subsequently count the radioactive fatty acid bands in an instant imager (Packers).

A.2 Fatty Acid Analysis with Gas Chromatography

The following steps were applied to extract total fatty acids from human cells for gas chromatography:

- Homogenize cells on ice with a hand hold homogenizer for 30 seconds, take per each 30 mg of cell tissue 2 ml of Chloroform:Methanol 2:1 containing 10mg/100ml Butylhydroxyltoluel.
- Add 100 μl (1mg/2ml) 17:0 fatty acid
- Transfer solution to new tube and add 1 ml of chloroform:methanol 2:1
- Add 1 ml of 0.01 M HCl and vortex
- Centrifuge 2500 rpm for 10 min
- Remove top layer and transfer bottom layer to new tube
- Add 350 μl 14 % bortrifluorid in methanol, 300 μl benzene and 350 μl methanol
- Add 100 μl of 15:0 (1 mg/ml) to each tube
- Heat in capped tubes for 90 minutes at 100 °C
- Add 1 ml Hexane to tubes and vortex each tube for at least 30 seconds
- Add 0.5 ml water and vortex briefly
- Centrifuge 2500 rpm for 5 minutes
- Transfer upper hexane phase to a new tube and evaporate under nitrogen
- Resuspend in 100 μl hexane
- Fill gas chromatograph with small amounts ($\sim$ 10 μl of solution)

B Lipids

B.1 Nomenclature

The following abbreviations of lipids were used:

DMPC	:	1,2-Dimyristoyl-sn-Glycero-3-Phosphocholine
DMPA	:	1,2-Dimyristoyl-sn-Glycero-3-Phosphate
DPPC	:	1,2-Dipalmitoyl-sn-Glycero-3-Phosphocholine
DPPG	:	1,2-Dipalmitoyl-sn-Glycero-3-[Phospho-rac-(1-glycerol)]
DMPS	:	1,2-Dimyristoyl-sn-Glycero-3-Phospho-L-Serine (sodium salt)
DPPS	:	1,2-Dipalmitoyl-sn-Glycero-3-Phospho-L-Serine (sodium salt)

B.2 Cardiolipin

Cardiolipin is a negatively charged lipid that features four fatty acid chains. The structure of the used form (14:0 CA, (sodium salt) or also 1',3'-bis[1,2-dimyristoyl-sn-glycero-3-phospho]-sn-glycerol (sodium salt)) was:

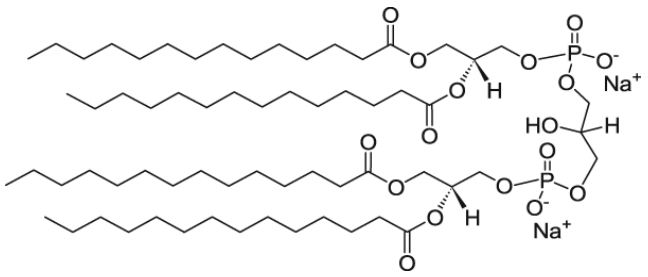

Bibliography

[1] B. Aloni and A. Livne. Acetylcholine esterase as a probe for erythrocyte-membrane intactness. *Biochim Biophys Acta*, 339(3):359–366, Mar 1974.

[2] V. F. Antonov, V. V. Petrov, A. A. Molnar, D. A. Predvoditelev, and A. S. Ivanov. The appearance of single-ion channels in unmodified lipid bilayer membranes at the phase transition temperature. *Nature*, 283(5747):585–586, Feb 1980.

[3] R. Apitz-Castro, M. K. Jain, and G. H. De Haas. Origin of the latency phase during the action of phospholipase a2 on unmodified phosphatidylcholine vesicles. *Biochim Biophys Acta*, 688(2):349–56, 1982.

[4] Avanti Polar Lipids, Inc., 700 Industrial Park Drive, Alabaster, Alabama 35007-9105, USA.

[5] A. D. Bangham. Lipid bilayers and biomembranes. *Annu Rev Biochem*, 41:753–76, 1972.

[6] P. L. Barton, A. H. Futerman, and I. Silman. Arrhenius plots of acetylcholinesterase activity in mammalian erythrocytes and in torpedo electric organ. effect of solubilization by proteinases and by a phosphatidylinositol-specific phospholipase c. *Biochem J*, 231(1):237–240, Oct 1985.

[7] Tobias Baumgart, Adam T Hammond, Prabuddha Sengupta, Samuel T Hess, David A Holowka, Barbara A Baird, and Watt W Webb. Large-scale fluid/fluid phase separation of proteins and lipids in giant plasma membrane vesicles. *Proc Natl Acad Sci U S A*, 104(9):3165–3170, Feb 2007.

[8] Tobias Baumgart, Samuel T Hess, and Watt W Webb. Imaging coexisting fluid domains in biomembrane models coupling curvature and line tension. *Nature*, 425(6960):821–824, Oct 2003.

[9] G. Beauregard, M. Potier, and B. D. Roufogalis. Modulation of erythrocyte acetylcholinesterase by cardiolipin: effect on subunit coupling revealed by irradiation inactivation. *Biochem Biophys Res Commun*, 96(3):1290–1295, Oct 1980.

[10] G. Beauregard and B. D. Roufogalis. Characterization of lipid-protein interactions in acetylcholinesterase lipoprotein extracted from bovine erythrocytes.

Biochem J, 179(1):109–117, Apr 1979.

[11] J. F. Blazyk and J. M. Steim. Phase transitions in mammalian membranes. *Biochim Biophys Acta*, 266(3):737–41, 1972.

[12] A. Blicher, K. Wodzinska, M. Fidorra, M. Winterhalter, and T. Heimburg. The temperature dependence of lipid membrane permeability, its quantized nature, and the influence of anesthetics. *Biophys J*, 96(11):4581–91, 2009.

[13] E. G. Bligh and W. J. Dyer. A rapid method of total lipid extraction and purification. *Can J Biochem Physiol*, 37(8):911–917, Aug 1959.

[14] G. Boheim, W. Hanke, and H. Eibl. Lipid phase transition in planar bilayer membrane and its effect on carrier- and pore-mediated ion transport. *Proc Natl Acad Sci U S A*, 77(6):3403–3407, Jun 1980.

[15] L. Boltzmann. Über die mechanische bedeutung des zweiten hauptsatzes der wärmetheorie. *Wien. Ber.*, 53:195–220, 1866.

[16] M. M. Bradford. A rapid and sensitive method for the quantitation of microgram quantities of protein utilizing the principle of protein-dye binding. *Anal Biochem*, 72:248–254, May 1976.

[17] Thomas A. Brasitus, David Schachter, and Theofanis G. Mamouneas. Functional interactions of lipids and proteins in rat intestinal microvillus membranes. *Biochemistry*, 18(19):4136–4144, September 1979.

[18] Brunswick Scientific, PO Box 4005 Edison, NJ 08818-4005 USA.

[19] J N Bryngelson JD FAU Onuchic, N D Onuchic JN FAU Socci, P G Socci ND FAU Wolynes, and Wolynes PG. Funnels, pathways, and the energy landscape of protein folding: a synthesis. (0887-3585 (Linking)):–, 1995.

[20] H.B. Callen. *Thermodynamics and an Introduction to Thermostatistics*. John Wiley & Sons, 1985.

[21] M. A. Casadei, P. Manas, G. Niven, E. Needs, and B. M. Mackey. Role of membrane fluidity in pressure resistance of escherichia coli nctc 8164. *Appl Environ Microbiol*, 68(12):5965–72, 2002.

[22] Gregor Cevc. *Phospholipids Handbook*, volume 1. Marcel Dekker, New York, 1993.

[23] D. Chapman. Phase transitions and fluidity characteristics of lipids and cell membranes. *Q Rev Biophys*, 8(2):185–235, 1975.

[24] C. H. Chen, B. M. Zuklie, and L. G. Roth. Elucidation of biphasic alterations on acetylcholinesterase (ache) activity and membrane fluidity in the structure-functional effects of tetracaine on ache-associated membrane vesicles. *Arch Biochem Biophys*, 351(1):135–140, Mar 1998.

[25] C. M. Chow and M. F. Islam. Colorimetric determination of red blood cell acetylcholinesterase activity. *Clin Biochem*, 3(4):295–306, Dec 1970.

[26] Jens Chr. Skou. Studies on the influence of the degree of unfolding and orientation of the side chains on the activity of a surface-spread enzyme. *Biochimica et Biophysica Acta*, 31(1):1–10, January 1959.

[27] E. F. DeLong and A. A. Yayanos. Adaptation of the membrane lipids of a deep-sea bacterium to changes in hydrostatic pressure. *Science*, 228(4703):1101–1103, May 1985.

[28] T. J. Denich, L. A. Beaudette, H. Lee, and J. T. Trevors. Effect of selected environmental and physico-chemical factors on bacterial cytoplasmic membranes. *J Microbiol Methods*, 52(2):149–82, 2003.

[29] P. W. Van Dijck, B. De Kruijff, L. L. Van Deenen, J. De Gier, and R. A. Demel. The preference of cholesterol for phosphatidylcholine in mixed phosphatidylcholine-phosphatidylethanolamine bilayers. *Biochim Biophys Acta*, 455(2):576–587, Dec 1976.

[30] L. Edman and R. Rigler. Memory landscapes of single-enzyme molecules. *Proc Natl Acad Sci U S A*, 97(15):8266–8271, Jul 2000.

[31] Lars Edman, Zeno Földes-Papp, Stefan Wennmalm, and Rudolf Rigler. The fluctuating enzyme: a single molecule approach. *Chemical Physics*, 247(1):11 – 22, 1999.

[32] Elena M. Egorova. Dissociation constants of lipid ionizable groups i. corrected values for two anionic lipids. *Colloids and Surfaces A: Physicochemical and Engineering Aspects*, 131(1-3):7–18, January 1998.

[33] M. Eigen and R. Rigler. Sorting single molecules: application to diagnostics and evolutionary biotechnology. *Proc Natl Acad Sci U S A*, 91(13):5740–5747, Jun 1994.

[34] A. Einstein. Über die von der molekularkinetischen theorie der wärme geforderte bewegung von in ruhenden flüssigkeiten suspendierten teilchen. *Annalen der Physik*, 322(8):549–560, 1905.

[35] A. Einstein. Theorie der opaleszenz von homogenen flüssigkeiten und flüssigkeitsgemischen in der nähe des kritischen zustandes. *Annalen der Physik*, 14(S1):368–391, 1910.

[36] Albert Einstein. Folgerungen aus den capillaritätserscheinungen. *Annalen der Physik*, 309(3):513–523, 1901.

[37] Fau A AndreasV Jr Feather-Stone RM Ellman GL, Courtney KD. A new and rapid colorimetric determination of acetylcholinesterase activity. (0006-2952

(Linking)):–, 1959.

[38] H. G. Enoch, A. Catala, and P. Strittmatter. Mechanism of rat liver microsomal stearyl-coa desaturase. studies of the substrate specificity, enzyme-substrate interactions, and the function of lipid. *J Biol Chem*, 251(16):5095–103, 1976.

[39] M. Esfahani, A. R. Limbrick, S. Knutton, T. Oka, and S. J. Wakil. The molecular organization of lipids in the membrane of escherichia coli: phase transitions. *Proc Natl Acad Sci U S A*, 68(12):3180–4, 1971.

[40] Alan Fersht. *Structure and Mechanism in Protein Science*. W. H. Freeman and Company, 1998.

[41] Bernhard Fichtl. Diploma thesis, University of Augsburg, 2010.

[42] Matthew T Flowers and James M Ntambi. Role of stearoyl-coenzyme a desaturase in regulating lipid metabolism. *Curr Opin Lipidol*, 19(3):248–256, Jun 2008.

[43] J. Folch, M. Lees, and G. H. Sloane Stanley. A simple method for the isolation and purification of total lipides from animal tissues. *J Biol Chem*, 226(1):497–509, May 1957.

[44] M. Foot, R. Jeffcoat, and N. J. Russell. Some properties, including the substrate in vivo, of the delta 9-desaturase in micrococcus cryophilus. *Biochem J*, 209(2):345–353, Feb 1983.

[45] E. J. Frenkel, B. Roelofsen, U. Brodbeck, L. L. van Deenen, and P. Ott. Lipid-protein interactions in human erythrocyte-membrane acetylcholinesterase. modulation of enzyme activity by lipids. *Eur J Biochem*, 109(2):377–382, Aug 1980.

[46] A. H. Futerman, R. M. Fiorini, E. Roth, M. G. Low, and I. Silman. Physicochemical behaviour and structural characteristics of membrane-bound acetylcholinesterase from torpedo electric organ. effect of phosphatidylinositol-specific phospholipase c. *Biochem J*, 226(2):369–377, Mar 1985.

[47] A. H. Futerman, D. Raviv, D. M. Michaelson, and I. Silman. Differential susceptibility to phosphatidylinositol-specific phospholipase c of acetylcholinesterase in excitable tissues of embryonic and adult torpedo ocellata. *Brain Res*, 388(2):105–112, Jul 1987.

[48] J. L. Garwin and Jr. Cronan, J. E. Thermal modulation of fatty acid synthesis in escherichia coli does not involve de novo enzyme synthesis. *J Bacteriol*, 141(3):1457–9, 1980.

[49] P. Gazzotti and S. W. Peterson. Lipid requirement of membrane-bound enzymes. *J Bioenerg Biomembr*, 9(6):373–86, 1977.

[50] Wolfgang Gebhardt. *Phasenübergänge und kritische Phänomene*. Friedr. Vieweg & Sohn Verlagsgesellschaft mbH, 1980.

[51] Peter Grabitz, Vesselka P Ivanova, and Thomas Heimburg. Relaxation kinetics of lipid membranes and its relation to the heat capacity. *Biophys J*, 82(1 Pt 1):299–309, Jan 2002.

[52] J. Griesbauer, A. Wixforth, and M. F. Schneider. Wave propagation in lipid monolayers. *Biophys J*, 97(10):2710–2716, Nov 2009.

[53] M. I. Gurr, M. P. Robinson, and A. T. James. The mechanism of formation of polyunsaturated fatty acids by photosynthetic tissue. the tight coupling of oleate desaturation with phospholipid synthesis in chlorella vulgaris. *Eur J Biochem*, 9(1):70–78, May 1969.

[54] C. W. Haest, A. J. Verkleij, J. De Gier, R. Scheek, P. H. Ververgaert, and L. L. Van Deenen. The effect of lipid phase transitions on the architecture of bacterial membranes. *Biochim Biophys Acta*, 356(1):17–26, 1974.

[55] J. R. Hazel. Thermal adaptation in biological membranes: is homeoviscous adaptation the explanation? *Annu Rev Physiol*, 57:19–42, 1995.

[56] T. Heimburg. Mechanical aspects of membrane thermodynamics. estimation of the mechanical properties of lipid membranes close to the chain melting transition from calorimetry. *Biochim Biophys Acta*, 1415(1):147–62, 1998.

[57] Thomas Heimburg. *Thermal Biophysics of Membranes*. Wiley-VCH Verlag GmbH & Co. KGaA, 2007.

[58] Thomas Heimburg and Andrew D Jackson. On soliton propagation in biomembranes and nerves. *Proc Natl Acad Sci U S A*, 102(28):9790–9795, Jul 2005.

[59] Helmut Hund GmbH, Wilhelm-Will-Str. 7, D-35580 Wetzlar.

[60] A. R. Honerkamp-Smith, S. L. Veatch, and S. L. Keller. An introduction to critical points for biophysicists; observations of compositional heterogeneity in lipid membranes. *Biochim Biophys Acta*, 1788(1):53–63, 2009.

[61] T. Honger, K. Jorgensen, R. L. Biltonen, and O. G. Mouritsen. Systematic relationship between phospholipase a2 activity and dynamic lipid bilayer microheterogeneity. *Biochemistry*, 35(28):9003–6, 1996.

[62] I. Horvath, Z. Torok, L. Vigh, and M. Kates. Lipid hydrogenation induces elevated 18:1-coa desaturase activity in candida lipolytica microsomes. *Biochim Biophys Acta*, 1085(1):126–30, 1991.

[63] Ibidi, GmbH, Am Klopferspitz 19, 82152 Martinsried, Germany.

[64] J. H. Ipsen, G. Karlström, O. G. Mouritsen, H. Wennerström, and M. J. Zuckermann. Phase equilibria in the phosphatidylcholine-cholesterol system.

Biochim Biophys Acta, 905(1):162–172, Nov 1987.

[65] M. B. Jackson and J. M. Sturtevant. Studies of the lipid phase transitions of escherichia coli by high sensitivity differential scanning calorimetry. *J Biol Chem*, 252(14):4749–51, 1977.

[66] A. L. Jones, D. Lloyd, and J. L. Harwood. Rapid induction of microsomal delta 12(omega 6)-desaturase activity in chilled acanthamoeba castellanii. *Biochem J*, 296 (Pt 1):183–8, 1993.

[67] P. D. Jones, P. W. Holloway, R. O. Peluffo, and S. J. Wakil. A requirement for lipids by the microsomal stearyl coenzyme a desaturase. *J Biol Chem*, 244(4):744–54, 1969.

[68] K. Jorgensen, J. Davidsen, and O. G. Mouritsen. Biophysical mechanisms of phospholipase a2 activation and their use in liposome-based drug delivery. *FEBS Lett*, 531(1):23–7, 2002.

[69] Morris Kates and Arnis Kuksis, editors. *Membrane Fluidity, Biophysical Techniques and Cellular Regulation*. The HUMANA press Inc., 1980.

[70] K. Kaufmann. *My Theory*, volume 2 & 3. Anahit AB publisher, 2009.

[71] K. Kaufmann and I. Silman. The induction of ion channels through excitable membranes by acetylcholinesterase. *Naturwissenschaften*, 67(12):608–609, Dec 1980.

[72] K. Kaufmann and I. Silman. The induction by protons of ion channels through lipid bilayer membranes. *Biophys Chem*, 18(2):89–99, Sep 1983.

[73] K. Kaufmann and I. Silman. Proton-induced ion channels through lipid bilayer membranes. *Naturwissenschaften*, 70(3):147–149, Mar 1983.

[74] H.K. Kimelberg. The influence of membrane fluidity on the activity of membrane-bound enzymes. *Cell Surf. Rev.*, 3:205–293, 1977.

[75] Lifschitz E. M. Landau L. D. *Lehrbuch der theoretischen Physik*, volume 5, Statistische Physik. Akademie-Verlag Berlin, 1987.

[76] A. G. Lee. Functional properties of biological membranes: a physical-chemical approach. *Prog Biophys Mol Biol*, 29(1):3–56, 1975.

[77] A. G. Lee. Lipid phase transitions and phase diagrams. i. lipid phase transitions. *Biochim Biophys Acta*, 472(2):237–281, Aug 1977.

[78] A. G. Lee. Lipid phase transitions and phase diagrams. ii. mictures involving lipids. *Biochim Biophys Acta*, 472(3-4):285–344, Nov 1977.

[79] A. G. Lee. Lipid-protein interactions in biological membranes: a structural perspective. *Biochim Biophys Acta*, 1612(1):1–40, May 2003.

[80] C. Leidy, L. Linderoth, T. L. Andresen, O. G. Mouritsen, K. Jorgensen, and G. H. Peters. Domain-induced activation of human phospholipase a2 type iia: local versus global lipid composition. *Biophys J*, 90(9):3165–75, 2006.

[81] A. Leikin and M. Shinitzky. Characterization of the lipid surrounding the delta 6-desaturase of rat liver microsomes. *Biochim Biophys Acta*, 1256(1):13–7, 1995.

[82] Christian Leirer. *Dynamik und Struktur in der Phasenkoexistenz von Lipidmembranen*. PhD thesis, University of Augsburg, 2008.

[83] Ruthven N A H Lewis and Ronald N McElhaney. The physicochemical properties of cardiolipin bilayers and cardiolipin-containing lipid membranes. *Biochim Biophys Acta*, 1788(10):2069–2079, Oct 2009.

[84] Sackmann E. Lipowski R. *Structure and Dynamics of Membranes*, volume 1. Elsevier Science B.V., 1995.

[85] H. P. Lu, L. Xun, and X. S. Xie. Single-molecule enzymatic dynamics. *Science*, 282(5395):1877–1882, Dec 1998.

[86] J. Massoulié, L. Pezzementi, S. Bon, E. Krejci, and F. M. Vallette. Molecular and cellular biology of cholinesterases. *Prog Neurobiol*, 41(1):31–91, Jul 1993.

[87] Harden McConnell. Complexes in ternary cholesterol-phospholipid mixtures. *Biophys J*, 88(4):L23–L25, Apr 2005.

[88] R. N. McElhaney and K. A. Souza. The relationship between environmental temperature, cell growth and the fluidity and physical state of the membrane lipids in bacillus stearothermophilus. *Biochim Biophys Acta*, 443(3):348–59, 1976.

[89] D. L. Melchior and J. M. Steim. Thermotropic transitions in biomembranes. *Annu Rev Biophys Bioeng*, 5:205–38, 1976.

[90] D. L. Melchior and J. M. Steim. Control of fatty acid composition of acholeplasma laidlawii membranes. *Biochim Biophys Acta*, 466(1):148–59, 1977.

[91] Wei Min, Brian P. English, Guobin Luo, Binny J. Cherayil, S. C. Kou, and X. Sunney Xie. Fluctuating enzymes: Lessons from single-molecule studies. *Accounts of Chemical Research*, 38(12):923–931, December 2005.

[92] Wei Min, Guobin Luo, Binny J. Cherayil, S. C. Kou, and X. Sunney Xie. Observation of a power-law memory kernel for fluctuations within a single protein molecule. *Phys. Rev. Lett.*, 94(19):198302–, May 2005.

[93] Makoto Miyazaki and James M Ntambi. Role of stearoyl-coenzyme a desaturase in lipid metabolism. *Prostaglandins Leukot Essent Fatty Acids*, 68(2):113–121, Feb 2003.

[94] W C Miyazaki M FAU Man, J M Man WC FAU Ntambi, and Ntambi JM. Targeted disruption of stearoyl-coa desaturase1 gene in mice causes atrophy of sebaceous and meibomian glands and depletion of wax esters in the eyelid.

[95] M. Montal and P. Mueller. Formation of bimolecular membranes from lipid monolayers and a study of their electrical properties. *Proc Natl Acad Sci U S A*, 69(12):3561–3566, Dec 1972.

[96] O. G. Mouritsen and M. Bloom. Mattress model of lipid-protein interactions in membranes. *Biophys J*, 46(2):141–153, Aug 1984.

[97] Ole G Mouritsen and Martin J Zuckermann. What's so special about cholesterol? *Lipids*, 39(11):1101–1113, Nov 2004.

[98] M. T. Nakamura and T. Y. Nara. Structure, function, and dietary regulation of delta6, delta5, and delta9 desaturases. *Annu Rev Nutr*, 24:345–76, 2004.

[99] H. Nakayama, T. Mitsui, M. Nishihara, and M. Kito. Relation between growth temperature of e. coli and phase transition temperatures of its cytoplasmic and outer membranes. *Biochim Biophys Acta*, 601(1):1–10, 1980.

[100] E. Neher and B. Sakmann. Single-channel currents recorded from membrane of denervated frog muscle fibres. *Nature*, 260(5554):799–802, Apr 1976.

[101] E. Neumann and D. Nachmansohn. Nerve excitability–toward an integrating concept. *Biomembranes*, 7:99–166, 1975.

[102] Jürgen Neumann. *Sensorische und aktorische Anwendungen akustischer Oberflächenwellen*. PhD thesis, University of Augsburg, Institut of Physics, 2009.

[103] Nima Technology Ltd, The Science Park, Coventry, England, CV4 7EZ.

[104] James N. Ntambi. Lipids, genes, and health. *Science*, 312:698a, 2006.

[105] Prof. Ntambi. University of Wisconsin Madison, USA, 2008.

[106] Nobuyasu Okazaki K FAU Koga, Shoji Koga N FAU Takada, Jose N Takada S FAU Onuchic, Peter G Onuchic JN FAU Wolynes, and Wolynes PG. Multiple-basin energy landscapes for large-amplitude conformational motions of proteins: Structure-based molecular dynamics simulations. (0027-8424 (Linking)):–, 1995.

[107] L. Onsager. Reciprocal relations in irreversibel processes. *Phys. Rev.*, 37:405–426, 1931.

[108] Lars Onsager. Reciprocal relations in irreversible processes. ii. *Phys. Rev.*, 38(12):2265–, December 1931.

[109] J. A. Op den Kamp, J. de Gier, and L. L. van Deenen. Hydrolysis of phosphatidylcholine liposomes by pancreatic phospholipase a2 at the transition temperature. *Biochim Biophys Acta*, 345(2):253–6, 1974.

[110] J. A. Op den Kamp, M. T. Kauerz, and L. L. van Deenen. Action of pancreatic phospholipase a2 on phosphatidylcholine bilayers in different physical states. *Biochim Biophys Acta*, 406(2):169–77, 1975.

[111] P. Ott. Membrane acetylcholinesterases: purification, molecular properties and interactions with amphiphilic environments. *Biochim Biophys Acta*, 822(3-4):375–392, Dec 1985.

[112] P. Ott, A. Lustig, U. Brodbeck, and J. P. Rosenbusch. Acetylcholinesterase from human erythrocytes membranes: dimers as functional units. *FEBS Lett*, 138(2):187–189, Feb 1982.

[113] P. Overath and H. Träuble. Phase transitions in cells, membranes, and lipids of escherichia coli. detection by fluorescent probes, light scattering, and dilatometry. *Biochemistry*, 12(14):2625–2634, Jul 1973.

[114] F. Pattus, C. Rothen, M. Streit, and P. Zahler. Structure, composition, enzymatic activities of human erythrocyte and sarcoplasmic reticulum membrane films. *Biochim Biophys Acta*, 647(1):29–39, Sep 1981.

[115] George Poste and Garth L. Nicolson. *Dynamic Aspects of Cell Surface Organization*. North-Holland Publishing Company Amsterdam- New York - Oxford, 1977.

[116] R A Prakash MK FAU Marcus and Marcus RA. An interpretation of fluctuations in enzyme catalysis rate, spectral diffusion, and radiative component of lifetimes in terms of electric field fluctuations.

[117] Ilya Prigogine. Time, structure, and fluctuations. *Science*, 201(4358):777–785, Sep 1978.

[118] E. L. Pugh and M. Kates. Characterization of a membrane-bound phospholipid desaturase system of candida lipolytica. *Biochim Biophys Acta*, 380(3):442–53, 1975.

[119] E. L. Pugh and M. Kates. Direct desaturation of eicosatrienoyl lecithin to arachidonoyl lecithin by rat liver microsomes. *J Biol Chem*, 252(1):68–73, Jan 1977.

[120] E. L. Pugh and M. Kates. Membrane-bound phospholipid desaturases. *Lipids*, 14(2):159–65, 1979.

[121] Daniel M. Quinn. Acetylcholinesterase: Enzyme structure, reaction dynamics, and virtual transition states. *Chem. Rev.*, 87:955–979, 1987.

[122] P. J. Quinn. The fluidity of cell membranes and its regulation. *Prog Biophys Mol Biol*, 38(1):1–104, 1981.

[123] S. Rainier, M. K. Jain, F. Ramirez, P. V. Ioannou, J. F. Marecek, and R. Wagner.

Phase transition characteristics of diphosphatidyl-glycerol (cardiolipin) and stereoisomeric phosphatidyldiacylglycerol bilayers. mono- and divalent metal ion effects. *Biochim Biophys Acta*, 558(2):187–198, Dec 1979.

[124] J. K. Raison. The influence of temperature-induced phase changes on the kinetics of respiratory and other membrane-associated enzyme systems. *J Bioenerg*, 4(1):285–309, 1973.

[125] T. L. Rosenberry. Acetylcholinesterase. *Adv Enzymol Relat Areas Mol Biol*, 43:103–218, 1975.

[126] M. A. Rothenberg and D. Nachmansohn. Studies on cholinesterase; purification of the enzyme from electric tissue by fractional ammonium sulfate precipitation. *J Biol Chem*, 168(1):223–231, Apr 1947.

[127] E. Sackmann, H. Träuble, H. J. Galla, and P. Overath. Lateral diffusion, protein mobility, and phase transitions in escherichia coli membranes. a spin label study. *Biochemistry*, 12(26):5360–5369, Dec 1973.

[128] Harini Sampath and James M Ntambi. Polyunsaturated fatty acid regulation of gene expression. *Nutr Rev*, 62(9):333–339, Sep 2004.

[129] Jr. Sandermann, H. Regulation of membrane enzymes by lipids. *Biochim Biophys Acta*, 515(3):209–37, 1978.

[130] Jr. Sandermann, H. Lipid-dependent membrane enzymes. a kinetic model for cooperative activation in the absence of cooperativity in lipid binding. *Eur J Biochem*, 127(1):123–8, 1982.

[131] Sabine Schmitz. *Der Experimentato: Zellkultur*. Spektrum Akademischer Verlag, 2 edition, 2009.

[132] Matthias F. Schneider. *Forces, Thermodynamics and Structure of Artificial Glycocalyx Models in Two and Three Dimensions*. PhD thesis, Technische Universität München, 2003.

[133] N. Schürer, A. Köhne, V. Schliep, K. Barlag, and G. Goerz. Lipid composition and synthesis of hacat cells, an immortalized human keratinocyte line, in comparison with normal human adult keratinocytes. *Exp Dermatol*, 2(4):179–185, Aug 1993.

[134] I. Shin, D. Kreimer, I. Silman, and L. Weiner. Membrane-promoted unfolding of acetylcholinesterase: a possible mechanism for insertion into the lipid bilayer. *Proc Natl Acad Sci U S A*, 94(7):2848–2852, Apr 1997.

[135] Sigma-Aldrich Co, 3050 Spruce St., St. Louis, MO 63103, USA.

[136] H. I. Silman and A. Karlin. Effect of local ph changes caused by substrate hydrolysis on the activity of membrane-bound acetylcholinesterase. *Proc Natl*

Acad Sci U S A, 58(4):1664–1668, Oct 1967.

[137] I. Silman and A. H. Futerman. Modes of attachment of acetylcholinesterase to the surface membrane. *Eur J Biochem*, 170(1-2):11–22, Dec 1987.

[138] Israel Silman and Joel L Sussman. Acetylcholinesterase: how is structure related to function? *Chem Biol Interact*, 175(1-3):3–10, Sep 2008.

[139] K. Simons and E. Ikonen. Functional rafts in cell membranes. *Nature*, 387(6633):569–572, Jun 1997.

[140] Kai Simons and Winchil L C Vaz. Model systems, lipid rafts, and cell membranes. *Annu Rev Biophys Biomol Struct*, 33:269–295, 2004.

[141] A. C. Simonsen. Activation of phospholipase a2 by ternary model membranes. *Biophys J*, 94(10):3966–75, 2008.

[142] M. Sinensky. Homeoviscous adaptation–a homeostatic process that regulates the viscosity of membrane lipids in escherichia coli. *Proc Natl Acad Sci U S A*, 71(2):522–5, 1974.

[143] S. J. Singer and G. L. Nicolson. The fluid mosaic model of the structure of cell membranes. *Science*, 175(23):720–731, Feb 1972.

[144] Dorette Christel Else Monika Spötter. *Der Retinoidmetabolismus in HaCaT-Zellen*. PhD thesis, Medizinische Fakultät der Rheinisch-Westfälischen Technischen Hochschule Aachen, 2003.

[145] J. M. Steim, M. E. Tourtellotte, J. C. Reinert, R. N. McElhaney, and R. L. Rader. Calorimetric evidence for the liquid-crystalline state of lipids in a biomembrane. *Proc Natl Acad Sci U S A*, 63(1):104–9, 1969.

[146] T. Frommelt W. Appelt A. Wixforth Steppich D., J. Griesbauer and M. F. Schneider. Thermomechanic-electrical coupling in phospholipid monolayers near the critical point. *PHYSICAL REVIEW E*, 81, 2010.

[147] Roman Stocker, Justin R Seymour, Azadeh Samadani, Dana E Hunt, and Martin F Polz. Rapid chemotactic response enables marine bacteria to exploit ephemeral microscale nutrient patches. *Proc Natl Acad Sci U S A*, 105(11):4209–4214, Mar 2008.

[148] P. Strittmatter, L. Spatz, D. Corcoran, M. J. Rogers, B. Setlow, and R. Redline. Purification and properties of rat liver microsomal stearyl coenzyme a desaturase. *Proc Natl Acad Sci U S A*, 71(11):4565–9, 1974.

[149] C. D. Stubbs and A. D. Smith. The modification of mammalian membrane polyunsaturated fatty acid composition in relation to membrane fluidity and function. *Biochim Biophys Acta*, 779(1):89–137, 1984.

[150] J. L. Sussman, M. Harel, F. Frolow, C. Oefner, A. Goldman, L. Toker, and

I. Silman. Atomic structure of acetylcholinesterase from torpedo californica: a prototypic acetylcholine-binding protein. *Science*, 253(5022):872–879, Aug 1991.

[151] P. E. Tiku, A. Y. Gracey, A. I. Macartney, R. J. Beynon, and A. R. Cossins. Cold-induced expression of delta 9-desaturase in carp by transcriptional and posttranslational mechanisms. *Science*, 271(5250):815–8, 1996.

[152] H. Träuble and H. Eibl. Electrostatic effects on lipid phase transitions: membrane structure and ionic environment. *Proc Natl Acad Sci U S A*, 71(1):214–219, Jan 1974.

[153] Hermann Träuble, Max Teubner, Paul Woolley, and Hansjörg Eibl. Electrostatic interactions at charged lipid membranes: I. effects of ph and univalent cations on membrane structure. *Biophysical Chemistry*, 4(4):319–342, July 1976.

[154] R. J. Trueman, P. E. Tiku, M. X. Caddick, and A. R. Cossins. Thermal thresholds of lipid restructuring and delta(9)-desaturase expression in the liver of carp (cyprinus carpio l.). *J Exp Biol*, 203(Pt 3):641–50, 2000.

[155] J. L. van de Vossenberg, A. J. Driessen, M. S. da Costa, and W. N. Konings. Homeostasis of the membrane proton permeability in bacillus subtilis grown at different temperatures. *Biochim Biophys Acta*, 1419(1):97–104, 1999.

[156] G. N. van Muijen, K. F. Jansen, I. M. Cornelissen, D. F. Smeets, J. L. Beck, and D. J. Ruiter. Establishment and characterization of a human melanoma cell line (mv3) which is highly metastatic in nude mice. *Int J Cancer*, 48(1):85–91, Apr 1991.

[157] S. L. Veatch, O. Soubias, S. L. Keller, and K. Gawrisch. Critical fluctuations in domain-forming lipid mixtures. *Proc Natl Acad Sci U S A*, 104(45):17650–5, 2007.

[158] Sarah L Veatch, Pietro Cicuta, Prabuddha Sengupta, Aurelia Honerkamp-Smith, David Holowka, and Barbara Baird. Critical fluctuations in plasma membrane vesicles. *ACS Chem Biol*, 3(5):287–293, May 2008.

[159] Sarah L Veatch and Sarah L Keller. Separation of liquid phases in giant vesicles of ternary mixtures of phospholipids and cholesterol. *Biophys J*, 85(5):3074–3083, Nov 2003.

[160] R. Verger and F. Pattus. Spreading of membranes at the air/water interface. *Chem Phys Lipids*, 16(4):285–291, Jul 1976.

[161] R. Verger and F. Pattus. Lipid-protein interactions in monolayers. *Chemistry and Physics of Lipids*, 30(2-3):189–227, May 1982.

[162] S. Wennmalm, L. Edman, and R. Rigler. Conformational fluctuations in single

dna molecules. *Proc Natl Acad Sci U S A*, 94(20):10641–10646, Sep 1997.

[163] B. Wunderlich, C. Leirer, A. L. Idzko, U. F. Keyser, A. Wixforth, V. M. Myles, T. Heimburg, and M. F. Schneider. Phase-state dependent current fluctuations in pure lipid membranes. *Biophys J*, 96(11):4592–7, 2009.

Danksagung

An dieser Stelle möchte ich gerne allen danken die zum Gelingen dieser Arbeit in irgendeiner Form beigetragen haben. Die Zusammenarbeit mit allen Lehrstuhlangehörigen des EXP 1 war mir immer eine Riesenfreude und hat mir einige wunderschöne Jahre mit euch eingebracht.

Eine namentliche Auflistung wird schwerlich vollständig sein. Trotzdem danke ich ganz besonders den folgenden Personen:

Prof. Dr. Achim Wixforth

für die Möglichkeit sowohl Diplom- als auch Doktorarbeit am Lehrstuhl anfertigen zu können. In den sehr angenehmen vergangenen Jahren am Lehrstuhl durfte ich ein Höchstmaß an menschlicher Führungskompetenz miterleben.

Prof. Dr. Matthias Schneider

für die begeisternde Betreuung während der letzten Jahre, die äußerts fruchtbaren Diskussionen, den forscherischen Freiraum und den Spaß tagsüber und am Abend.

Prof. Dr. Armin Reller

für die Begutachtung der Arbeit.

Dr. Konrad Kaufmann

für das enorme Wissen, dass du an uns weitergegeben hast, die Diskussionen, deine einzigartige Art und den “anderen” Blick auf die Physik.

Bernhard Fichtl

für deine Hilfe, deine tolle Arbeit und deine offene voranschreitende Art die mir immer eine Freude war.

Daehyun Eom

für deine Hilfe, dein erheiterndes Wesen und den kleinen Einblick in Südkorea.

Babak Fallah, Chris Westerhausen, Daniel Steppich, Josef Griesbauer, Jürgen Neumann, Stefan Bössinger, Stefan Völk

für die interessanten Gespräche und Diskussionen innerhalb und außerhalb der Uni, die netten Abende, die grandiose Stimmung und nicht zuletzt die daraus entstandenen Freundschaften.

Christian Leirer, Jochen Oelke, Kumudesh Sritharan, Lothar Schmid, Marcin Malecha, Markus Regler, Rolf Anders, Susanne Braunmüller, Dr. Thomas Franke

den Mitdoktoranden und Kollegen für die stets gute Laune und die kleinen Unterstützungen jedweder Art.

Funda Cevik, Alexander Hupfer, Sidonie Lieber, Andreas Spörhase, Olga Ustinov, Pouya Vaziri

für die organisatorischen und technischen Hilfen.

Prof. Dr. Israel Silman (Weizmann Institute of Science, Israel)

für die angenehme Zusammenarbeit und die zur Verfügung gestellten Acetylcholinesterase Proben.

Prof. Dr. James Ntambi, Mad, Chad und Harini (University of Madison, USA)

für ihre Gastfreundschaft, ihre Unterstützung bei den Desaturaseexperimenten und die ernüchternde kleine Einführung in die Mausforschung.

Prof. Dr. Hans Sturm

für die Einführung in strukturtheoretische Aspekte in philosophischer Hinsicht die durchaus nicht ohne Einfluss auf meine Arbeit waren.

Meinen Eltern und Geschwistern

für all ihre Unterstützung bei meinem bisherigen Weg. Ohne euch wäre diese Arbeit nicht zustande gekommen.

Karin

für deine moralische Unterstützung und deine Geduld über all die Jahre. Du warst immer für mich da.

Curriculum Vitae

Persönliche Angaben

Name	Stefan Nuschele
Geburtsdatum	28.08.1976
Geburtsort	Füssen
Familienstand	Ledig

Schule / Berufsausbildung / Zivildienst

09/1983 – 07/1987	Grundschule in Seeg
09/1987 – 07/1990	Gymnasium in Füssen
09/1990 – 06/1993	Realschule in Füssen
09/1993 – 02/1997	Otto Bihler Maschinenfabrik GmbH & Co. KG in Halblech Berufsausbildung zum Energieelektroniker
02/1997 – 07/1997	Otto Bihler Maschinenfabrik GmbH & Co. KG in Halblech Berufstätigkeit als Energieelektroniker
08/1997 – 08/1998	Alten- und Pflegeheim St. Martin in Füssen Zivildienst
09/1998 – 06/2000	Berufsoberschule in Kempten

Hochschulausbildung an der Universität Augsburg

10/2000 – 10/2005	Studium der Physik, Nebenfach: Philosophie Diplomarbeit: „Untersuchung und Nachahmung hämodynamischer Vorgänge mit Oberflächenwellen“
12/2006 -	Wissenschaftlicher Mitarbeiter Promotion in Biophysik: “The Role of Interfaces on Enzyme Activity and Cell Adaptation“
04/2007 - 06/2010	Förderung durch das „Elitenetzwerk Bayern” (ENB) Im Rahmen des internationalen Doktorandenkollegs „Material Science of Complex Interfaces” (CompInt)

Auslandsaufenthalte

11/2005 – 11/2006	Jahresreise durch verschiedene Kontinente
09/2008 – 12/2008	University of Wisconsin, Madison USA (2 Monate)
01/2010 – 02/2010	Boston University, Boston USA